PART II

FINAL REPORT
CAPILLARY MATRIX AND FUEL CELL DEVELOPMENT STUDY

Contract NAS9-10443

ALLIS-CHALMERS

ADVANCED ELECTROCHEMICAL PRODUCTS DIVISION • GREENDALE, WISCONSIN 53129

3.2.2.2 Weight and Configuration

- Weight Reduction

A detailed review of current systems has been performed which indicates that significant reductions in system weight can be achieved without employing high-risk design changes.

The present hardware exhibits a 98 lb/kW specific weight with a 2.0 kW rating; the projected 5 kW system, employing two 2 kW modules uprated to 2.5 kW each, represents a 44 lb/kW specific weight.

The present stack weight of 92 pounds can be reduced to 69 pounds by means of the following improvements:

- Polysulfone water removal plates (material substitution)
- Thinner hydrogen and oxygen plate nickel plating (process control)
- Lightweight end plates (material reduction)
- Lightweight compression device (component modification)

Weight reduction in the reactant controls can be achieved by modular packaging of existing components, reduction of tubing and fittings, and cold-plated preheaters. The present weight of 8.4 pounds per stack can be reduced to 5 pounds per 5 kW system.

The water delivery unit is a prime candidate for weight reduction as the existing hardware is far from weight-optimized. From a present weight of 24.2 pounds for a 2 kW rating, the weight of this assembly can be reduced to less than 19 pounds for a 5 kW system. A modular approach would be used with one set of components servicing two 2.5 kW stacks.

The weight of the electrical control and regulation equipment will increase to 33 pounds from the present 18.6 pounds due to the addition of a power conditioner to meet the voltage requirements. Controls and instrumentation for two stacks can be packaged as a unit to save enclosure and cold plate

weight. The following changes can be incorporated:

- Delete inverter (ac power supplied by spacecraft if required)
- Delete moisture controller (thermomechanical MRV is self-controlled)
- Delete coolant controller
- Add voltage regulator
- Optimize packaging

Significant weight reductions are achievable in the thermal control area. Helium fans and the coolant pump should be deleted to minimize rotating parts. Cold-plate cooling of the stack allows elimination of the canister, end dome, and heat exchanger coils. The weight of thermal control items for the 5 kW system is 13.6 pounds compared with 34.2 pounds for existing 2 kW hardware.

Mounting structure weight reductions can be achieved by repackaging components and integrating the stack supports with end plate hardware. An 11-pound structure weight is projected for the 5 kW system compared with 18 pounds for the 2 kW hardware.

- Volume and Mounting

In consonance with the requirements for minimum volume and simplified mounting, the techniques and requirements of MIL-C-172, MS 91403, and ARINC Specification 404 can be used as goals for packaging design. Physically, the Advanced Centerline is expected to be packaged into rectangular boxes which may be hard mounted to the vehicle surface or incorporated into an electronic equipment rack.

Internal to the units, related functions should be packaged into removable assemblies. An example of this technique is a repackaged bottom end plate for the EPU presented in Figure 3.2-7. The end plate contains integral manifolding of gases and fluids, allowing removal and replacement at the

first shop level of maintenance.

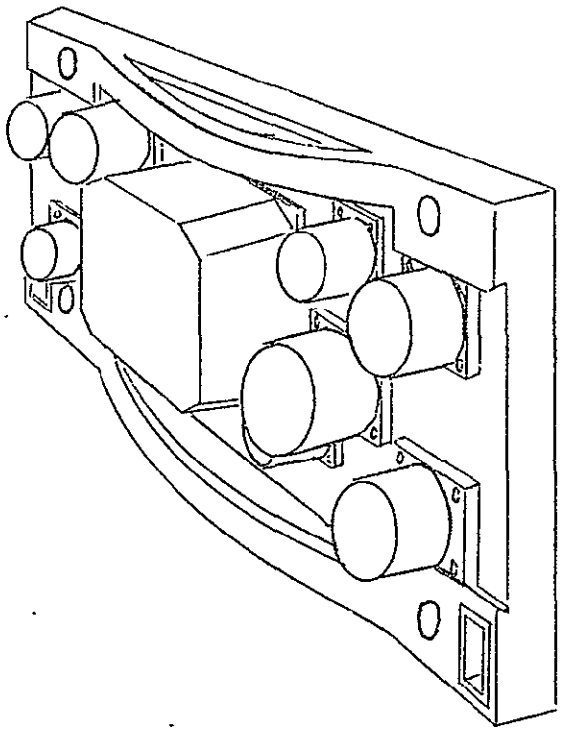

Figure 3.2-7. Bottom End Plate Assembly

3.2.2.3 Reactant Management

Advanced system goals identified in connection with reactant utilization require improvements over existing hardware designs. These include operation with propellant grade reactants, source pressures as low as 20 psia and (simultaneously) minimum fuel cell reactant consumption rates.

A complete study of propellant grade reactant usage was conducted under Subtask 2.3 and is reported there. General considerations of the basic approaches toward reactant management are discussed below:

- Propellant Grade Reactant Usage

  Two types of impurities are of concern in the use of propellant grade H_2 and O_2: inerts and chemically active species.

  Two basic concepts investigated for management of high inert levels are reactant recirculation and use of an inert accumulation cell. Reactant recirculation by means of jet pumping is reliable, requires no parasitic power, and has been demonstrated in over 13,000 cell-hours of testing under the High Performance Fuel Cell program. Recirculation flows from 50% to 100% of consumption flow, and purge sensitivity improvements as high as a factor of four, have been achieved.

  Inerts can be accumulated in a single cell of a stack by providing reactant feed flow in series through the stack. It is possible to obtain equivalent results by a "cascade" arrangement whereby reactants flow in parallel through the next quarter of the stack, and so on to the final cell in the assembly. The need for purging can be detected by measuring the output potential of the inert accumulation cell. With this approach, a wide range of reactant purities can be tolerated while minimizing the amount of reactants lost through purging.

  Active impurities in the inlet gases must be captured upstream of the reactor assembly. This can be accomplished by scrubber techniques. The scrubber must be removable for routine, scheduled maintenance.

- Low-Pressure Reactants

  The requirement to operate with low inlet pressures has the dual effect of constraining cell/stack performance and limiting the choice of techniques for dealing with impure gases. Efficiency and reactant consumption suffer at low operating pressures, and jet pumping for example, is ineffective at low feed pressures. The use of compressor techniques for boosting feed pressure have been traded against the option of accepting and compensating

for reduced performance at low pressures (see Subtask 2.3 report).

- Reactant Consumption

  Reactant consumption for future space missions should be minimized and an ambitious goal for the advanced system has been established at .7 to .8 lb/kW-hr at rated power.

  These goals require operation at cell potentials from 0.925 to 1.058 volts. For existing cell performance levels, operation must be limited to power densities far below the cells' inherent capability, resulting in large stack weight penalties.

  The low-risk cell improvements presented earlier relative to life and performance will improve efficiency and hence, reactant consumption substantially but higher-risk improvements would be required to meet the consumption rate goals and maintain an attractive specific weight. A trade study should be performed to identify the optimum balance between stack weight (with the proposed low-risk improvements) and total reactant consumption specifically related to the shuttle mission.

3.2.2.4 Thermal Control

Thermal requirements are specified in qualitative terms and call for a high-temperature, minimum heat load interface with the spacecraft radiator loop. Dual mode heat rejection is permitted, to avoid thermal spike inputs to the radiator loop. Various thermal control methods were investigated under Subtask 2.3 and reported on there. General thermal control considerations are presented below.

- Cold Plate Cooling

  Removal of waste heat from the stack by means of cold plates significantly reduces weight as well as permitting increased system coolant outlet temperatures. Testing of this approach was accomplished at the full-stack level under contract NAS 8-20573. Results of this evaluation verified that

the concept is practical and the stack-to-cold plate interface is not a critical one in terms of manufacturing tolerance. A design trade-off is required to compare liquid cooling versus heat pipe cooling of the stack cold plates for the shuttle application.

- Improved Water Removal

  The present 2 kW condenser design is thermally limited and not weight optimized. An improved condenser conceptual design was developed under Subtask 2.3. Development testing of an integrated water removal assembly (condenser, deionizer, and water pump) should be conducted to demonstrate integrated operation of the improved condenser with its interfacing elements.

3.2.2.5 Operational Flexibility

System adaptability to a variety of applications, and operational modes within a given application, require a flexible concept in terms of packaging, performance, and operation. Modular packaging, as previously discussed, is expected to facilitate installation and interfaces. Dual mode heat rejection permits sustained overload operation under water venting conditions. Maintainability and automatic checkout features enable system readiness to be defined rapidly and sustained over the vehicle life cycle. Specific performance and operational features are described below.

- High Voltage Output

  Generation of power at voltages higher than the usual 28 volt level permits optimization of the spacecraft power distribution system in terms of copper weight and power losses. Fuel cells are adaptable with modifications to a 56-Volt output due to the use of series-parallel cell connections in present hardware. Each series-connected cell section in the 2 kW stack consists of two single cells in parallel. The modifications required to reconnect these in series stem from the two cells/sharing of a common oxygen plate.

Options for operation at the 112 volt level include series connection of two 56-volt stacks, parallel connection of two stacks modified for 112 volt capability, and boost-regulation power conditioning. These approaches should be evaluated and a tradeoff study prepared assessing hardware implications, development requirements, and cost.

- Power Conditioning

Fuel cell systems have traditionally been operated as unregulated power supplies due to the relative flatness of their Voltage-Current characteristic from rated power down to 20 or 30% of full load.

More recent flight applications requiring large power turndown ratios have resulted in number of techniques for limiting output voltage at light loads, including variable temperature operation, voltage suppression by means of parasite loads, and switching of stacks off load at low power levels.

The requirement for voltage regulation down to open circuit, coupled with minimum reactant consumpiton goals, necessitates consideration of high-efficiency voltage regulation methods.

The AAP Prototype power regulator developed for NASA by Allis-Chalmers under Contract NAS 9-8639 is a demonstrated method of achieving the required regulation at high efficiency. Exploitation of this advanced technology by means of full-scale system demonstration should be conducted.

- Multiple Start/Stop

A straightforward engineering effort is recommended to fabricate an automatic start/stop sequencer and demonstrate multiple restarts on a multi-cell stack under sequencer control. This will verify, at a high level of assembly, stack/controller compatibility, minimum degradation, and stable control of startup/shutdown parameters.

3.2.2.6 Cost and Schedule

Costs and schedules for a program to utilize the above improvements have been developed. Table 3.2-7 shows the overall schedules and costs for the recommended improvements. It should be noted that they are for the individual improvements and not a complete program.

3.2.2.7 System Concept Definition

The Part 3 Design Requirements document starting on page 1 of Appendix B was used as the basis for the system concept. A complete functional block diagram network was prepared to definitize the concept. (Refer to Monthly Report #4 - 80045-141.) In addition, a complete set of input/output block diagram was prepared to identify internal and external interfacing. (Refer to Monthly Report #4 - 80045-141.) Figure 3.2-8 is the fluid diagram for the system concept. Detailed performance requirements and subsystem component descriptions were prepared to define the system. These are presented in Appendix C.

COST ESTIMATE

Catagory	Months ARO 1	2	3	4	5	6	7	8	9	10	11	12	13	TOTAL
Engineer	4.5	7.3	7.2	7.0	7.3	6.9	5.5	5.4	5.4	4.6	4.0	3.0	0.8	68.8
Technician	-	1.3	1.8	1.7	4.1	6.1	6.5	5.1	5.2	4.9	3.5	3.0	0.4	42.6
Draftsman	-	1.1	1.1	0.6	0.6	0.6	0.6	0.6	0.6	1.1	1.2	1:0	9.7	9.7
Total Manpower	4.5	9.7	10.1	9.3	12.0	12.6	12.6	11.1	11.2	10.1	8.6	7.2	2.2	121.1MM
Material	-	1448	1540	3722	4664	3953	4500	1800	1000	1956	1600	1715	-	$27,898

SCHEDULE ESTIMATE

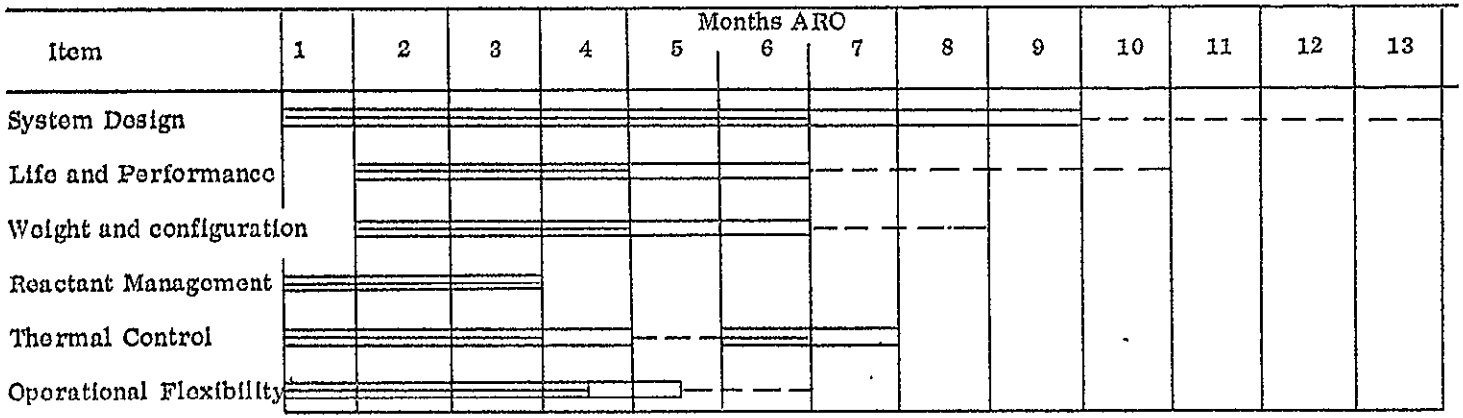

Table 3.2-7. Advanced System Development Cost and Schedule

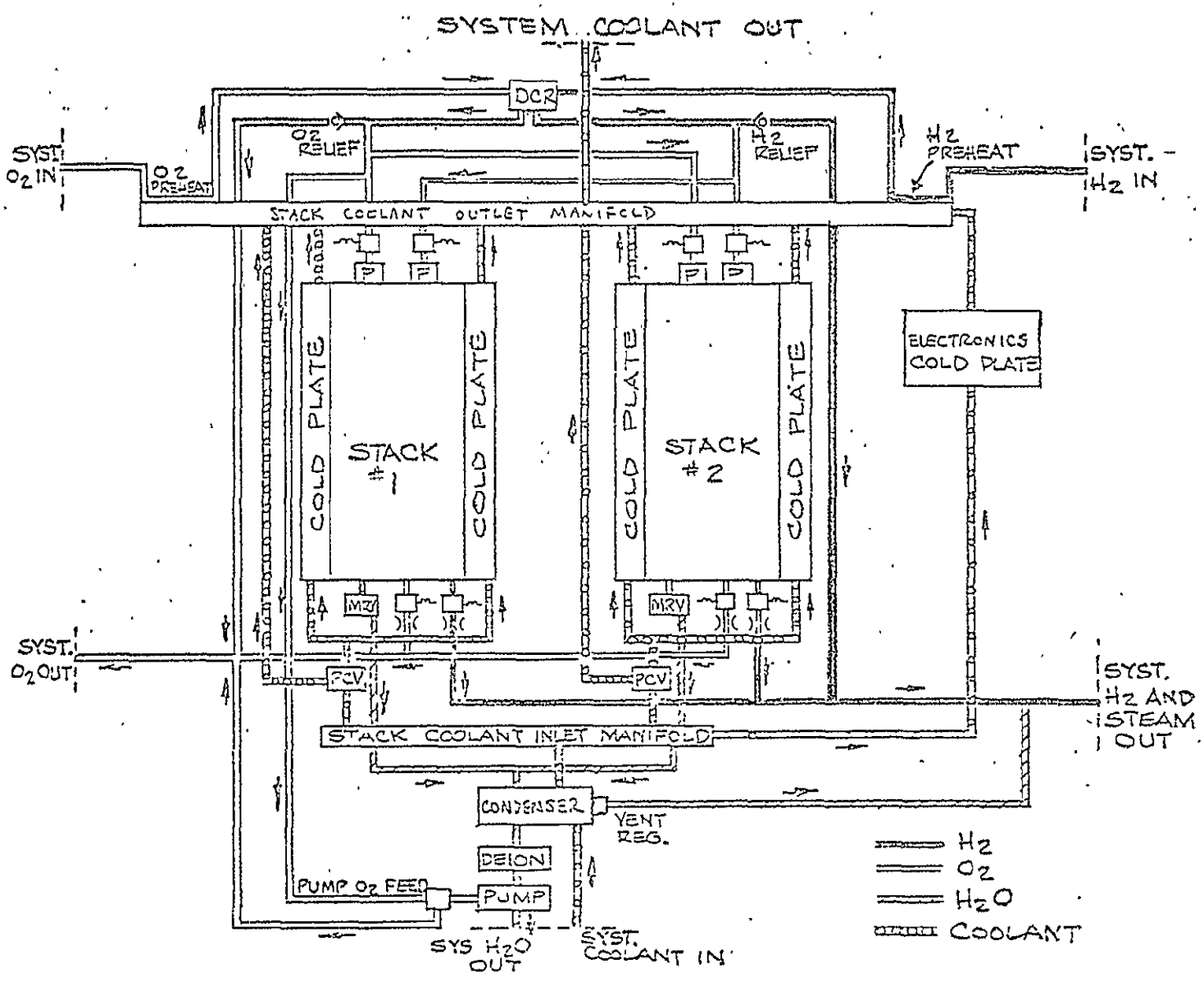

Figure 3.2-8. 5kW Building Block Approach - A Preliminary Sketch

3.2.3 Subtask 2.3 - Applications Analysis

The objectives of the Applications Analysis subtask were as follows:

- Determine vehicle/mission power system requirements
- Evaluate system improvements in the areas of maintainability, propellant gas utilization and thermal control
- Define system operational concepts and automated checkout

Contractual effort performed toward meeting these objectives consisted basically of customer/prime contractor coordination, and subsequent design definition and tradeoff studies.

3.2.3.1 Coordination

The magnitude of the coordination efforts is illustrated in the shuttle customer contact summary, Table 3.2-8.

All of the design requirements gathered in these contacts were used to develop a system requirements specification. An initial centerline system design was then developed from this specification. The centerline design was documented by means of a functional logic network, interface block diagrams, and subsystem data packages containing detailed technical requirements allocated and expanded from the system specification.

The initial issue of the above documents was based primarily on the composite requirements obtained from the shuttle study contractors. Major updating of these documents was performed after release of the MSC Fuel Cell Technology Program RFP to bring the centerline design into conformance with NASA's specific requirements, which differed significantly in some respects from the vehicle contractor design philosophies.

The latest versions of these system documents were presented in Section 2.2 and are not repeated here. They include the system operational concepts and checkout interface definition.

The balance of this section presents the results of the system improvement studies conducted under this subtask.

Organization Contacted	Type of Contact: Telecon	Type of Contact: Visit
Aerospace Corporation	3	1
Boeing	3	-
General Dynamics	16	3
Grumman	10	-
Lockheed	6	4
Martin	2	2
McDonnell/Douglas	6	5
NASA-ERC	1	-
NASA-HQ (DART)	3	3
NASA-HQ (OMSF)	10	3
NASA-Lewis	2	-
North American	11	5
USAF-SAMSO	-	3
Conferences*	-	3
Total	73	32

*Meetings with Space Shuttle on agenda:

IECEC Meeting, Washington, D.C.
Shuttle Conference, Washington D.C.
AIAA Conference, Cape Kennedy, Florida

Table 3.2-8. Customer/Prime Contractor Coordination Summary

3.2.3.2 Maintainability

The maintenance concept is an important part of total systems engineering. Early maintenance analysis and planning can minimize field support requirements for sparing, service time, and special equipment.

As a part of the Applications Analysis subtask, various maintenance techniques were evaluated. The concepts assessed are depicted in Figure 3.2-9; the results of these evaluations are presented in this section.

- Maintenance Concepts

  The maintenance concept assessment considered system test, scheduled maintenance, servicing, detection and isolation of malfunctions, replacement and repair of equipment, skill categories of maintenance personnel, and supply requirements.

  The primary objectives that guided the maintenance concept development were:

  - Minimum vehicle downtime in the event of a malfunction
  - Minimum requirements for qualification, quantity and training of maintenance personnel
  - Minimum requirements for repair capability
  - Minimum special support equipment

  These objectives along with the constraints and requirements of both NASA and the vehicle contractors were factored into the concept development.

  The maintenance concept that was evolved for the present centerline system was based on the following guidelines:

  - Design simplicity to reduce the number and complexity of components
  - Functional packaging of equipment to minimize fault isolation and correction time

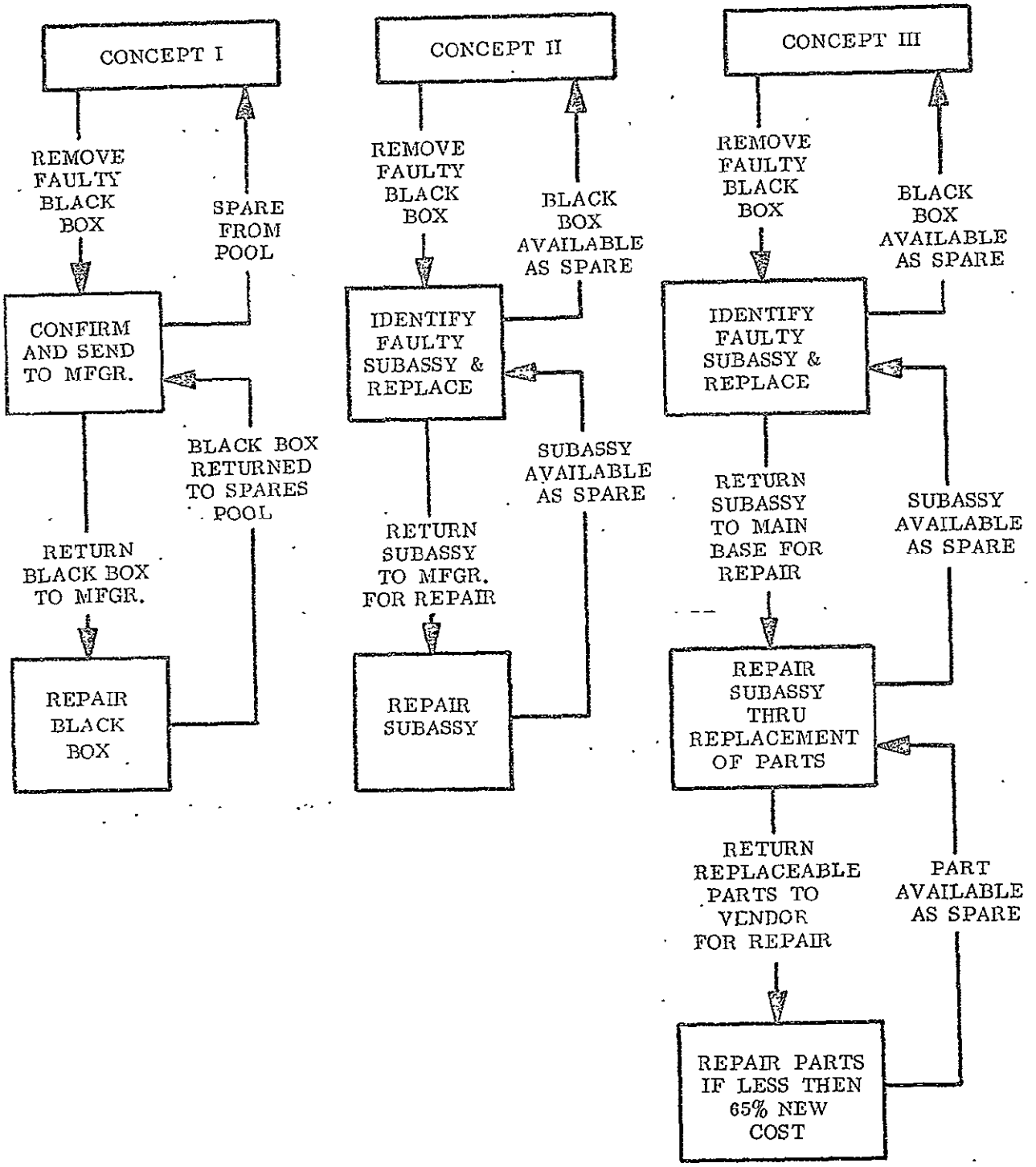

Figure 3.2-9. Examples of Maintenance Concepts

- Utilization of standard maintenance policies for NASA
- Minimum vehicle servicing, requiring less than 30 minutes to accomplish
- No special equipment required at the vehicle to support corrective maintenance actions
- Preventive maintenance actions to be consistent with vehicle certification and overhaul intervals
- Maximum corrective action capability at the shop level with minimum dependence on the depot

Several features have been incorporated into the centerline system design to meet the maintenance guidelines. The most significant feature is that the design allows the user to choose any desired level of maintenance, ranging from simple return of Line Replaceable Units to the manufacturer to complete customer repair capability.

The selection of all the features has been based upon minimizing maintenance costs at all levels of maintenance, maximizing the ease of maintenance and minimizing the degradation of equipment reliability because of maintenance errors. Additional general features are as follows:

Sufficient built-in test equipment has been incorporated to insure detection and isolation of all malfunctions of the Fuel Cell Power Systems (FCPS) to a Line Replaceable Unit (LRU). Operation in conjunction with an on-board computer allows continuous automatic detection of failures which can be recorded in memory, identifying intermittent failures for future maintenance actions.

Degradation type failures are detected by the on-line evaluation of system condition before and during each flight through the automatic monitoring and processing of the data items being monitored. The quality of the system is indicated in a performance index displayed to the crew during ground or in-space startup. Degradation type errors can also be detected by comparing the outputs of the different fuel cell units installed in the vehicle. All system performance information is processed to the computer

and from there to the common display unit, thus providing a complete end-to-end check of system condition. Therefore, no test equipment is required on the flight line to detect and isolate malfunctions internal to the FCPS. Test equipment may occasionally be necessary for vehicle cabling malfunctions and ancillary equipment malfunctions.

The packaging of the FCPS subsystems into functionally contained LRU's represents a balance between the constraints of small size, minimum weight, rapid fault isolation, simple replacement and low cost spares. Each functional subsystem is self contained in a separate LRU. Each LRU will be a plug-in unit, rack mounted, allowing easy access for maintenance actions. Figure 3.2-10 is a sketch of the rack mount concept.

The LRU's are easily attached to test equipment in the same manner as originally mounted in the vehicle, with sufficient test points to enable rapid fault isolation to the faulty subassembly.

Fluid and gas passages have been integrated into the structure of each LRU, thereby minimizing interconnect tubing and fittings. The result is ease of maintenance and reduced reliability risks.

The general concepts for NASA maintenance of the FCPS are predicted upon four principal requirements:

1. Quality and reliability of maintenance - all maintenance actions must be planned so that the likelihood of degrading the reliability or performance of the equipment is minimized.
2. Economy of maintenance - the total cost of maintenance must be minimized.

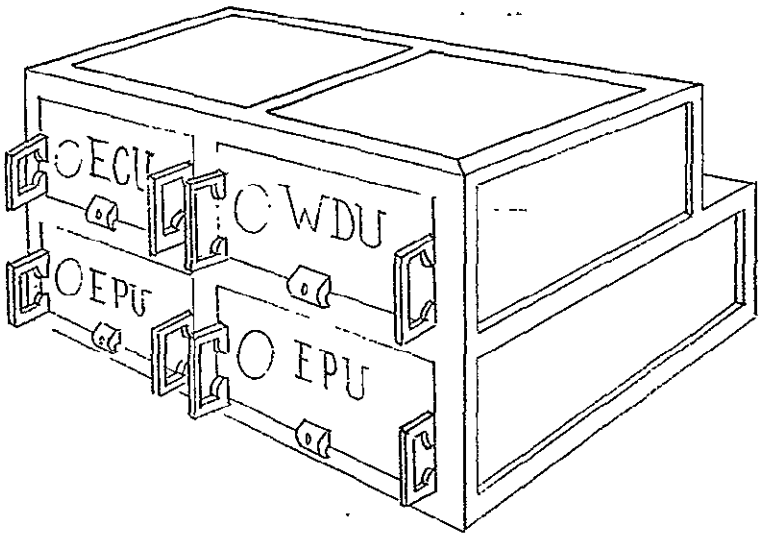

Figure 3.2-10. Integrated System Configuration Concept

3. Flexibility of maintenance planning - the choice of possible maintenance concepts (or variations of one concept) must be wide enough to permit the user to choose a specific plan to meet its particular needs.

4. Independence of user maintenance - it must be possible for the user to conduct a maximum of maintenance or repair by itself, independent of any external repair organization.

This section describes two user maintenance facilities (Basic and Expanded) as illustrations of the types of maintenance plans possible. It is recognized that, with the minimum shuttle fleet size presently identified, only the Basic maintenance facility is cost effective. However, if shuttle fleet sizes become comparable to that of a commercial airline, the Expanded maintenance facility is most desirable. A detailed discussion of the concepts is given below.

Implicit in the discussion of the maintenance facilities is a common ramp flight line maintenance concept, described in the first subparagraph.

Ramp maintenance of the shuttle must be performed quickly to assure that vehicle departures remain on schedule. In the event of a FCPS malfunction, ramp maintenance involves replacement of the defective LRU and ground startup of the FCPS. Under this concept, only those corrective maintenance actions which can be performed in a short time without degrading reliability or performance will be conducted at the ramp.

Maintenance functions to be performed at the ramp consist of detection and isolation of the malfunction, removal and replacement of the LRU and runup and checkout of the system. Automatic inflight and preflight detection of malfunctions is performed through the continuous monitoring of the system performance by the system monitoring equipment and the onboard computer. Detection of a malfunction can be indicated either on an integrated cockpit display unit or a separate control and display unit.

Since malfunction detection is continuous and automatic, the normal isolation action is simply a visual check for a malfunction indication. No test equipment is required for ramp maintenance, and the isolation, removal and replacement can be accomplished by relatively unskilled personnel.

Removal and replacement of the LRU can be accomplished quickly without special tools or adjustments. All the units can be removed and replaced by one man, except the Electrical Power Unit (EPU) which weighs approximately 75 pounds. EPU removal and replacement will require two men. All the gas, liquid and electrical connections are made automatically when the unit is placed in position in the mounting rack.

Flight worthiness of a newly installed LRU will be verified by monitoring initial startup, monitoring the fault indicators and visually monitoring the displayed status indicator. Check out is complete when sequencing is completed and no malfunction indication is observed.

The Basic shop concept provides for repair of the LRU's by replacement of subassemblies and electronic modules. The Expanded shop concept includes the basic shop capability with the added capability of testing and trouble shooting removed subassemblies, electronic modules, and components.

In general, an electronics shop environment is satisfactory for LRU level test and the repair and replacement of the various subassemblies; a semiclean area is required for repair of the stack assembly.

The Basic maintenance facility is intended for use while the fleet of shuttle vehicles is small. It provides minimum cost in GSE and personnel skills, but a larger investment in major spares elements is required over that of the Expanded shop.

The corrective maintenance actions to be performed in the Basic maintenance facility are shown in Figure 3.2-11. The LRU's that are removed from the

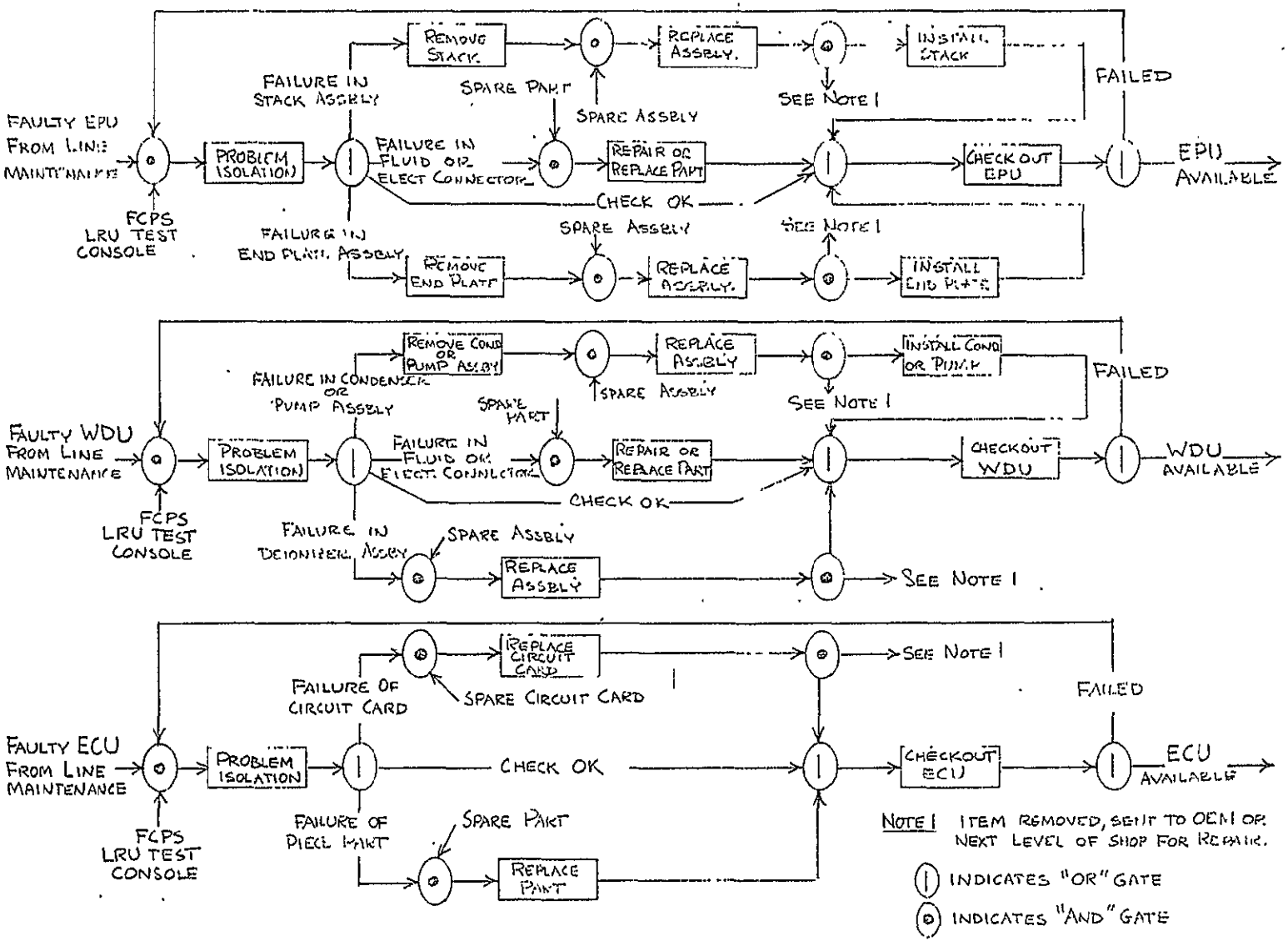

Figure 3.2-11. Basic Shop Maintenance Functions

vehicle are installed in the appropriate rack position on the FCPS LRU test console. The console will verify the malfunction and isolate it to a replaceable subassembly or electronics module. The test console control panel has the capability of exercizing the faulty LRU's individually or in any combination. A complete system is not required to test an individual LRU. Test results will be displayed on the control console panel and also printed out on tape for future reference. In some instances it may be necessary to perform some manual probing of test points within an LRU. Quick and easy access will be made to these test points through removal of a cover plate on the front panel of the LRU behind which all the test points for the LRU will be located.

Functional elements within each LRU will be integrally packaged for easy removal. Electronic modules will be of the plug-in type and will not require soldering as a part of the replacement action. Electrical harnesses and fluid and gas piping within the LRU will be individually replaceable as all spares will include fittings and connectors. This will require only simple mechanical hand tools.

Post maintenance LRU checkout is accomplished by the test console exercizing the repaired item to assure conformance to all maintenance manual test criteria.

Removed subassemblies and electronic modules will be sent to the Original Equipment Manufacturer (OEM) for further repair or overhaul.

The Expanded shop maintenance facility allows customer maintenance on those items repaired by the OEM under the Basic shop concept. Specifically, the Expanded facility permits lower level of assembly repair, including replacement of components, piece parts, and printed circuit boards within a subassembly or electronic module. The expansion can be accomplished incrementally as the fleet size increases, making the investment in additional GSE a financially sound undertaking. Those items for which the largest return on investment can be realized, can be undertaken

first with additional items being added as it is found that they will pay their own way.

The maintenance operations for the aforementioned maintenance levels, and their corresponding resource requirements, are summarized in Table 3.2-9.

- Maintenance Analysis

A maintenance analysis was performed to quantitatively establish the MTTR values for FCPS repair at the ramp and in both Basic and Expanded maintenance shops. The details of the ramp analysis resulted in an MTTR of approximately 25 minutes. The details of the shop maintenance analysis resulted in an MTTR of approximately 92 minutes.

In both analyses, the calculations of MTTR were based on the failure rates in Table 3.2-10. The maintenance analysis was based on the ramp maintenance concept the shop maintenance actions previously described.

The ramp maintenance analysis included consideration of ramp maintenance actions required to isolate faults, remove and replace LRU's, and check out the system. The results of this analysis, shown in Table 3.2-11 shows a MTTR of approximately 25 minutes for repair of the FCPS while installed in the vehicle. A review of the projection shows that the greatest amount of time is required for checkout to establish a high confidence in system integrity. This checkout is automatically accomplished in conjunction with the onboard computer, thus eliminating the possibility of human error by limiting the operators participation to turning on the system and monitoring the displayed data.

The shop maintenance analysis results appear in Tables 3.2-11'a) and 3.2-11(b) and show an MTTR of approximately 92 and 150 minutes for the Basic and Expanded shops, respectively.

Typical Operations / Support Factors	MAINTENANCE LEVELS		
	Ramp	Basic Shop	Expanded Shop or OEM
	• Simple adjustments • Item replacements • Fault isolation • Checkout	• Simple repairs • Calibration • Selected component and piece-part replacement • Retest	• Detail overhaul • Complex repair • Seal, diaphragm replacements • Electronic piece parts
Personnel Skill and Training Needed	Low	Average	High
Facilities	None	Semi-clean room	Clean rooms
Special Test Equipment	None	Subassembly test consoles	Complete in-process to system-level equipment
Tooling	Hand tools	• Handling fixtures • Special tools	Overhaul tooling
Spares	None	• Subassemblies • Selected components • Selected piece-parts	Complete backup to piece-part level

Table 3.2-9. Maintenance Operations and Supporting Resources

	Failure Rate x 10^{-6}	
	Assembly	Component
EPU (2 Each)		
Stack assembly (1)	9.0	
End plate assembly (1)	33.2	
Inlet valves (2)		1.6
Pressure transducers (2)		20.0
Proportional moisture removal valve (1)		4.0
Purge valves (2)		4.0
Restrictors		0.6
Proportional coolant valve (1)		3.0
Cold plates (2)	1.0	
Sensors (Temperature-Pressure-Amps)	6.0	
Miscellaneous (Tubing-Connectors-Etc.)	10.0	____
	59.0	
WDU (1 Each)		
Condenser	0.4	
Vent regulator	4.0	
Deionizer	0.1	
Pump assembly	13.0	
Water pump		2.0
Check valves		3.0
Pump valve		4.0
Vacuum regulator		4.0
Miscellaneous (Manifold-Tubing-Connectors-Etc.)	7.5	____
	25.0	
Rack Assembly (1 Each)		
Tubing	5.0	
Electrical wiring	5.0	
Connectors	30.0	
Hard fittings		5.0
QD's		15.0

Table 3.2-10. (Page 1 of 2) Failure Rates

	Failure Rate x 10^{-6}	
	Assembly	Component
Rack Assembly (Continued)		
Electrical connectors		10.0
DCR	8.0	
Relief Valves	2.0	____
	50.0	
ECU (1 Each)		
Purge controller assembly	10.0	
Signal conditioning	20.0	
Temperature		5.0
Pressure		5.0
Current		5.0
Valve indication		5.0
Start/stop logic	20.0	
Voltage regulator	75.0	
Miscellaneous (Wiring-Connectors)	10.0	____
	135.0	
Approximate System Failure Rate		
EPU (2) 59.0 x 2	118.0	
WDU (1) 26.0 x 1	25.0	
Rack (1) 50.0 x 1	50.0	
ECU (1) 135.0 x 1	135.0	
	328.0	

MTBF = 3050 Hours

Table 3.2-10. (Page 2 of 2) Failure Rates

UNIT	Failed Item	Active Corrective Maintenance Time (minutes)					% of Total Failures	Contribution to MTTR (minutes)
		Set Up	Malfunction Isolation	Remove & Replace	Checkon	Total		
FUEL CELL POWER SYSTEM	Electrical Power Unit (2)	-	1.0	3.0	12.0	16.0	36.0%	5.56
	Water Delivery Unit	-	1.0	3.0	20.0	24.0	7.6%	1.90
	Electrical Control Unit	-	1.0	3.0	15.0	19.0	41.1%	7.60
	Reactant Control Assembly	-	1.0	3.0	5.0	9.0	3.1%	0.28
	Rack Assembly	-	20.0	30.0	30.0	80.0	12.2%	9.76
					FCPS Total MTTR Average (Ramp)			25.10

Table 3.2-11. Ramp Maintenance Time Requirements

UNIT	Failed Item	Active Corrective Maintenance Time (minutes) Set Up	Malfunction Isolation	Remove & Replace	Checkout	Total	% of Total Failures	Contribution to MTTR
E	Stack Assembly	5	25	60	20	105	15.3%	16.1
	End Plate Assembly	5	30	120	40	190	56.2%	107.0
P	Cold Plate Assembly	5	30	60	30	120	1.7%	2.1
	Sensors	5	15	30	15	60	10.1%	6.1
U	Misc (Tubing - Connectors - etc.)	5	20	75	30	125	16.7%	20.8
								152.1
W	Condenser Assembly	5	30	15	15	60	17.6%	10.6
	Deionizer Assembly	5	5	5	15	25	0.1%	0.3
D	Pump Assembly	5	15	15	15	45	52.3%	23.5
	Misc (Manifold - Tubing - Connectors - etc.)	5	45	10	15	70	30.0%	21.0
U								55.4
E	Purge Control Assembly	5	15	10	10	35	7.4%	2.6
	Signal Conditioners	5	15	10	10	35	14.8%	5.2
C	Start/Stop Assembly	5	15	10	10	35	14.8%	5.2
	Voltage Regulator	5	15	15	15	45	55.6%	25.0
U	Misc. (Wiring - Connections)	5	45	30	10	85	7.4%	6.3
								44.3

EPU	152.1	42.5%	64.7
WDU	55.4	9.0%	5.0
ECU	44.3	48.5%	21.5
			91.2

Table 3.2-11(a) Shop Maintenance Time Requirements - Level I Repairs Performed in Basic Shop

UNIT		Active Corrective Maintenance Time (minutes)					% of Total Failures	Contribution to MTTR
		Set Up	Malfunction Isolation	Remove & Replace	Checkout	Total		
	End Plate Assembly							
E	Inlet Valves (2)	5	10	5	5	20	4.8%	1.0
	Pressure Transducers (2)	5	10	5	10	25	60.4%	15.1
P	Prop Moisture Removal Valve	5	20	5	20	45	12.0%	55.4
	Purge Valves (2)	5	10	5	5	20	12.0%	2.4
U	Restrictors (2)	5	5	5	5	15	1.8%	0.3
	Prop Coolent Valves	5	15	5	15	35	9.0%	3.2
								27.4
	Condenser Assembly							
W	Condenser	5	20	15	20	55	2.3%	1.3
	Vent Regular	5	5	10	5	20	23.0%	4.6
D	Pump Assembly							
	Water Pump	5	10	10	10	30	11.5%	3.4
U	Check Valves	5	10	5	5	20	17.2%	3.4
	Pump Valves	5	5	5	5	15	23.0%	3.5
	Vacuum Regulator	5	15	5	5	25	23.0%	5.7
								21.9
E	Purge Controller Cards	5	20	5	20	45	8%	3.6
	Signal Conditioner Cards	5	30	5	20	55	16%	8.8
C	Start/Stop Logic Cards	5	30	5	20	55	16%	8.8
	Regulator Cards	5	40	5	20	65	60%	39.0
U								60.2

Table 3.2-11(b) (Sheet 1 of 2). Shop Maintenance Time Requirements - Level II Repairs Performed in Expanded Shop

UNIT		Active Corrective Maintenance Time (minutes)					% of Total Failures	Contribution to MTTR
		Set Up	Malfunction Isolation	Remove & Replace	Checkout	Total		
RACK ASSEMBLY	Rack Assembly							
	Tubing	10	45	15	5	65	12.5%	8.3
	Electrical Wiring	10	45	15	5	65	12.5%	8.3
	Quick Disconnects	10	15	10	5	30	37.5%	11.2
	Hard Fitting	10	15	10	5	30	12.5%	3.8
	Electrical Connectors	10	30	30	30	90	25.0%	22.5
								54.1
	Reactant Control Assembly							
	Regulator	5	10	5	10	25	80%	20.0
	Relief Valves	5	10	10	10	30	20%	6.0
								26.0
	EPU					27.4	14.7%	4.0
	WDU					21.9	7.8%	1.7
	ECU					60.2	55.5%	33.4
	DC Assembly					26.0	4.4%	1.2
	Rack Assembly					54.1	17.6%	9.5
								49.8
	Total Average Maintenance Time							
	Ramp					25.1	100%	25.1
	Shop Level I					91.2	85%	77.5
	Shop Level II					60.2	69%	41.5
								144.1 or 2.42 hours

Table 3.2-11. (Sheet 2 of 2) Shop Maintenance Time Requirements - Level II Repairs Performed in Expanded Shop

The conceptual AC Fuel Cell Power System has been designed to assure simplicity with reliability of maintenance actions. Minimum time is required for ramp maintenance action as a result of the system self check capability and integral packaging. Maintenance at the shop level is flexible and expandable to the point where the user may become completely independent of the OEM for maintenance support when it proves to be economically beneficial.

3.2.3.3 Propellant Gas Utilization

Two advanced system goals identified by NASA relative to reactant utilization require improvements over existing hardware designs. These are operation with source pressures as low as 20 psia and use of propellant grade reactant purities.

Low Pressure Reactants

Two approaches for operating the system with 20 psia reactant feed pressures were evaluated; these are illustrated schematically in Figure 3.2-12. One approach is to operate the stacks at low pressure, compensating for the resulting low performance by adding extra cells; the other approach is to boost reactant pressure by means of compressors.

The effects of reactant pressure upon cell performance are shown in Figure 3.2-13. These curves are based on demonstrated volt-amp performance and demonstrated degradation rates of Allis-Chalmers fuel cell sections, at an age level of 2500 hours.

The curves show that a stack operating with reactant pressures of 13 psia requires 9% more cell sections (and consumes 9% more reactants) that a 37 psia stack at loads in the neighborhood of 100 amperes. These penalties will be counteracted by the weight, volume, and additional parasitic power consumption of the compressors and accumulators required to supply 37 psia reactants from a 20 psia source.

Compressor System Design

The power required for adiabatic compression is given by the following relationship:

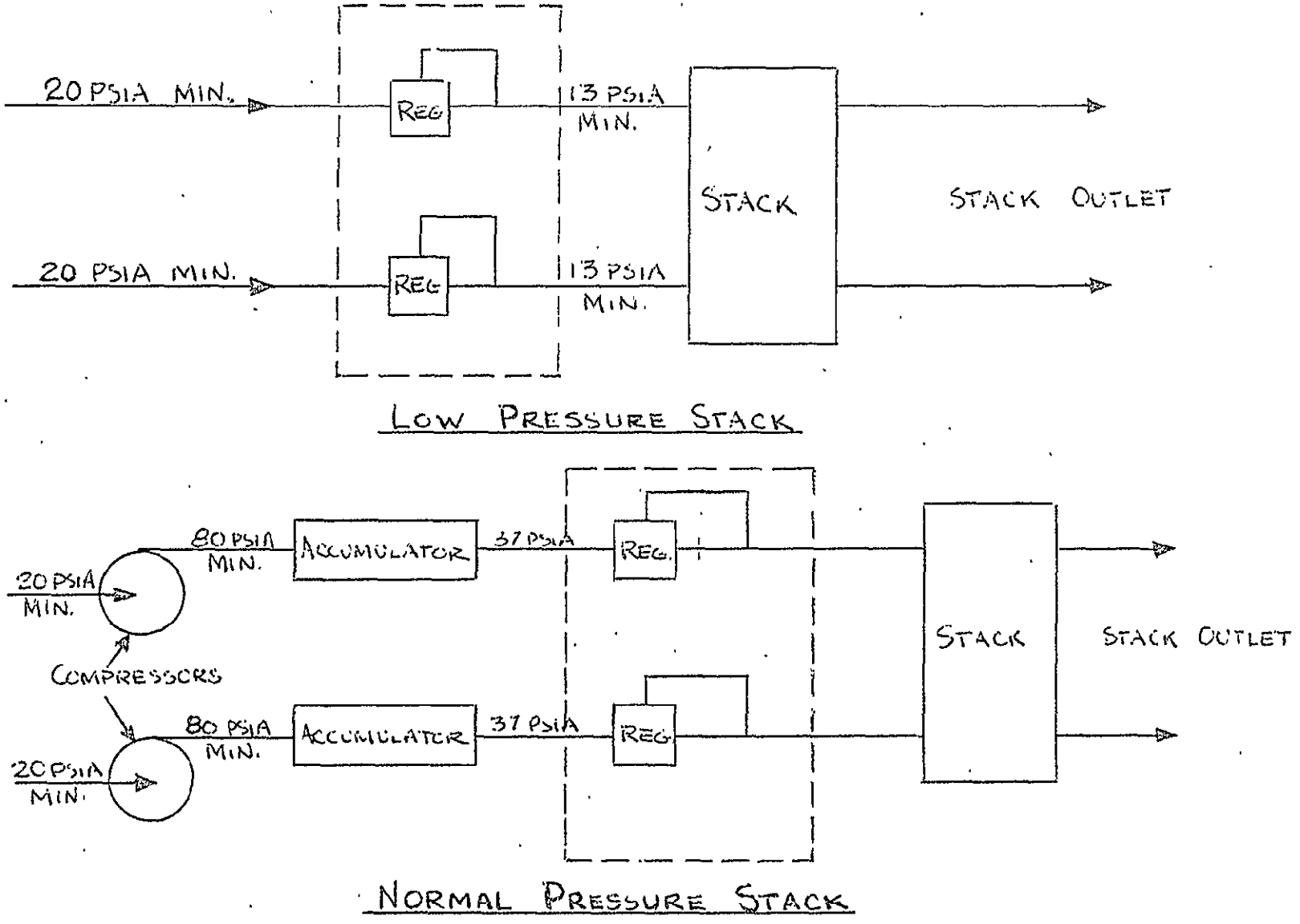

Figure 3.2-12. Simplified Schematics for Low Pressure Operation

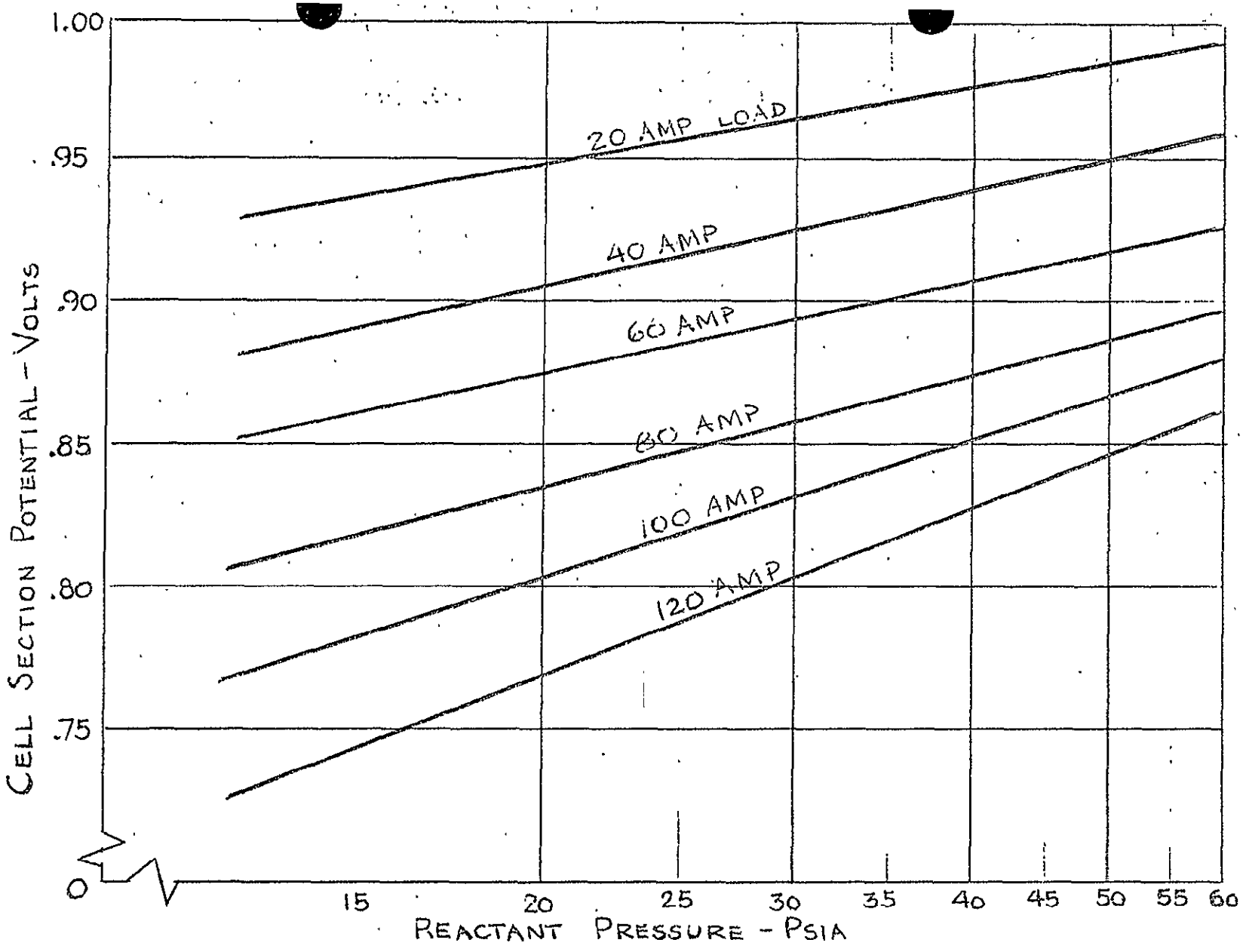

Figure 3.2-13. Pressure and Load Effects on Section Voltage

$$P = \dot{m}RT\left[\left(\frac{k}{k-1}\right)\left(r_p^{\frac{k-1}{k}} - 1\right)\ 3.77 \times 10^{-4}\right]$$

where:

P = compressor power, watts

$\dot{m}$ = gas flow rate, lb/h

R = gas constant, 766.4 for H_2, 48.3 for O_2

T = absolute gas temperature, °R

k = adiabatic exponent, 1.404 for H_2, 1.395 for O_2

r_p = discharge-to-intake pressure ratio

For a pressure ratio of 7.5, the quantity in brackets is 1.028×10^{-3}; for gas temperatures of 559°R (100°F), the power equation reduces to:

$P_{H_2} = 441.5\ \dot{m}$ for hydrogen and,

$P_{O_2} = 27.8$ in for oxygen

Correcting the above for non-adiabatic conditions (assuming compressore efficiencies of 80% for both gases) the compressor power equation is:

$$P_{Total} = 551\ \dot{m}_{H_2} + 34.8\ \dot{m}_{O_2}$$

For typical reactant consumption rates, the total power penalty for compressing reactants by a factor of 7.5 will be approximately 80 watts per kilowatt equivalent flow. The total reactant consumption is thus increased by 8% to provide for compressor parasitic power.

The compressor and accumulator sizes are derived from several interdependent considerations. These are listed below with the assumed quantitative goals and rationale for each criterion:

- Maximum Sustained Load - The compressors must have the capacity to provide for total fuel cell consumption at the maximum required steady

load. The maximum sustained load requirement for the "5 kw" system is 10 kW net, resulting in a total gross load of 11.1 kW (100 watts parasitic power plus 1000 watts compressor power).

- Maximum Accumulator Volume - The accumulator volume should not increase system volume by more than 50%. The packaging concept presently envisioned results in a 5 kW system volume of approximately 5 cubic feet; the total accumulator volume should, therefore, not exceed 2.5 cubic feet.

- Compressor Cycling - The number of compressor on-off cycles over the system design lifetime should be "reasonable"; a limit of 25,000 cycles in 3000 hours of operation is selected as a design goal. This consideration establishes the lower limit for accumulator volume, since a very small accumulator would fill and discharge rapidly, causing a large number of compressor cycles.

- Purge and Water Pumping Surges - The accumulator must be capable of handling flow surges required for fuel cell purging and operation of the water pump with O_2. Each hydrogen purge requires 0.0011 pounds of H_2 at 0.66 lb/h. A simultaneous oxygen purge and water pump cycle requires 0.0112 pounds of O_2 at 7.45 lb/h.

- Startup - The compressor/accumulator combination must reach design operating conditions within 10 minutes from start initiation.

- The 11.1kW operating point results in reactant flow rates of 1.22 lb/h hydrogen and 9.70 lb/h oxygen, which sizes the compressors in accordance with the first of the above criteria. The compressor/accumulator interactions are governed by the relationship:

$$pV = \dot{m}tRT$$

where:

p = accumulator pressure

V = accumulator volume

t = time

$\dot{m}$ = net accumulator flow rate

R and T are as defined previously

Differentiating the above expression with respect to flow rate at constant accumulator volume; we have:

$$(\Delta p)V = (\Delta \dot{m})\, tRT$$

where:

Δp = accumulator pressure rise during compressor on-cycle

$\Delta \dot{m}$ = compressor flow minus fuel cell consumption

The values of R and T are fixed for the two gases; the accumulator volume V is related to the remaining quantities Δp, t, and $\Delta \dot{m}$. The interdependence of these variables is plotted in Figures 3.2-14 and 3.2-15 with values for $\Delta \dot{m}$ of 0.61 lb/h for hydrogen and 4.85 lb/h for oxygen. These values of $\Delta \dot{m}$ are based on the following conditions for the compressor "on" cycle:

	Hydrogen		Oxygen
Compressor Flow, lb/h	1.22		9.70
Compressor Power, watts	675		338
Gross FC Power, watts		6113	
Consumption Flow, lb/h	0.61		4.85
Delta Flow, lb/h ($\Delta \dot{m}$)	0.61		4.85

These figures show that a compressor on-time of 3.5 minutes and an accumulator Δp of 67 psi correspond to accumulator volumes of 1.60 cu. ft. for H_2 and 0.80 cu. ft. for O_2. The pressure decay time during the "off" position of the compressor duty cycle is as follows for the 67 psi Δp:

	Hydrogen		Oxygen
Gross FC Power, watts		5100	
Consumption Flow, lb/h	0.490		3.90
Pressure Decay Time, minutes	4.3		4.3

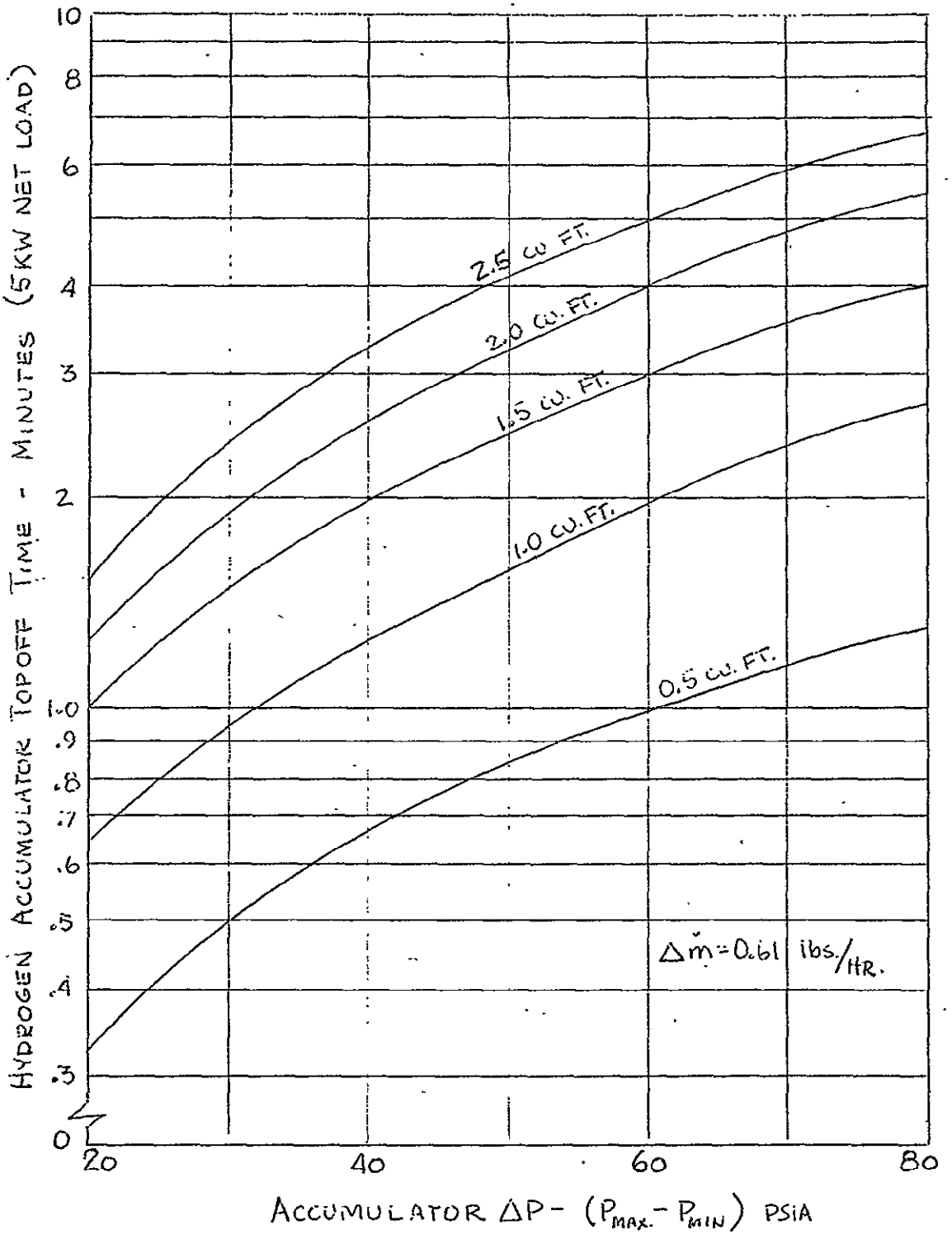

Figure 3.2-14. Hydrogen Accumulator Characteristics

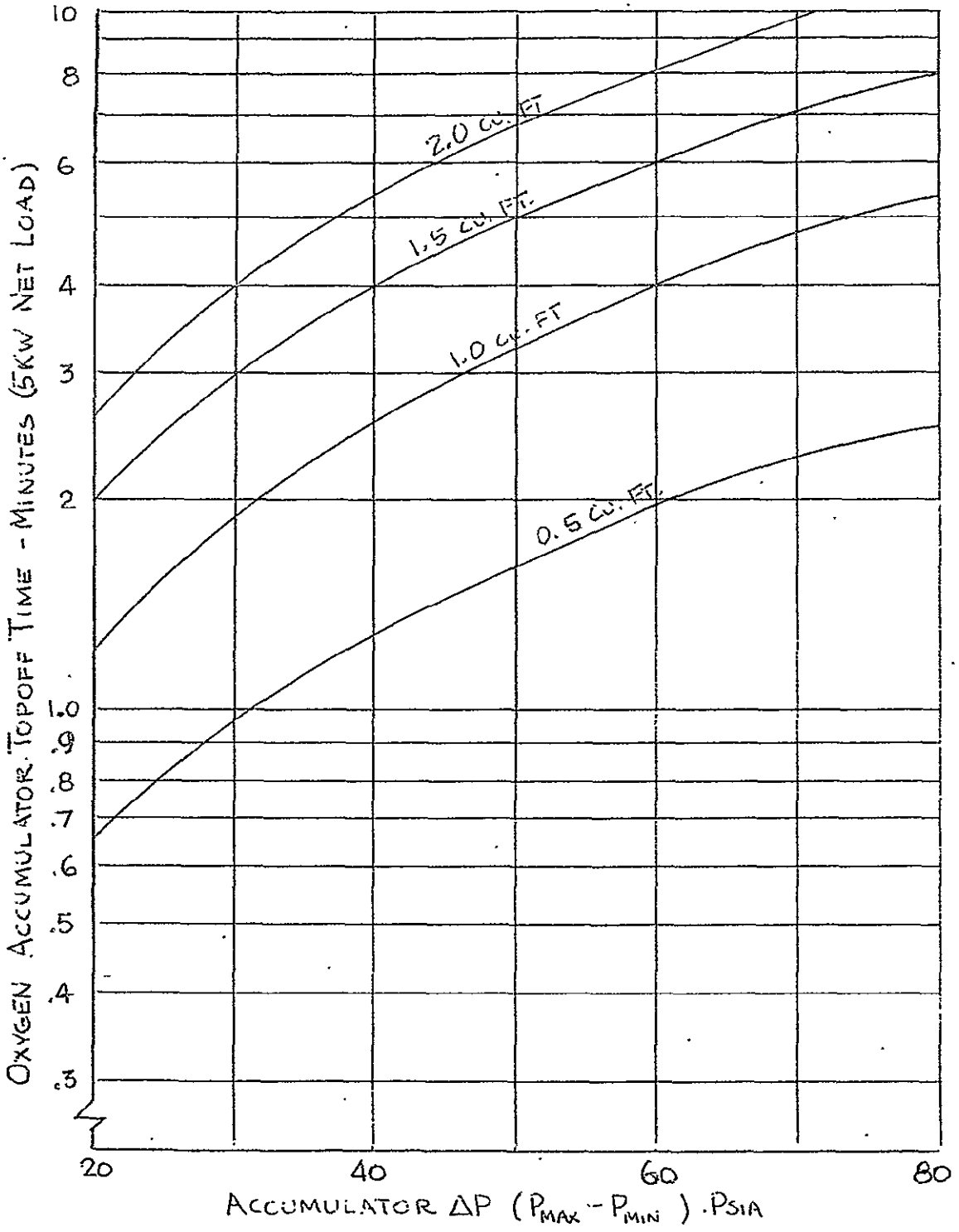

Figure 3.2-15. Oxygen Accumulator Characteristics

The overall cycle time on the compressors is, therefore, 7.8 minutes, resulting in a total of 23,000 cycles in 3000 hours.

With a source pressure of 20 psia and a compression ratio of 7.5, the maximum accumulator pressure (at compressor shutoff) is 150 psia. The 67 psi accumulator Δp results in a minimum steady state accumulator pressure of 83 psia. The gas quantities in the accumulators at this pressure are 0.0507 pounds of H_2 and 0.404 pounds of O_2. The purge and water pumping gas quantities are less than 3% of these values, and hence do not impose low-pressure spikes of any significance on operation of the system; reactant regulator inlet pressure will remain above 79 psia under all normal operating modes. This condition is adequate to supply the stacks with properly regulated 37 psi reactants.

Startup time for the compressor/accumulator assembly sized as described above is determined from

$$t = \frac{V \Delta p}{RT \Delta \dot{m}}$$

The quantitative values are:

	Hydrogen	Oxygen	
V, ft^3	1.60	0.80	
Δp, psi	130	130	Initial 20 psia, Final 150 psia
$\Delta \dot{m}$	1.22	9.70	
R, T	as defined earlier		

Using these values, the startup time is within 3.5 minutes.

Weight and volume estimates for the compressors and accumulators defined in the above design analysis are as follows:

	Hydrogen		Oxygen	
	Weight lb	Vol., ft^3	Weight lb	Vol., ft^3
Compressor	12.7	0.19	10.0	0.16
Accumulator Vessel	7.0	1.6	3.6	0.8
Hardware & Plumbing	0.8	0.6	0.8	0.5
Subtotal	20.5 lb	2.29 ft^3	14.4 lb	1.46 ft^3
Total	34.9lb		3.75 ft^3	

System Comparison

The compressor system incurs overall weight and volume penalties compared to the low-pressure system. Furthermore, the addition of a compressor/accumulator assembly would decrease system reliability. With the above disadvantages and no apparent advantages, the use of as-delivered low-pressure reactants without pressure boosting, clearly seems to be the preferred approach. However, the NASA requirement for operation with low reactant purities as well as low pressure imposes additional constraints which must be evaluated. The next section considers low-purity operation in the light of the operating pressure level in order to permit an integrated conclusion as to the combined effects of propellant gas utilization.

Propellant Purity Reactants

This section deals with system configurations and operational modes for using reactant gases of propellant-grade purity. Since use of low purity reactants is a departure from prior Allis-Chalmers aerospace fuel cell requirements, a brief review of the fundamentals of reactant purging is presented to serve as a point of departure from which to evaluate alternate impurity management techniques.

Purging Fundamentals

Fuel cell reactants invariably contain some inert gaseous impurities. These inert gases enter the cells along with the reactants. Since the inerts are not consumed by

the fuel cell reaction, they accumulate over a period of time. Accumulation of inert gases causes a decrease in cell performance by blocking a portion of the electrode or, if the cell contents are adequately mixed, by dilution of the reactants. In general, dead-ended operation of the fuel cell will lead to the former condition.

In order to maintain acceptable cell performance, it is necessary to periodically purge the accumulated inert gases from the cells. If the cell is not purged, it will eventually become filled with inerts and be unable to support a load.

When a cell is purged, useful reactants are vented from the cell along with the impurities. This loss of reactants represents a reactant utilization penalty, and effort must be made to maintain losses within acceptable limits.

In a practical power system, purging is accomplished automatically according to a predetermined purge program. The purge program must maintain acceptable levels of inert gases within the cells (to prevent loss of system performance) and must minimize the loss of useful reactants. The factors affecting specification of the purge program parameters (purge interval, duration, and flow rate) are discussed in the following paragraphs.

The total quantity of inert gases contained in a single operating cell can be calculated from knowledge of the inlet gas purity and the number of amp-hours produced by the cell. The total quantity of inert gases contained in a multicell module can also be determined from the same data. However, the distribution of inerts among the cells in the module is not, in general, uniform. Each cell is fed reactants from a common manifold and is ported to a common purge manifold. The cells and manifolds form a flow resistance network as illustrated in Figure 3.2-16A. Any variation among the resistances will cause cell-to-cell flow of reactants via the purge manifold. Cells with higher flow resistance will receive some reactants from the manifold; cells with lower resistance will vent some reactants to the manifold.

Although back-flow of reactants into a cell may be small, the gas in the purge manifold will be relatively rich in inert gases, and will contribute markedly to the accumulation of inerts in the high-resistance cell. In the limiting case where all cells have the same

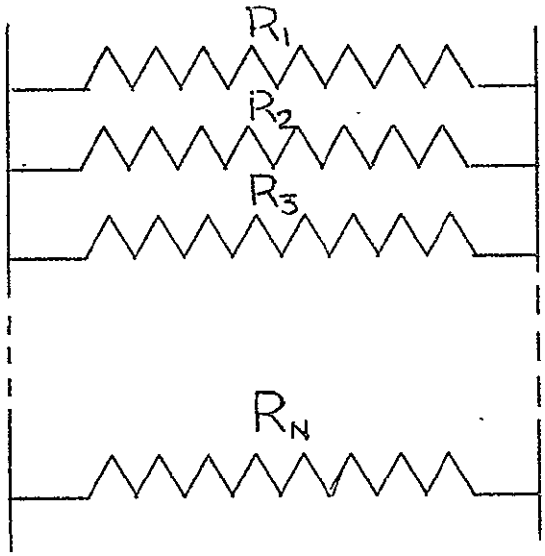

A. Module Flow Resistance Network

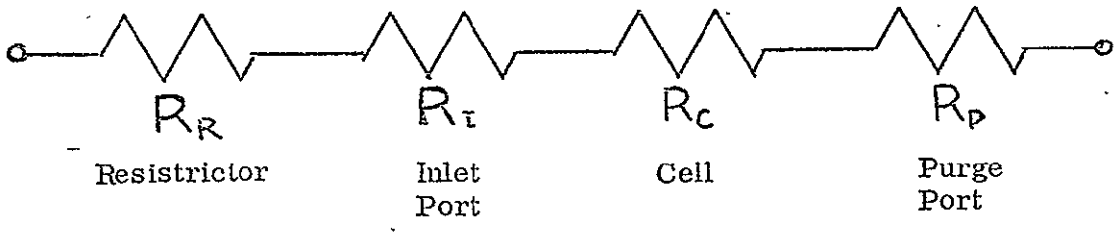

B. Cell Flow Resistance Components

Figure 3.2-16. Flow Resistance Networks

flow resistance except one, which has a higher resistance, essentially all of the inert gases entering the module would accumulate in the high-resistance cell. The purge interval could be set to accommodate this "worst-case" condition. However, this would result in unnecessarily high losses of reactants since real modules will exhibit variation of flow resistance among the cells, and hence will tend to distribute the inerts among more cells.

In order to treat realistic cell flow resistance distributions, a Quicktran computer program was developed to determine the net flow through each purge port for a specified flow resistance network. This program has been used to investigate a number of resistance networks and purge flow requirements. The resistances for each flow path is considered to consist of four series resistances as indicated in Figure 3.2-16B.

Inlet port and purge port resistances are relatively small, and are assumed to be the same for all cells. Flow resistance of the reactant distribution channels in the cell plate is assumed to vary over a range of ±25% for a new stack. Physical changes in the cell geometry can occur over the operating life of the cells, due to such factors as electrode swelling, plate corrosion, and liquid film formation. These changes can affect the purge characteristics of the module by increasing the flow resistance of certain cells. The high-resistance cells accumulate inerts faster than other cells in the module, and the purge interval must be selected to prevent excessively high inert concentrations in these cells. In addition, the high-resistance cells will receive the least reactant through-flow during a purge, and the duration of the purge must be selected to assure adequate removal of the inerts.

Flow variation among cells of unequal resistance is shown in Figure 3.2-17.

Tables 3.2-12 and 3.2-13 present actual cell pressure drop variations for a multicell 2 kW stack (EDS-1). Table 6 shows the beginning-of-life O_2 plate pressure drops, with a variance on the order of ±30% of nominal. Performance of the same cells after 3000 hours of stack operation is shown in Table 7. Leakage of reactant around some of the restrictors is evident from the low pressure drops in some of the cells, distorting the data; however, the behavior of cells 4, 10, 11, and 12 does illustrate a significant increase in

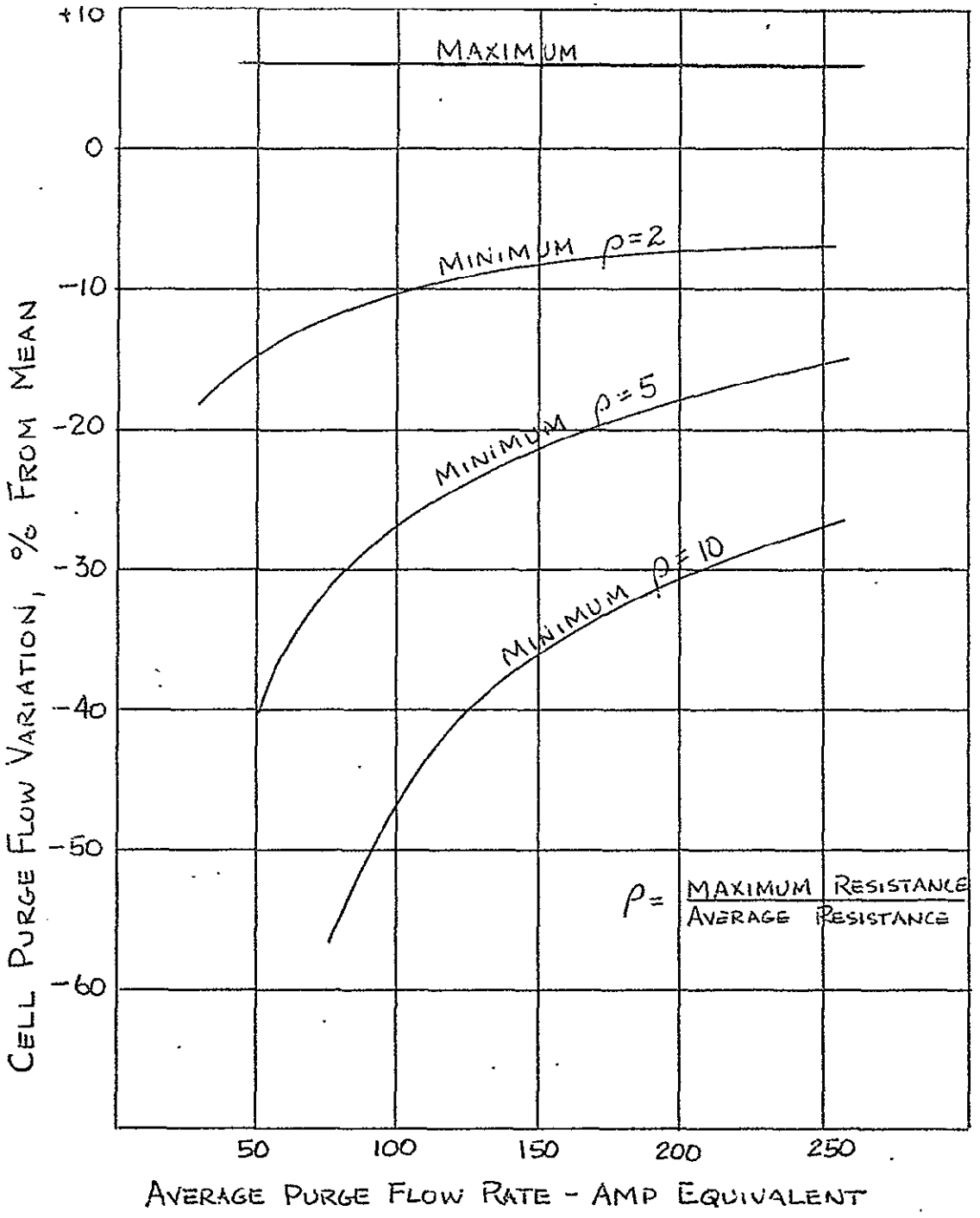

Figure 3.2-17. Oxygen Purge Flow Variation (Cell to Cell)

the max-to-average flow resistance ratio with operating time. Based on these data, a max-to-average resistance of 5 is appropriate for oxygen purge design.

Similar experience with hydrogen shows that the H_2 plate flow resistance tends to remain more nearly at the initial value. This is explained as being due to less corrosive conditions in the hydrogen atmosphere. The design value for the max-to-average H_2 flow resistance ratio is 2.

[redacted]ing the above flow resistance variances, the purge flow rates and durations can be determined. Figures 3.2-18 and 3.2-19 illustrate the worst-cell flow rate as a function of total stack purge flow. The duration required for one complete volume exchange at these flow rates is also indicated. Minimum allowable flow rate for each reactant is determined by the requirement for sufficient pressure differential to clear a cell port blocked with liquid film. These minimum flows correspond to stack H_2 purge flows of approximately 220 amps equivalent and O_2 purge flows of 140 amps equivalent. Including a 20% flow margin, the minimum flows are 264 and 168 amp equivalent for H_2 and O_2, respectively. From Figures 3.2-18 and 3.2-19, the required purge durations at these flows are 3.8 seconds for H_2 and 5.7 seconds for O_2.

It will be noted that the purge flow and duration design values are independent of inlet gas purity. The remaining variable, purge interval, has major impact on the reactant consumption penalty for purging and is a strong function of purity.

The required purge interval for the 2 kW cell geometry, considering flow imbalance effects and the resulting back-feed of inerts from the manifold to high resistance cells, has been determined and is shown on Figure 3.2-20. The dependence of purge interval upon operating pressure is included in the Figure.

Cell Number	ΔP (psi) at 150 AMP Equiv. Flow	ΔP (psi) at 250 AMP Equiv. Flow
1	.21	.525
2	.135	.345
3	.205	.525
4	.18	.425
5	.16	.415
6	.215 max., 1.30 x avg.	.550 max., 1.315 x avg.
7	.16	.395
8	.16	.390
9	.15	.390
10	.16	.415
11	.16	.410
12	.17	.420
13	.185	.470
14	.12 min., .728 x avg.	.310 min., .741 x avg.
15	.14	.365
16	.19	.510
17	.165	.425
18	.21	.540
19	.16	.410
20	.19	.480
21	.21	.360
22	.175	.440
23	.145	.345
24	.16	.415
25	.14	.345
26	.165	.435
27	.21	.345
28	.175	.410
29	.16	.425
30	.15	.360
31	.175	.445

Table 3.2-12. Oxygen Plate Pressure Drops, With Restrictors EDS-1 At Acceptance Test

Cell Number	ΔP (psi) at 150 AMP Equiv. Flow	ΔP (psi) at 250 AMP Equiv. Flow
1	.294	1.11 max., 2.66 x initial avg.; 2.96 x 3000 h avg.
2	.172	.75
3	.24	.58
4	.77 max., 4.66 x initial avg.; 4.48 x 3000 h avg.	1.05
5	.04	.11
6	.06	.14
7	.11	.22
8	.62	.96
9	.09	.22
10	.45	.92
11	.57	1.06
12	.47	.99
13	.12	.27
14	.10	.21
15	.11	.23
16	.18	.34
17	.04	.12
18	.08	.18
19	.21	.45
20	.17	.35
21	.03 min., .182 x initial avg.	.08
22	.10	.24
23	.04	.11
24	.07	.16
25	.03 min., .182 x initial avg.	.06 min., .143 x initial avg.
26	.09	.20
27	.03 min., .182 x initial avg.	.08
28	.05	.11
29	.03 min., .182 x initial avg.	.08
30	.09	.17
31	.04	.07

Table 3.2-13. Oxygen Plate Pressure Drops, With Restrictors EDS-1 at 3012 Hours

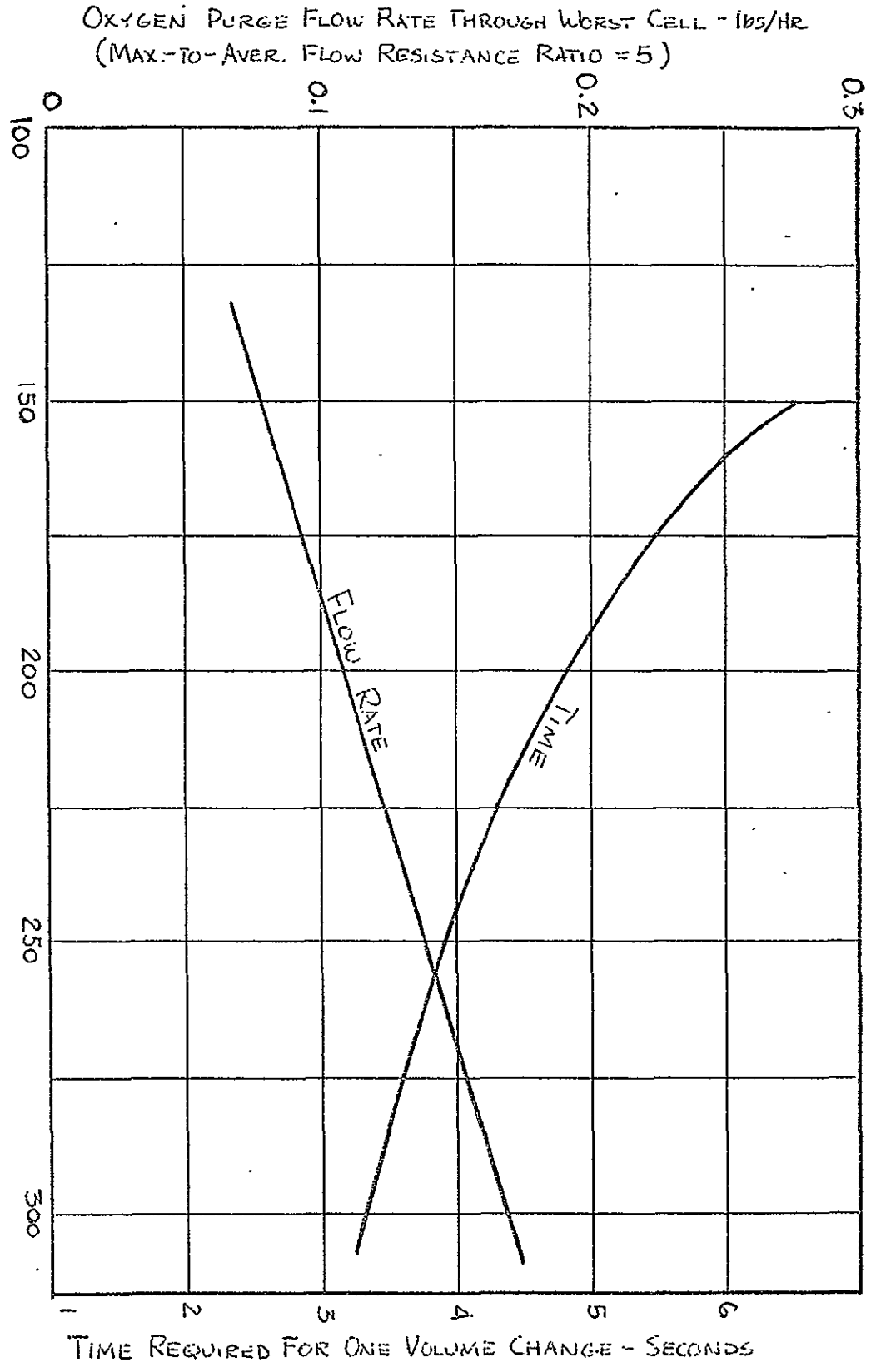

Figure 3.2-18. Oxygen Purge Flow and Duration Relationship

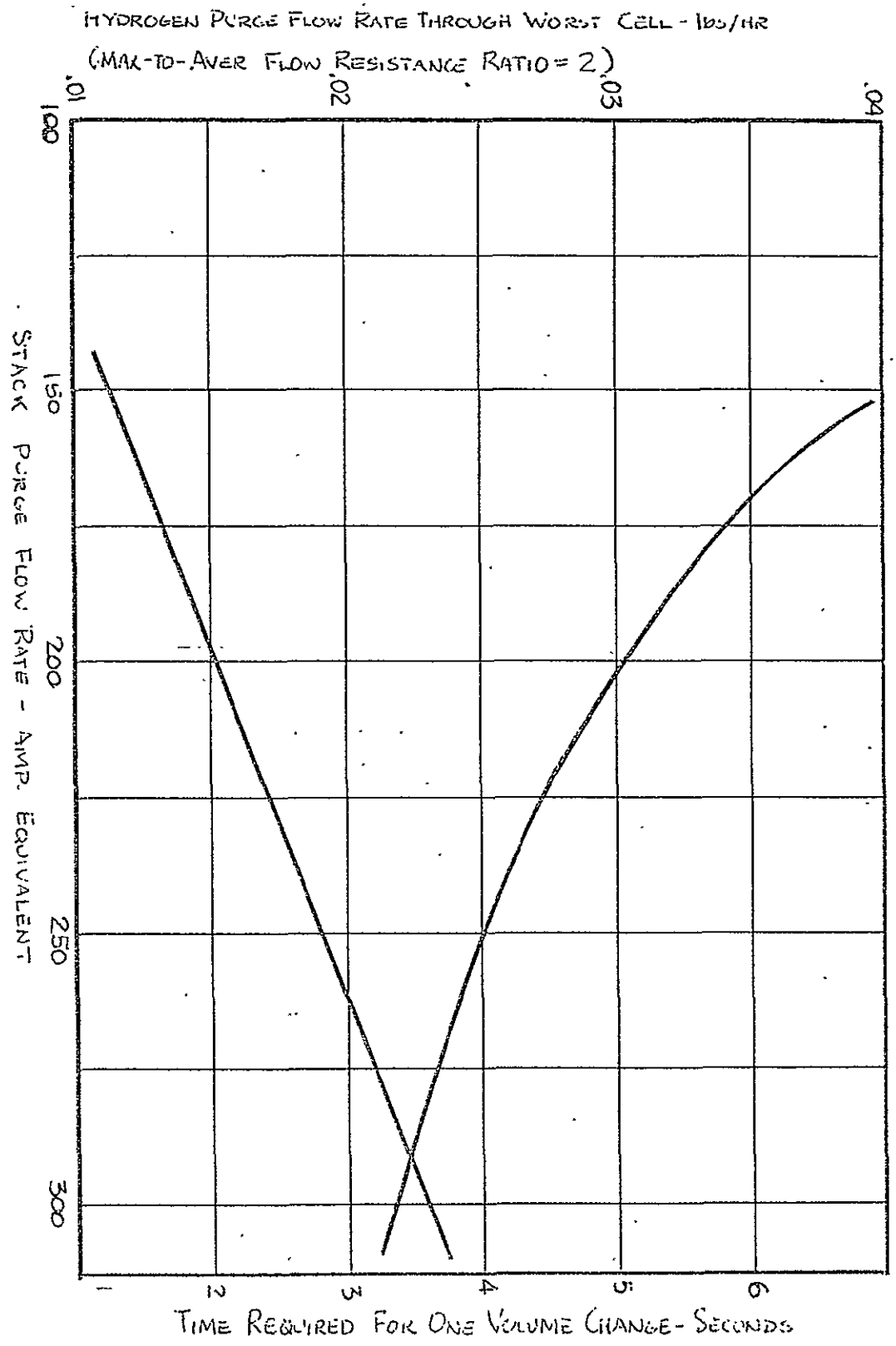

Figure 3.2-19. Hydrogen Purge Flow and Duration Relationship

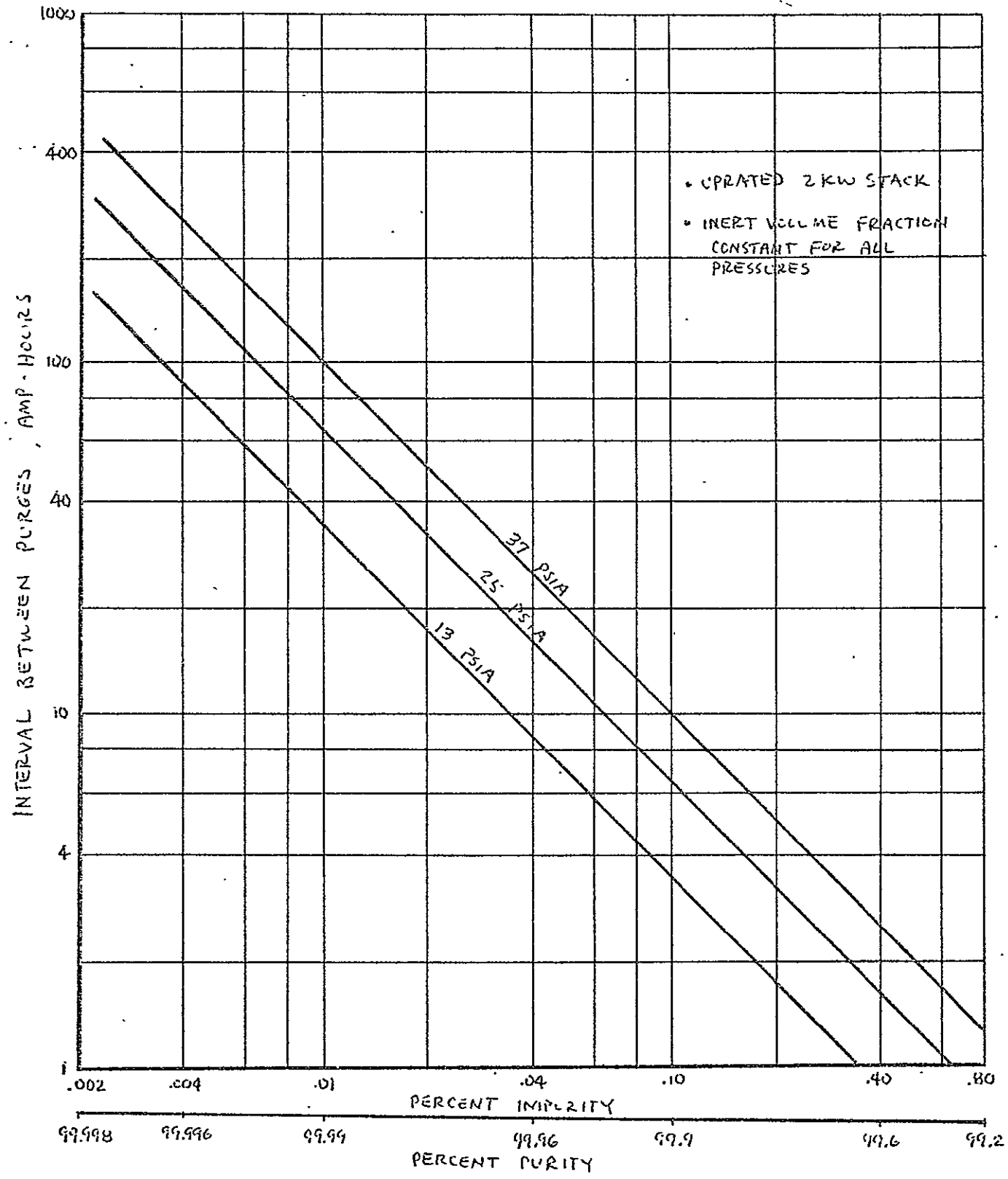

Figure 3.2-20. Purge Interval versus Purity

The overall penalty for purging can be determined from the data presented thus far. In prior space fuel cell applications, the specified reactant purities generally have been high enough to permit the use of conservative purge programs without incurring significant reactant weight penalties. As an example, the minimum purge requirements as derived above are compared with the AAP fuel cell purge parameters in the following table.

	Minimum Requirement		AAP Design	
	H_2	O_2	H_2	O_2
Specified Purity, %	99.995	99.995	99.995	99.995
Purge Interval, A-H	200	200	128	128
Purge Flow, Amp Equiv.	264	168	290 (.75 $\frac{lb}{hr}$)	270 (5.5 $\frac{lb}{hr}$)
Purge Duration, sec.	3.8	5.7	6	6
Purge %, $\frac{Qty.Purged}{Qty.Reacted} \times 100$	0.14%	0.14%	0.38%	0.37%

The conservative approach used for AAP was thus still very practical at the high specified purities, in terms of reactant quantity utilization.

For space shuttle type applications, reactant purities commensurate with the use of residual propellant gases must be accommodated. These are shown in the table below:

O_2	– MIL-P-25508D	
	Purity	0.995
	Total Hydrocarbons	66.7 ppm as Methane
	Moisture	26.3 ppm
	Remainder unspecified but found to be mainly Argon	
H_2	MIL-P-27201	
	Purity	0.99995
	Same as ultra pure	

NOTE: ppm by volume

With these specified purities, prior experience remains applicable to hydrogen purging while oxygen purging clearly requires further treatment. Five methods have been evaluated for O_2 purge management; these are shown in simple schematic form in Figure 3.2-21 and are discussed below.

Increased Purge Frequency

The standard purging technique used for relatively pure reactants can be applied to propellant grade reactants; the weight penalty for purge gas becomes appreciable at decreasing purities, however. For O_2 of 99.5% purity, the purge penalty is from 14 39% of the quantity required for reaction, depending upon operating pressure. The combined consumption for reaction and purge is plotted in Figure 3.2-22, illustrating the severity of the purge penalty at purities worse than 99.9%.

In addition to the reactant weight penalty, water removal by the purge gas becomes appreciable and will increase the probability of cell dryout and cross leaks unless compensated for by reactant prehumidification. The following table shows this effect quantitatively.

Operating Pressure, psia	37		13	
System gross power, kW	2.5	5.0	2.5	5.0
O_2 Purge flow rate, lb/h/stack	3.72(1)	3.72	3.93(2)	3.93
No. purges/h/stack	20	42	54	116
H_2O removed by purging, lb/h/stack	0.0078	0.0165	0.0212	0.0455
H_2O produced by reaction, lb/h/stack	0.96	2.06	1.04	2.18

(1) 33 sections per stack

(2) 35 sections per stack

The data in the table shows that 1 to 2% of the product water must be retained in the stacks to offset the drying effects of the high purge duty cycle. The large number of purge valve operating cycles is also evident in the table.

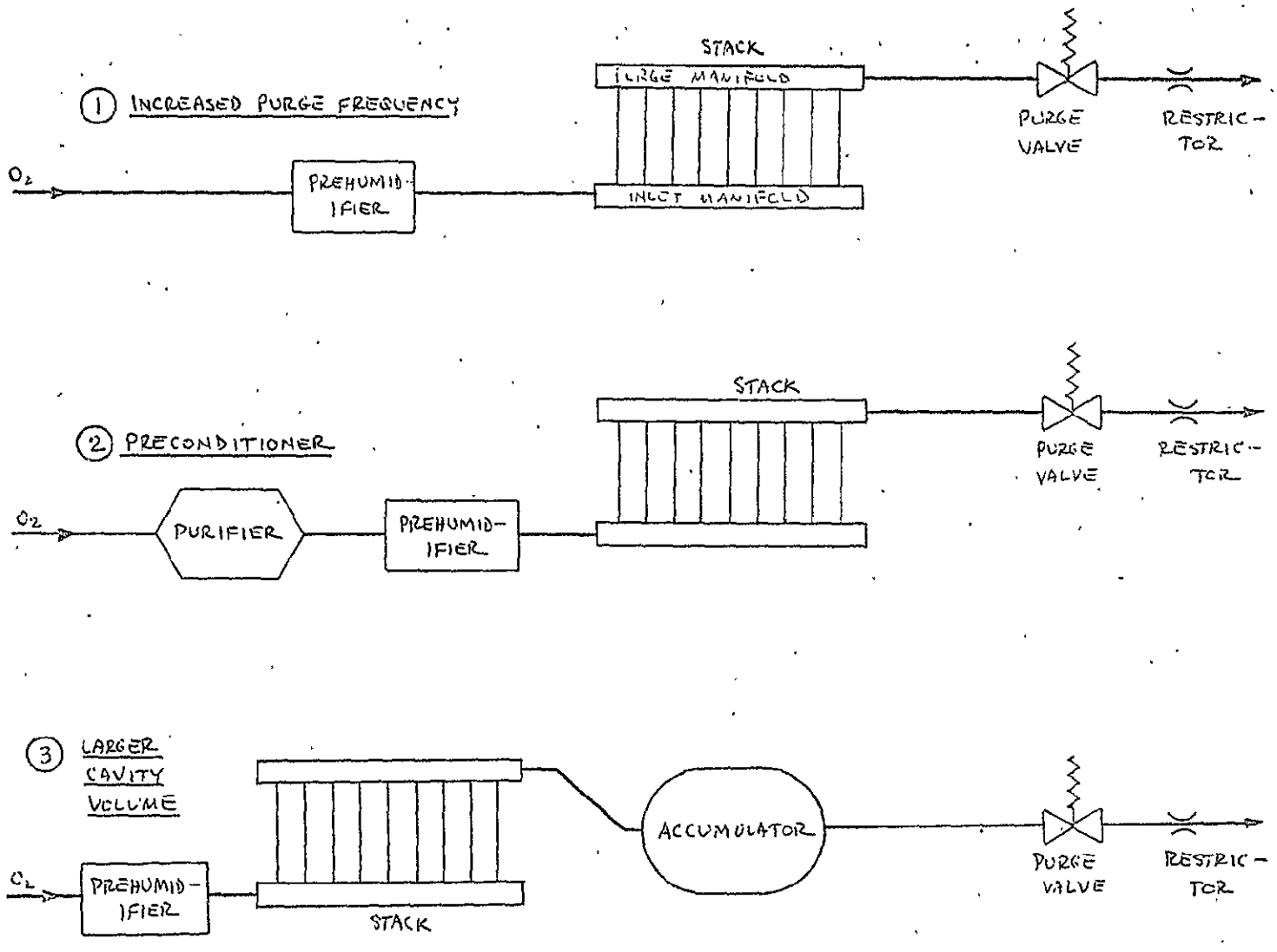

Figure 3.2-21. (Sheet 1 of 2). Techniques for Low Reactant Purity Operation.

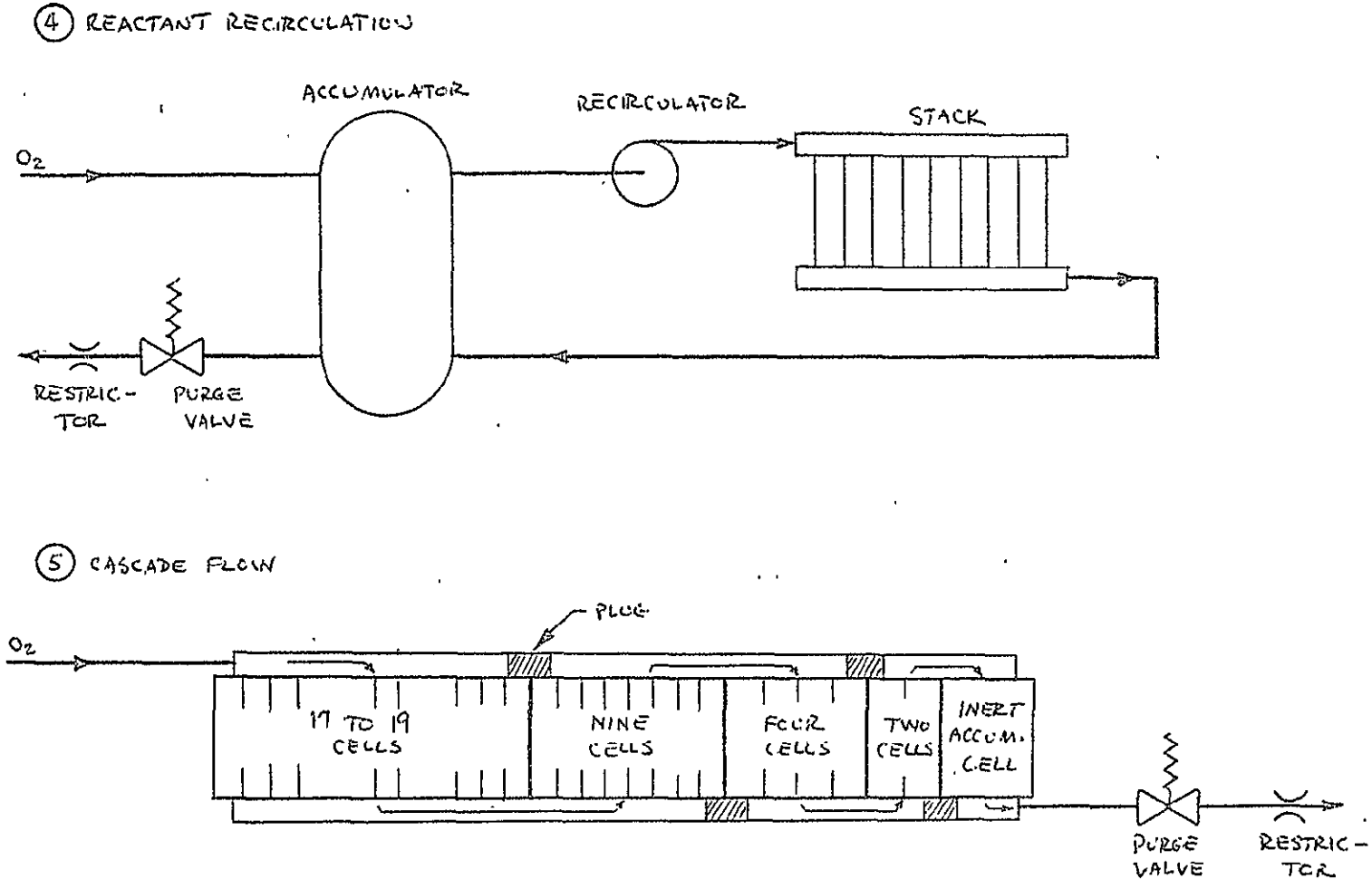

Figure 3.2-21. (Sheet 2 of 2). Techniques for Low Reactant Purity Operation

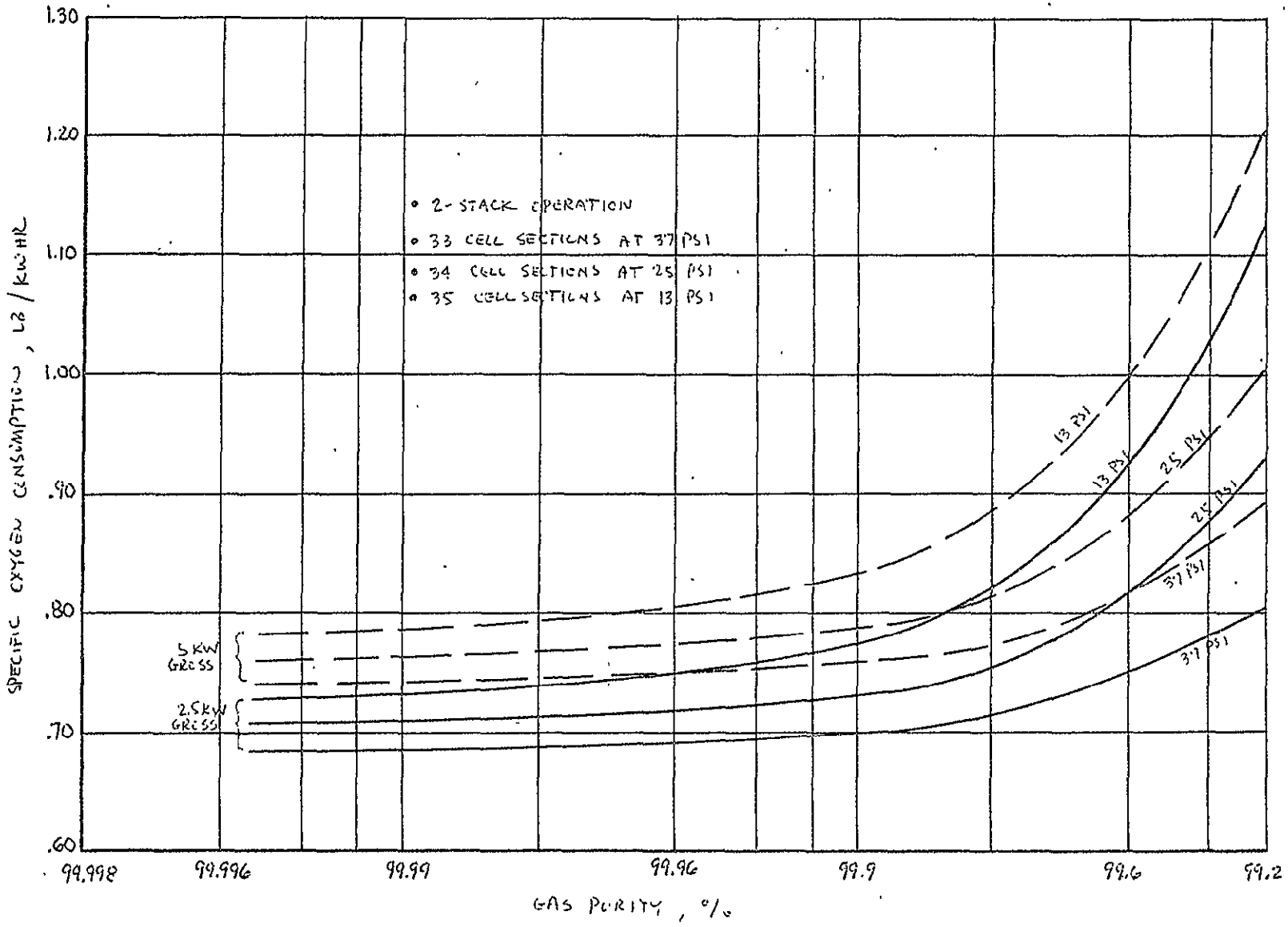

Figure 3.2-22. Effects of Gas Purity and Pressure on O_2 Consumption

Preconditioner

Oxygen can be supplied to the fuel cell stacks at a purity higher than the inlet purity by means of a purifier at the system inlet. The figure below illustrates the flow concept for delivering gas of various purities with a fixed purity at the inlet:

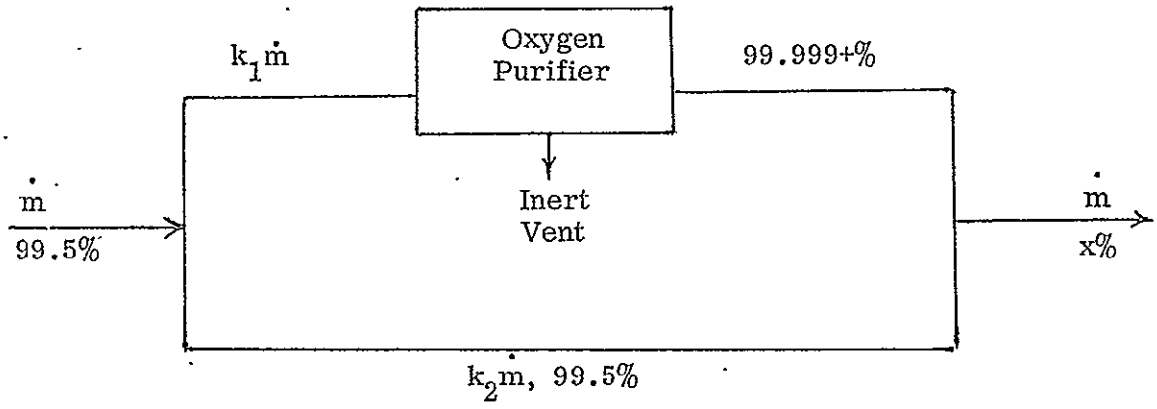

For an inlet purity of 99.5%, the flow split coefficients are as follows for various stack purities:

X = Stack Purity	k_1	k_2	Impurities to Stack, ppm
99.5	0	1.0	5000
99.6	0.2	0.8	4001
99.75	0.5	0.5	2502
99.9	0.8	0.2	1004
99.95	0.9	0.1	505
99.975	0.95	0.05	255
99.99	0.98	0.02	105
99.995	0.99	0.01	55
99.997	0.995	0.005	30

The overall O_2 Consumption of the purifier approach varies with stack purity as discussed in the previous section and also with the power consumption characteristics of the purifier device. Figure 3.2-23 depicts the total O_2 usage for two gas pressures and three sets of purifier power levels. The curves show significant reactant usage penalties unless purifier power consumption is on the order of 250 watts per pound/hour of O_2 purified. Since the state-of-the-art for O_2 concentration (electrowinning) techniques is on the order of 1200 watts per pound/hour of O_2 processed, the gas consumption inefficiency of this method for using propellant purity oxygen is apparent. Its chief advantage is the reduction in purge frequency and cell drying effects discussed earlier.

Larger Cavities

The amp-hour interval required to reach a given inert volume fraction in the cell cavities can be extended by increasing the total cavity volume: an N-fold increase in total volume permits an N-fold increase in the purge interval. The flow resistance effects, discussed previously, remain applicable as long as the connection between the purge manifold and accumulator permits adequate diffusion of inerts into the accumulator without large concentration gradients.

While the purge interval varies with total cavity volume, total reactant loss due to purging is not improved by the added volume, because the duration of each purge must be increased to achieve a complete volume exchange of gas. The oxygen consumption at 2.5 kW for an increased cavity volume system using 99.5% pure oxygen is thus 0.770 lb/kWh at 37 psi and 0.978 lb/kWh at 13 psi.

Reactant Recirculation

A fourth method of low-purity reactant management is to continuously recirculate the gas through a mixing chamber in a closed loop, purging the loop periodically as required.

The gas recirculation has the advantage of equalizing inert buildup among all of the cells. The purge interval can thereby approach the theoretical value for equal inert volume fractions in all cells, which is an order of magnitude longer than the interval required

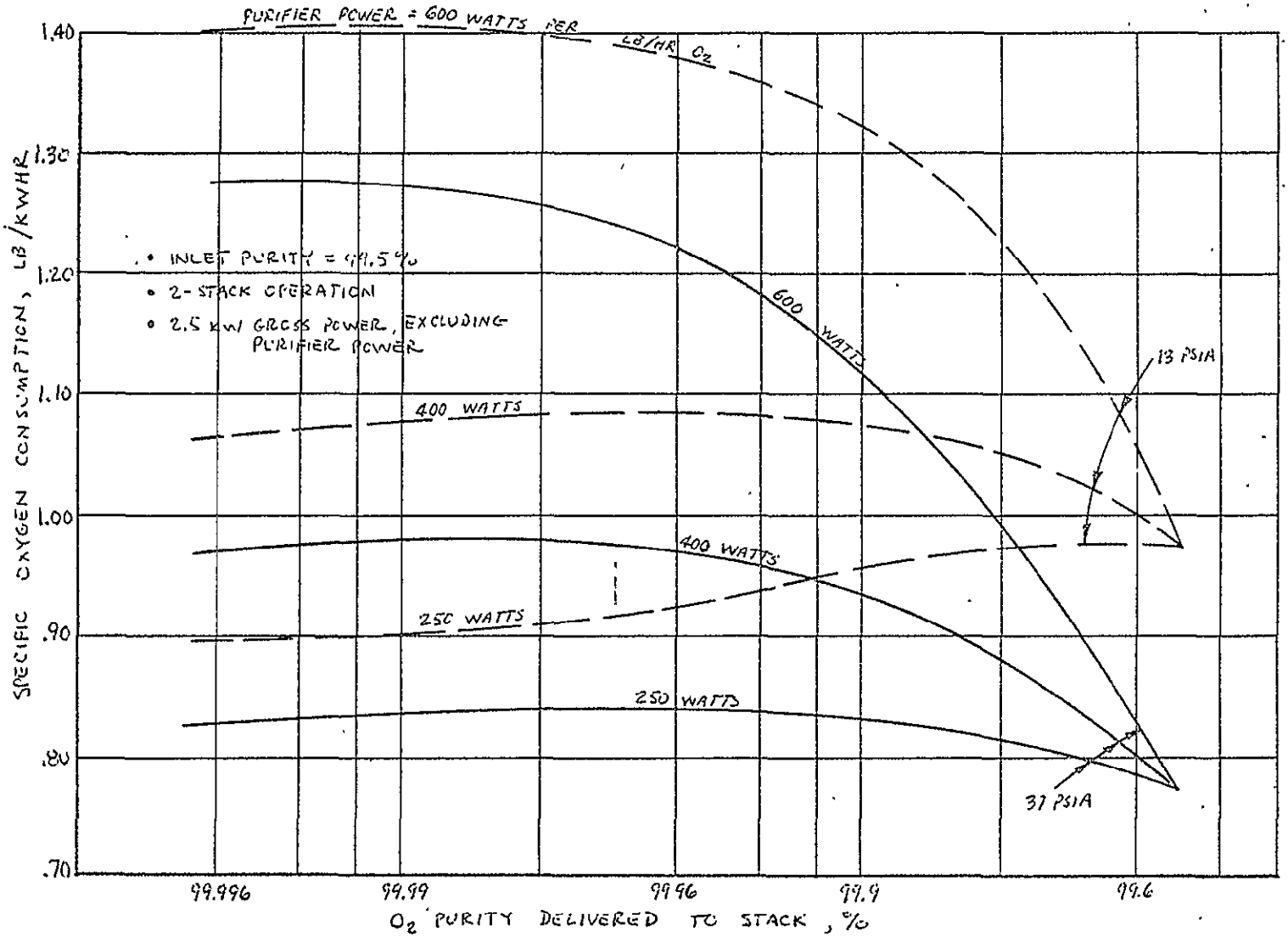

Figure 3.2-23. Oxygen Consumption Characteristics with Purifier

for unequal distributions. Thus for any given inlet purity, the purge interval and purge quantity for a recirculating system are improved ten-fold over that of a static system of equal cavity volume. Specific O_2 consumption of a recirculated system with 99.5% inlet purity at 2.5 kW output is 0.694 lb/kWh at 37 psi and 0.754 lb/kWh at 13 psi.

Cascade Flow

A continuous reactant flow through the cells can be achieved with an inert accumulator cell and the manifold path shown in Figure 3.2-21. This arrangement provides each normal cell with 1.5 to 2 times the flow required for consumption, sweeping the incoming inerts into the accumulator cell volume.

The purge interval for this design is proportional to the volume of the accumulator cell rather than the total stack plus accumulator volume. The total purge gas usage is independent of the accumulator volume but is always less than that of the recirculating reactant system. For a 2.5 kW output, O_2 consumption is 0.685 lb/kWh at 37 psi and 0.728 lb/kWh at 13 psi.

With the cascade flow arrangement, purging can be controlled by periodically switching the accumulator cell to a fixed load and measuring its performance dropoff as inerts build up. This permits the system to adapt to varying inlet reactant purities without adjustment.

Comparison of Purity Management Approaches

From the above discussion, the use of a purifier can be eliminated from further consideration. It offers no reactant consumption improvement, requires additional interfaces for purifier power input and inert vent, and adds additional fixed weight for the purifier itself. The remaining four options for utilization of 99.5 % pure O_2 are compared in Table 3.2-14. Approaches B, C, and D are sized on the basis of equal volume added to the stacks. The total oxygen required for 200 hours at 2.5 kW average is included to illustrate typical mission reactant weight. Methods A and B are characterized by significant reactant weight penalties and short purge intervals. The corresponding high purge valve duty cycles and cell drying effects make these two

	A Increased Purge	B Larger Cavities	C Recircu-lation	D Cascade Flow
Δ Volume, in^3 per Stack				
37 psi	0	85 (2 x stack O_2 vol.)	85	85
13 psi	0	180 (4 x stack O_2 vol.)	180	180
Purge Interval, Amp-h per Stack				
37 psi	2.0	6.0	60	40
13 psi	0.7	3.5	35	28
O_2 Consumption, lb/kWh at 2.5 kW				
37 psi (33 sections)	0.770	0.770	0.694	0.685
13 psi (35 sections)	0.978	0.978	0.754	0.728
System Δ Weight, lb*				
37 psi	0	2.75	3.75	1.30
13 psi	0	3.60	4.60	2.30
Mission O_2 Weight, lb (200 hour mission at 2.5 kW)				
37 psi	385	385	347	343
13 psi	489	489	377	364

*Includes accumulator and recirculator weights as applicable, for two stacks; does not include Δ weight of extra cell sections for 13 psi system.

Table 3.2-14. Comparison of Low Purity O_2 Management Systems

options undesirable relative to methods C and D. The purge intervals for C and D are in an acceptable range from valve cycling and cell drying standpoints. The cascade flow approach shows a slight advantage in hardware and reactant weight, and offers the additional advantages of its passive nature (no recirculator required) and its isolation of impurities by entrapment rather than continuous recirculation through all of the cells. For these reasons, the cascade flow technique is the preferred method for using low-purity reactants in advanced fuel cell applications.

Conclusions

Considering the combined effects of reactant source pressure and purity, the overall system concept for utilizing propellant gases as fuel cell reactants can be finalized. From the foregoing section, a cascade flow/accumulator cell design is preferred for utilization of low-purity oxygen at all pressures in the range of interest. A comparison of the significant features of a pressure-boosted system and a low-pressure system, both using the selected purge technique, is given in Table 3.2-15. The table shows the low-pressure system to be superior on the basis of weight and volume. Even if the reactant weights and volumes are considered "free", i.e. residuals that will be lost if not used by the fuel cells, the pressure-boosted system is at a disadvantage. Cost and reliability factors also favor the low-pressure system.

The preferred design for utilization of propellant grade reactants, then, is as summarized below:

Selected Propellant Utilization System Characteristics

	H_2	O_2
Supply Pressure, psia	20	20
System Operating Pressure, psia	13	13
Supply Purity, %	99.995	99.50
Purge Technique	Amp-Hour Count	Cascade Flow & Accumulator Cell
Accumulator Cell Volume, in^3	N/A	180
Purge Interval, Amp-hours	70	28
Reactant Consumption at 2.5 kW net, lb/h	0.244	2.025
Number of Cell Section per Stack	36	

	Pressure Boosted System		Low Pressure System	
Operating Pressure, psia	37		13	
No Cell Sections/Stack	34		36	
Average Net Power, Watts	2500	5000	2500	5000
Average Gross Power, Watts	2820	5535	2600	5100
H_2 Consumption, lb/kWh	0.0890	0.0970	0.0941	0.1020
O_2 Consumption, lb/kWh(1)	0.721	0.786	0.779	0.844
Average Reactant Flow, lb/h	2.28	4.88	2.27	4.82
WEIGHTS:				
Stack Δ Weight, lb(2)	9.1	9.1	17.9	17.9
Compressors/Accumulators, lb	34.9	34.9	-	-
Reactants for 200 h, lb	456.0	976.0	454.0	964.0
Net Δ Weight, lb	+28.1	+38.1		
VOLUMES:				
Stack Δ Volume, ft^3(3)	0.144	0.144	0.306	0.306
Compressors/Accumulators, ft^3	3.75	3.75	-	-
Reactants for 200 h, ft^3	17.75	38.00	17.70	37.60
Net Δ Volume, ft^3	+3.63	+3.98		

(1) Based on cascade flow/accumulator cell purity management, 99.5% O_2 purity.
(2) Δ weight relative to two 32-section stacks; 1.95 lb/per std. section, 2.60 lb per accumulator section at 37 psi, 3.10 lb per accumulator section at 13 psi.
(3) Δ volume relative to two 32-section stacks; 0.013 ft^3 per std section, 0.059 ft^3 per accumulator section at 37 psi, 0.114 ft^3 per accumulator section at 13 psi.

Table 3.2-15. Comparison of High and Low Reactant Pressure Systems

3.2.3.4 Thermal Control

Fuel cell systems for spacecraft require reliable and efficient management of the thermal energy produced in the stack; efficient fuel cell operation is dependent on close temperature control and temperature uniformity throughout the system. A feasibility study and prototype hardware development program aimed at thermal design improvement of the existing A-C/NASA 2-kW Fuel Cell has been completed, whose primary objectives were to investigate static heat removal methods to eliminate the need for forced flow systems such as helium canister heat exchangers and liquid coolant loops, to improve condenser and MRV reliability and thermal performance, and to reduce weight.

The study conducted under this program indicates that substantial improvement can be achieved in the following areas:

- Internal cooling of the fuel cell stack using heat pipes
- Edge cooling of the stack using heat pipes as a thermal link with the spacecraft cooling system
- Improved condenser design employing either heat pipes or conventional forced liquid coolant loop
- Heat pipe thermal link between a proportional moisture removal valve and the stack.

Generally, the feasibility study results indicated that weight reductions of up to one-fourth and thermal performance improvement ranging from one-half to one-fourth of existing temperature drops can be achieved. In addition, the basic feasibility of heat pipe cooling of the entire fuel cell, which would result in a completely passive and self-controlled (no moving parts) system, was established.

The final objective of this effort was to design, develop and test a heat pipe demonstration prototype to substantiate the result of the feasibility study. Edge cooling of the fuel cell stack using heat pipes as the thermal link with the spacecraft cooling system was selected since this concept can be applied directly to the existing 2 kW fuel cell stack. A thermal model simulating a portion of the stack was developed and fabricated. Basically,

it consists of series of plates (to simulate the stack) with electrical heaters, two heat pipes clamped to the edge of the plates, and a liquid cooled heat sink. Tests performed on this prototype were correlated with analytical predictions which conclusively demonstrated validity of the concepts developed in this program.

The following paragraphs present a summary of the work accomplished, along with descriptions of the various concepts generated and the test results of the demonstration prototype.

Cell Plate Cooling

Two basic methods for removing heat from individual cells were studied: evaporative cooling and the use of heat pipes.

- Evaporative Cooling:

  Evaporative cooling was studied in order to improve the capability of the system to meet higher power requirements. Water was selected as the cooling medium because:

  - It is compatible with the cell electrolyte and can be introduced directly into the cell assembly
  - It has the highest latent heat of vaporization of all known potential coolants in the temperature range of interest
  - It is available on board in continuous supply as a product of the fuel cell reaction

  Two basic design concepts were considered for evaporative cooling. The first involves direct injection of atomized water droplets into the electrochemical cell, either into the cell proper or into the water removal section. The second concept is that of a cooling section within the stack that is completely isolated and independent of the electrochemical cells. Each concept is described in more detail below.

The direct injection of atomized water droplets into the electrochemical cell was demonstrated under Contract NAS 8-20573 and reported in NAS 8-20573-QPR-003 dated January, 1967. Water was injected directly into the oxygen cavity with subsequent boil-off from the water removal matrix. The resultant cell performance degradation rate over the 165-hour test period under steady-load condition was approximately 170 μV/h/section. The cause of this degradation is postulated to be the severe local electrolyte concentration gradients in the cell due to the water injection.

Under variable load conditions, an injection rate controller would have to be devised which would inject water as a function of the current level.

The amount of water delivered to the condenser would include not only the water produced by the electrochemical action within the fuel cell to satisfy the vehicle electrical load but also the water vapor evolved in cooling the stack. The vapor pressure in the water removal cavity would be decreased in order to remove the additional water.

Direct injection of atomized water droplets into the water removal section of the cell assembly would relieve the problem of local concentration gradients resulting from the direct injection of atomized water droplets into the electrochemical cell. Other problems, however, present themselves depending on where the water is injected within the physical boundaries of the water removal section.

The injection of water into the water removal matrix would affect the control and heat exchanger requirements the same as the direct injection of water droplets into the electrochemical cell, but without the accompanying local concentration gradients in the cell proper. In addition, the KOH would tend to diffuse into the water inlet path, thus reducing the concentration in the water matrix, and foul up the water injection controlling device.

The direct injection of water droplets into the water cavity would cause the droplets to coalesce locally in the water cavity. In order that its vapor

pressure be in equilibrium with the vapor pressure in the water removal matrix, the temperature of the water would drop forming local cold spots. The temperature of these cold spots would be as much as 40°F below that of the matrix.

To alleviate the local cold spots, a wick assembly can be incorporated into the water removal cavity (see Figure 3.2-24). This approach, however, would make operation at the design temperature impossible if pure water is used because the temperature-pressure relationship differs from that of the electrolyte in the cell. By impregnating the wick with KOH, its temperature can be adjusted to the desired level. However, the KOH would tend to migrate upstream via the water path and would eventually diffuse. With a wick in the water cavity, the lag time (due to water inventory) would make it difficult to maintain constant temperature at variable power levels.

The second concept involves the introduction of independent evaporator sections into the stack. A separate evaporator inserted between the cells can control the temperature of the cells by venting steam through a back pressure regulator. The evaporator is shown in Figure 3.2-25. It consists of cooling plates between oxygen plates. Water is transported in the center of the evaporator via a wick, with a steam chamber on each side of the wick formed by the grooves in the cold plate. The heat is conducted to the wick by the lands of the cold plate.

The evaporator is a straight-forward design problem. It has no impact on basic fuel cell technology or on electrochemical performance because it is isolated from the cell. It is essentially a form of an open-cycle heat pipe. The basic principle is amply demonstrated by the static moisture removal system in A-C Fuel Cells.

The present 2 kW System design has approximately one-third of the by-product heat rejected in the water recovery condenser at a temperature corresponding to the condenser operating pressure of 3.6 psia or less. The maximum rejection temperature for this heat load then, is about 120°F. The remaining

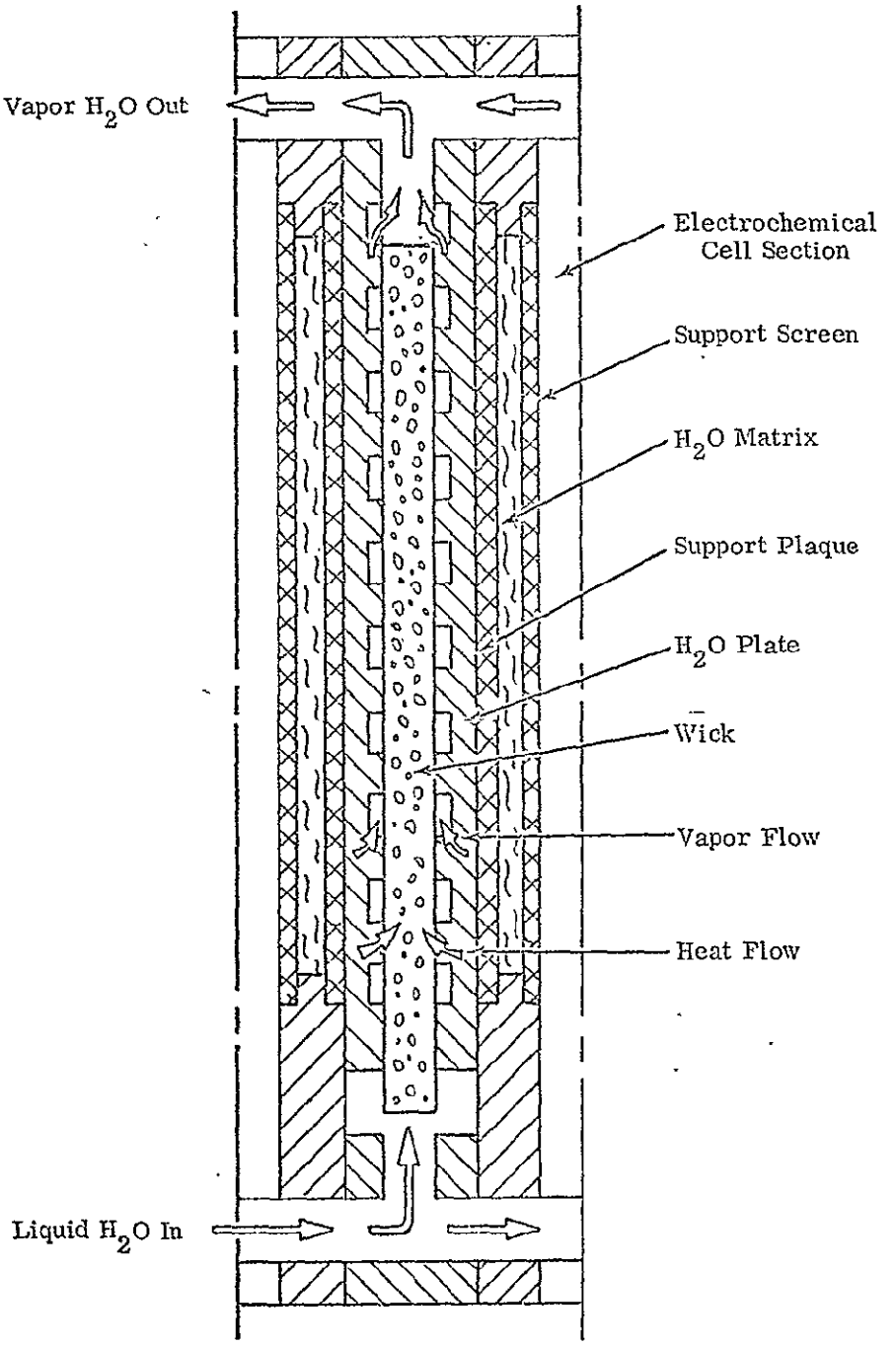

Figure 3.2-24. Heat and Moisture Removal Section

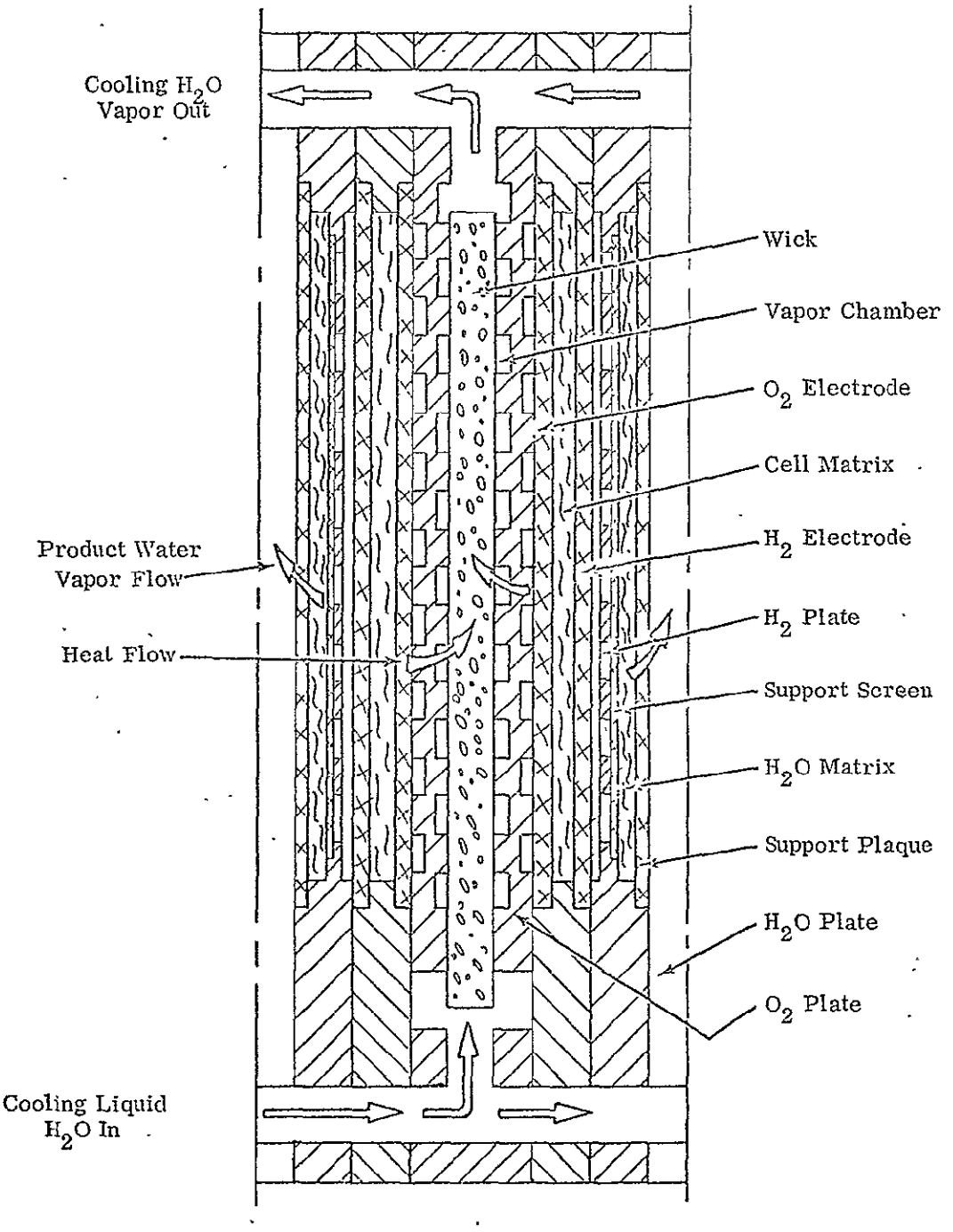

Figure 3.2-25. Evaporative Cooler

two-thirds of the by-product heat is rejected from the stack which operates at a nominal temperature of 190°F. Thus, the majority of the total waste heat is rejected at high temperature.

Any form of direct cooling by water injection into the cell necessitates removal of more than one-third of the by-product heat via the condenser. This will result in a vehicle radiator size penalty because a greater fraction of the heat load is rejected as low grade heat (temperature below 120°F).

Furthermore, the control system to handle direct injection of water into the cell would be complex and highly sophisticated since the electrolyte concentration level is a precisely controlled parameter that affects electrical output and cell life.

Therefore, the evaporative cooling design approach considered most adaptive to the 2 kW type fuel cell is that of the independent cooling plate located in the stack but completely isolated from the electrochemical cell. The basic principle of this concept is well established and is very similar to the static moisture removal system presently employed on all A-C aerospace fuel cells. The development effort in this instance is centered about the actual flight hardware that would be compatible with the fuel cell. Significant redesign of the stack and plate manifolds would be required to mechanize this approach.

- Heat Pipe Cooling of Fuel Cell Plates:

Improved plate conductance can be achieved by integrating heat pipes directly into the H_2, O_2, and H_2O plates. The conventional ribbed cross members used in the present plate design can be replaced by grooved heat pipes as shown in Figure 3.2-26.

An alternate cell cooling approach uses a heat pipe cooling plate imbedded in a split oxygen plate. Construction of the latter type of plate typically consists of a series of small (1/8 inch diameter) heat pipes embedded in a homeycomb core as shown in Figure 3.2-27. The honeycomb serves to retain internal pressure of the cell. An edge member is

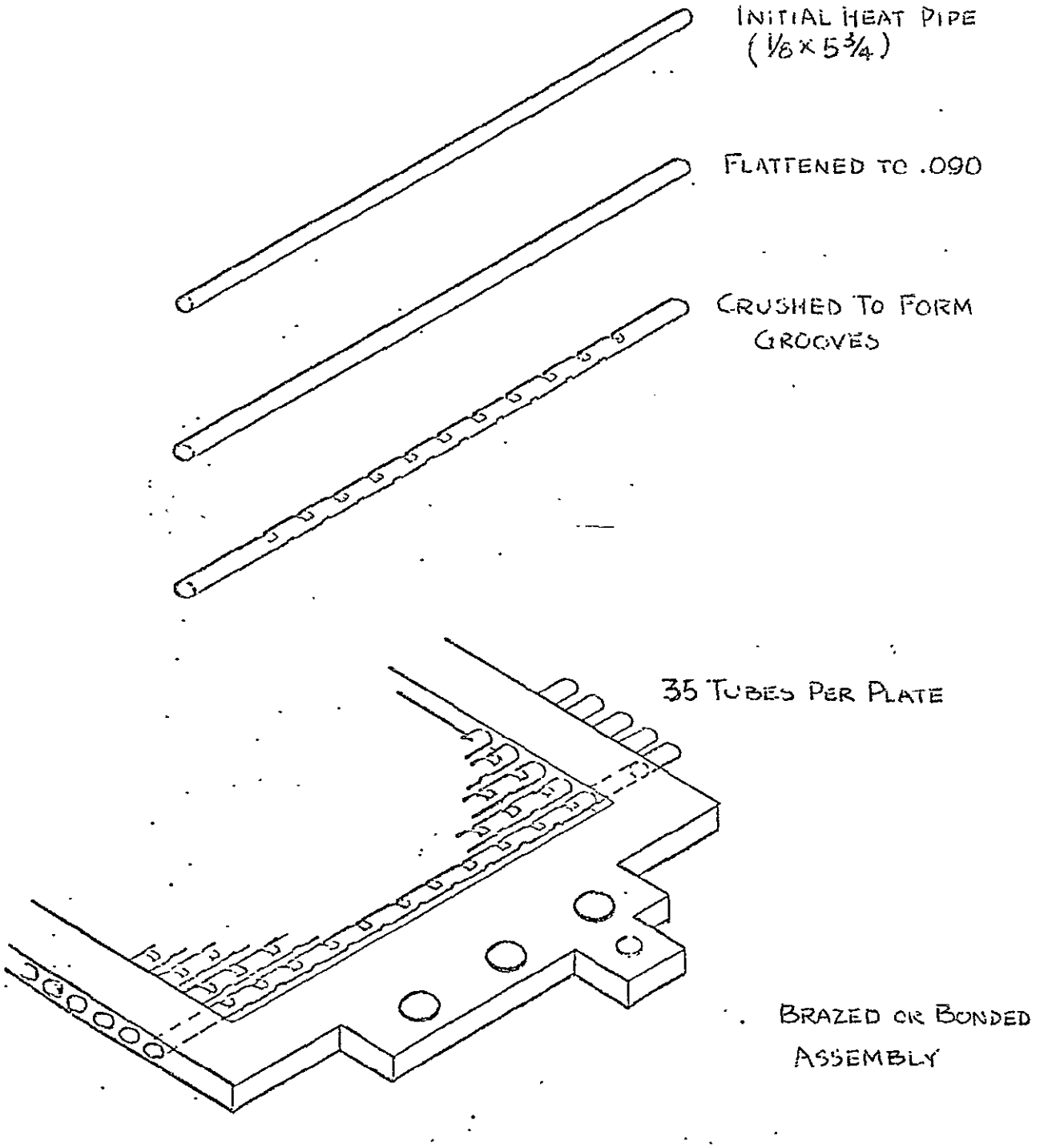

Figure 3.2-26. Heat Pipe/Cell Plate Assembly

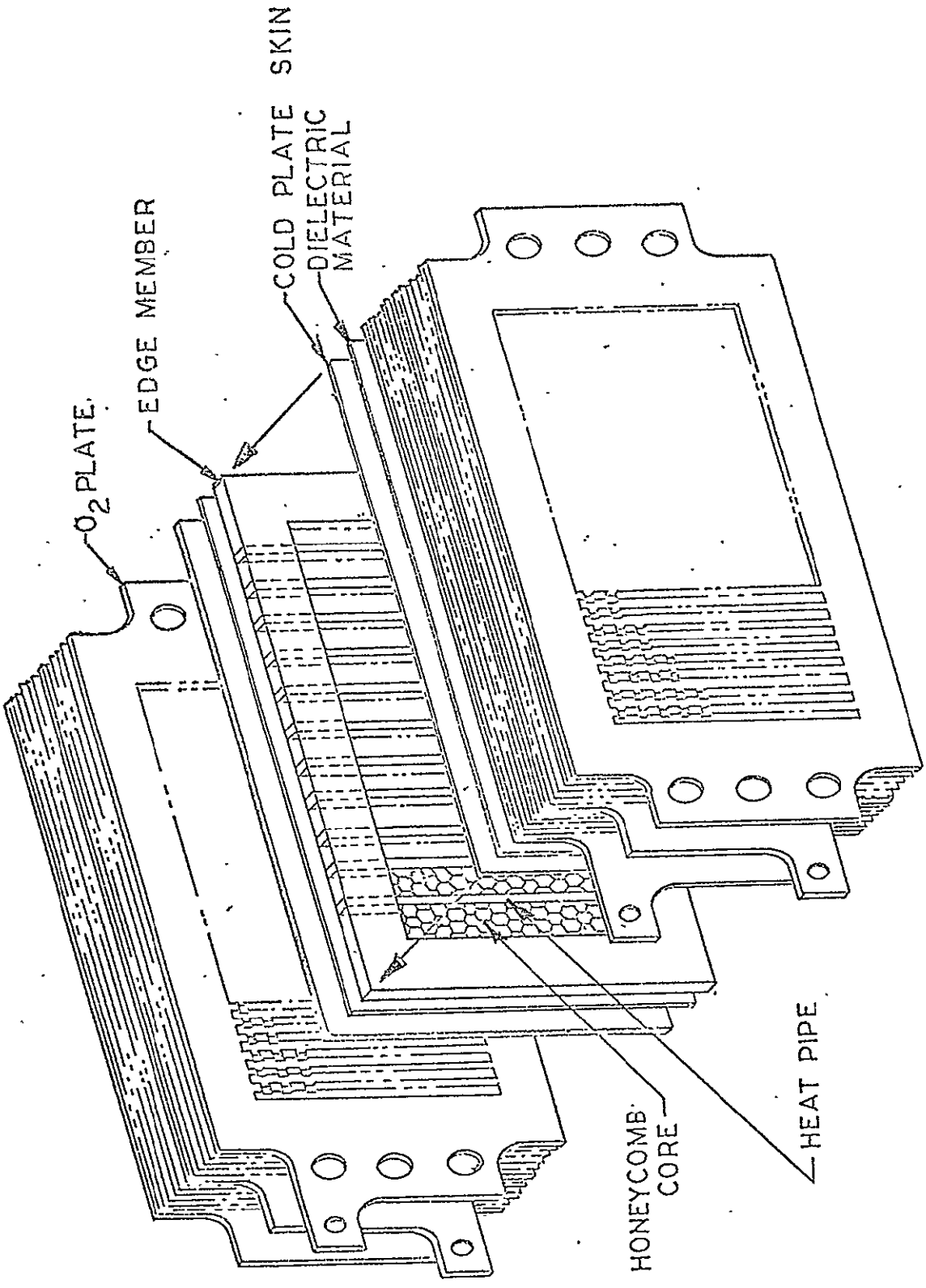

Figure 3.2-27. Intercell Heat Pipe Construction

provided for interfacing with transverse heat pipes or a forced flow liquid coolant loop. Electrical insulation and honeycomb skins complete the assembly.

A preliminary evaluation of these heat pipe approaches revealed that the intercell heat pipe cold plate results in nearly the same thermal performance as the integral heat pipe-cell plate. This is due to the fact that 70% of the heat in the cell is generated in the O_2 plate region, which is in direct contact with the separate cooling plate. Thus, only 15% of the heat from each of the H_2 plates has to be conducted through the cell matrix. Because of the similarity in thermal characteristics, the separate cooling plate approach was selected for further evaluation since it offers two distinctive advantages:

(1) The heat pipe cooling plate can be designed and optimized independently of the cell plate reactant flow requirements. Thus, the cooling plate can be of lighter weight construction, require fewer heat pipes, will be less complicated in design and be more easily integrated into the stack.

(2) The fuel cell plates can be optimized independently of the heat pipes. Thinner H_2 and O_2 plates and alternate H_2O plate material (such as plastic) can be considered.

When compared with evaporative cooling of the individual cells, the intercell heat pipe plate is clearly more desirable because it is (in the macroscopic sense) a "dry" technique, with no requirement for bulk coolant input and controlled discharge from the stack.

Stack Heat Removal

Techniques to provide a thermal link between the fuel cell stack and the spacecraft coolant loop were also considered. The objective was to provide improved thermal performance while eliminating any moving components. By employing heat pipes to provide this thermal link, elimination of the canister, helium and associated circulating fans of the existing 2 kW fuel cell is made possible.

Two approaches for providing a heat pipe interface between the fuel cell stack and primary coolant are shown in Figure 3.2-28 and 3.2-29. Figure 3.2-28 shows a concept of attaching heat pipes to the edge of the present 2 kW fuel cell stack plates. The heat pipes are electrically insulated and connected to two liquid cooled cold plates. An alternate heat pipe thermal link is shown in Figure 3.2-29. In this case, the heat pipes are attached to the stack in the axial direction. Straps are provided to maintain a pressure contract interface between the edges of the fuel cell plates and the heat pipe mounting saddles. This arrangement allows relative motion between the heat pipe and the plates to account for stack contraction. Electrical insulation is also provided at this interface. The latter approach (heat pipes parallel to the stack axis) is preferred for the following reasons:

(1) Fewer number of heat pipes (larger diameter) are required reducing design complexity.

(2) Primary coolant heat exchanger can be varied in size and geometry for optimum configuration.

(3) Larger diameter heat pipes are more amenable to static temperature control.

(4) The arrangement is structurally much more rugged.

Preliminary Design of a Heat Pipe Thermal Control Subsystem

The thermal performance of a heat pipe TCCS employing the concepts discussed in the previous section was evaluated. A configuration which combines internal and external cooling of the fuel cell stack was developed. The configuration consists of intercell heat pipe plates within the stack, integrated with a series of larger diameter heat pipes running along the edge of the stack. The latter heat pipes provide the required thermal link between the fuel cell plates and the spacecraft coolant loop.

In order to obtain maximum thermal conductance between the intercell cold plates and the transverse heat pipes an arrangement as shown in Figure 3.2-30 is used. The intercell heat pipes extend beyond the edge of the stack and are bonded to aluminum saddles. These are assembled as part of the stack. After the fuel cell stack assembly is completed, the transverse heat pipes are inserted in premachined grooves in the saddles and

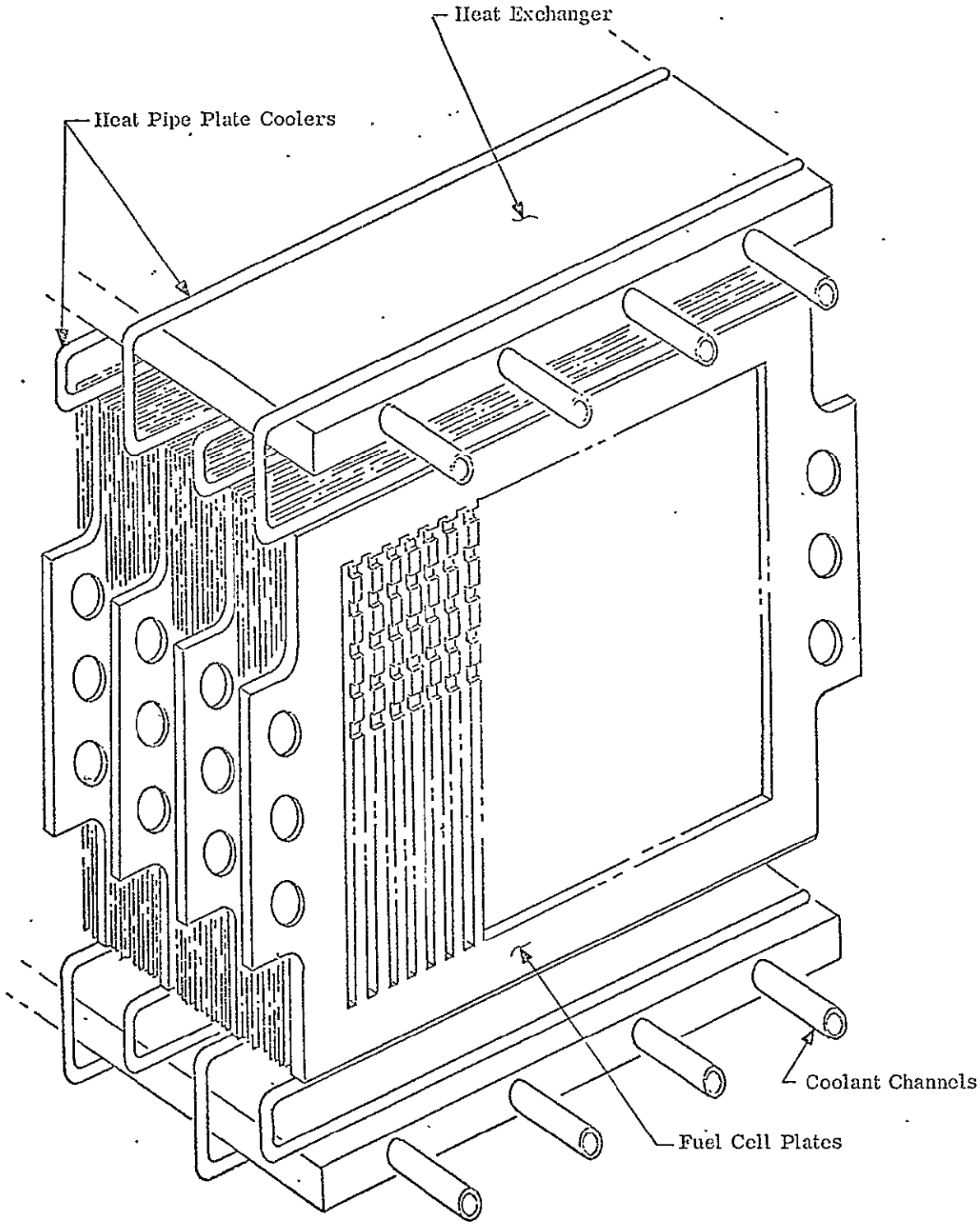

Figure 3.2-28. Heat Pipe Cooled Fuel Cell Plates Integrated with Heat Exchanger

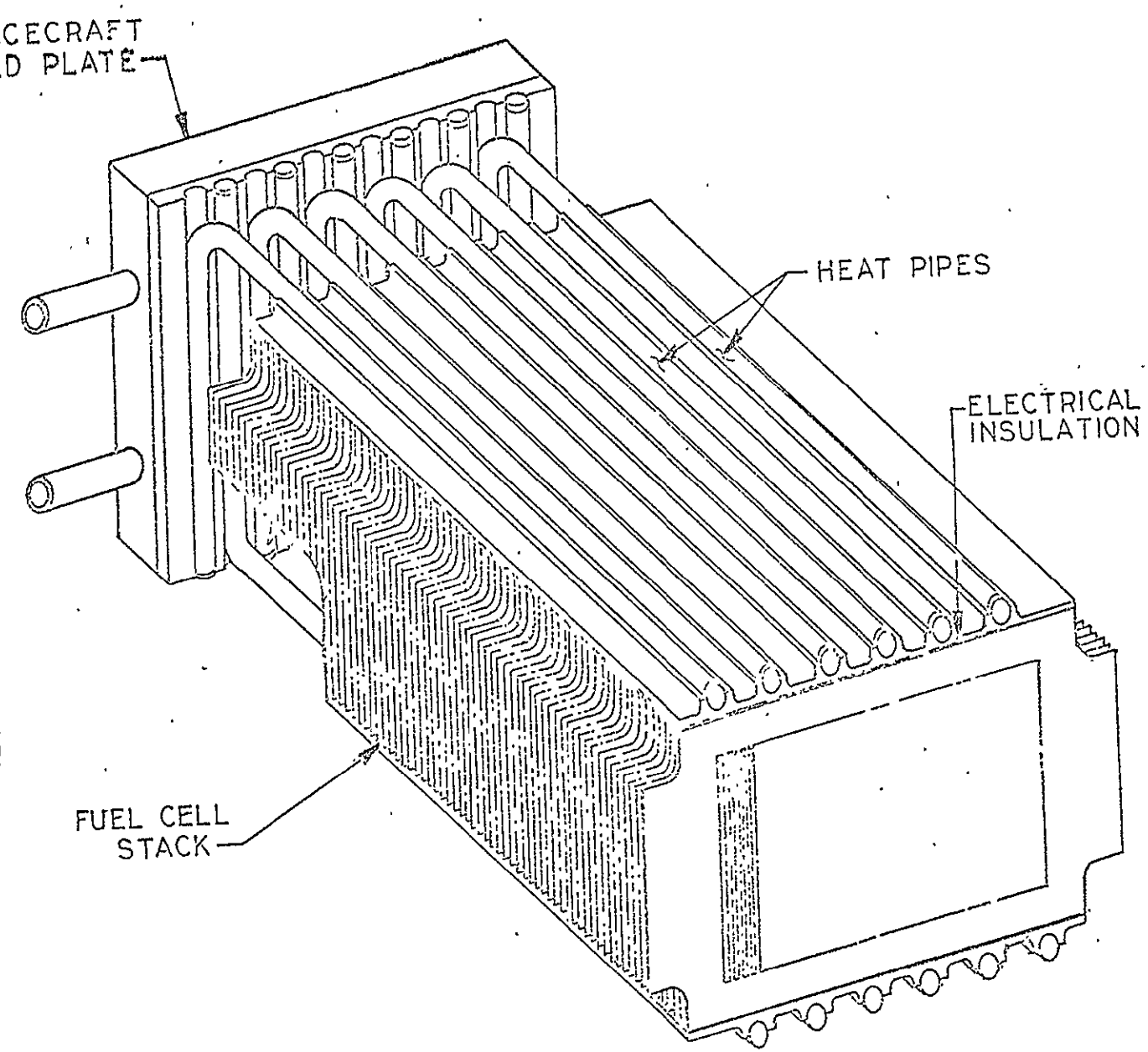

Figure 3.2-29. Fuel Cell Stack Edge Cooling Concept-Heat Pipes

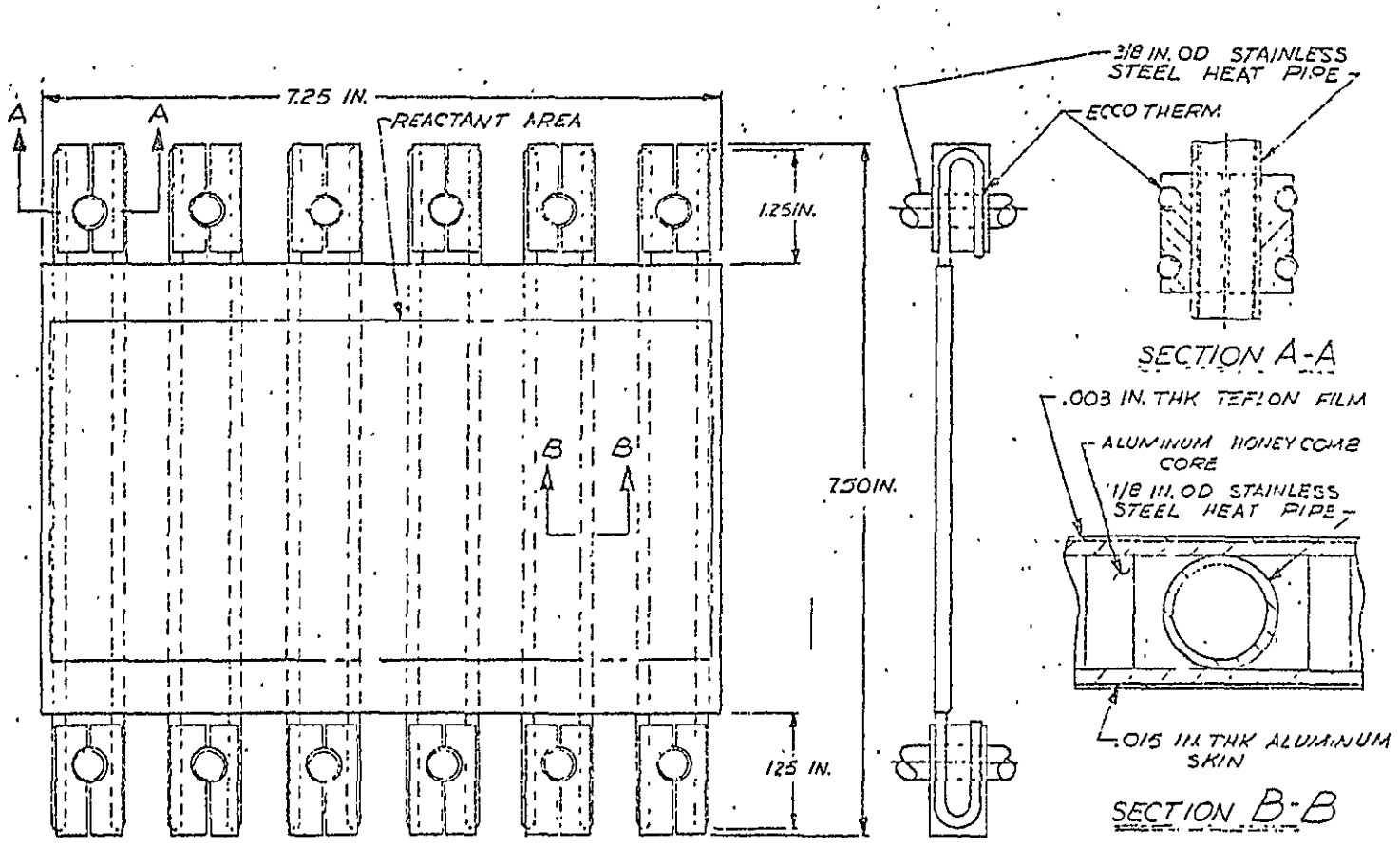

Figure 3.2-30. Heat Pipe Internal Cooling Plate

mechanically clamped. A thermally conductive epoxy (such as Eccotherm) is applied at this interface to improve the thermal conductance of the mechanically clamped interface.

Performance for this configuration was computed based on the thermal loads and geometry of the existing A-C/NASA 2kW fuel cell. With the existing fin cooling design, each cell section (two cells) has the capability of dissipating 250 Btu/hr-ft^2 per cell with a grid plate temperature gradient of approximately 6°F and a temperature gradient of approximately 100°F between the edge of the stack and the liquid cooled canister. With a heat pipe thermal control system, the goal is to dissipate 500 Btu/hr-sq ft per cell at a fuel cell stack temperature of 190° ± 10°F while maintaining nearly uniform temperature in the cell active zone. The major assumption made during this evaluation is that the heat generation is evenly distributed over the existing reactive area of 0.19 sq ft (6.74" x 4.06"). The intercell cold plate utilizes twelve evenly spaced 1/8" O.D. heat pipes. Since these heat pipes will be required to operate in any orientation during "One-G" testing, the wetting height capability is extremely improtant for reliable operation. For the 200 mesh stainless steel wick and water as the working fluid, the calculated wetting height is .86 feet (10.35 inches). The maximum vertical height of the heat pipes is only 7 inches. Therefore, these pipes will be capable of operating in any orientation in a "One-G" field.

The design heat input is 2 x 500 Btu/hr-ft^2 since the cooling plate serves to remove heat from two cells. Assuming twelve heat pipes embedded in the cold plate, the individual heat pipe transport requirement is calculated to be:

$$q = \frac{1000 \times 0.19}{12} = 15.84 \frac{\text{Btu}}{\text{Hr}} \quad (4.64 \text{ Watts}) \qquad (1)$$

The maximum heat pumping capability in the vertical position is calculated from the following equation:

$$q/A_w = \frac{a F_L}{L} \left(\frac{\epsilon D_L^2}{32 r}\right) (1 + \gamma) N_L \qquad (2)$$

where: A_w = Wick cross-sectional area

F_L = Liquid pressure drop fraction

L = Transport distance

η = Gravitation factor

N_L = Liquid transport factor

ϵ = Wick porosity

r = Capillary radius

a = Capillary constant

$$q/A_w = 2.36 \times 10^6 \ \frac{\text{Btu}}{\text{hr-ft}^2} \tag{3}$$

$$\text{or} \quad q_{Max} = \frac{2.36 \times 10^6 \times 1.45 \times 10^{-5}}{3.413} = 10 \text{ Watts} \tag{4}$$

Therefore, each intercell heat pipe has the maximum transport capability in the "one-G" vertical position of 10 watts as compared to the design requirement of only 4.54 watts.

A similar analysis was performed to evaulate the heat transport capability of the transverse heat pipes. In this case, it was assumed that the spacecraft cold plate would be located at one end of the fuel cell stack and that the transverse heat pipes would be mechanically clamped to the cold plate as shown in Figure 3.2-29. The spacecraft cold plate was assumed to measure approximately 8" x 8" to conform with the overall size of the stack. It was also assumed that the heat pipes should be able to operate in any orientation in a "One-G" field except in a stack-on-end orientation. For the case of a cell thermal power density of 500 Btu/hr-ft^2 and a configuration utilizing twelve 1/2" O.D. transverse heat pipes, the heat load per heat pipe was calculated to be:

$$q = \frac{1000 \ (0.19) \ (31)}{12} = 490 \ \frac{\text{Btu}}{\text{Hr}} \ (144 \text{ watts}) \tag{5}$$

Using equation (2) the heat transport capability of the transverse pipes was determined to be 250 watts in horizontal orientation and 150 watts with the heat pipe condenser in the spacecraft cold plate pumping against gravity. Since in the latter case only six heat pipes would be pumping against gravity while the other six heat pipes would be pumping with gravity, the transport is more than adequate.

The total thermal gradient between the oxygen grid plate and the primary coolant is made up of a series of small resistances which are depicted in Figure 3.2-31. The calculated temperature drops are presented in Table 3.2-16. The performance of the heat pipe cold plate compared to a solid aluminum plate of equal thickness is shown in Figure Figure 3.2-32(a) shows the relative temperature uniformity of the fuel cell active area, while Figure 3.2-32(b) shows the relative temperature drop between the cell and transverse heat pipes located on the edge of the stack.

In order to complete the evaluation of a heat pipe TCCS subsystem, it is necessary to include the temperature drops between the transverse heat pipes and the spacecraft cold plate. Assuming a water-glycol system and cold plate pressure drops of up to 4 psia at 100 #/hr flow rate, a cold plate capable of accepting 300 watts/°F can be achieved. In combination with the pressure contact interface and a water-glycol cold plate, the heat pipe condenser temperature drop would be approximately 30°F. The total system temperature drop would be approximately 40°F for a 500 Btu/hr-ft^2 cell power density or 20°F for a 250 Btu/hr-ft^2 cell power density. The latter case compares quite favorably with the 100°F drop in the existing helium cooled system at 250 Btu/hr-ft^2 cell power density.

Improved Condenser

The objectives of this evaluation were to define improvements in the thermal performance of the condenser subsystem to permit operation with higher coolant temperature, and to reduce the weight of the MCS condenser to 8.5 lb or less. The basic design approach used in the condenser modification studies was as follows:

(1) Relocate the coolant passages from the condensate to the vapor side of the asbestos separator. (Improve thermal conductance).

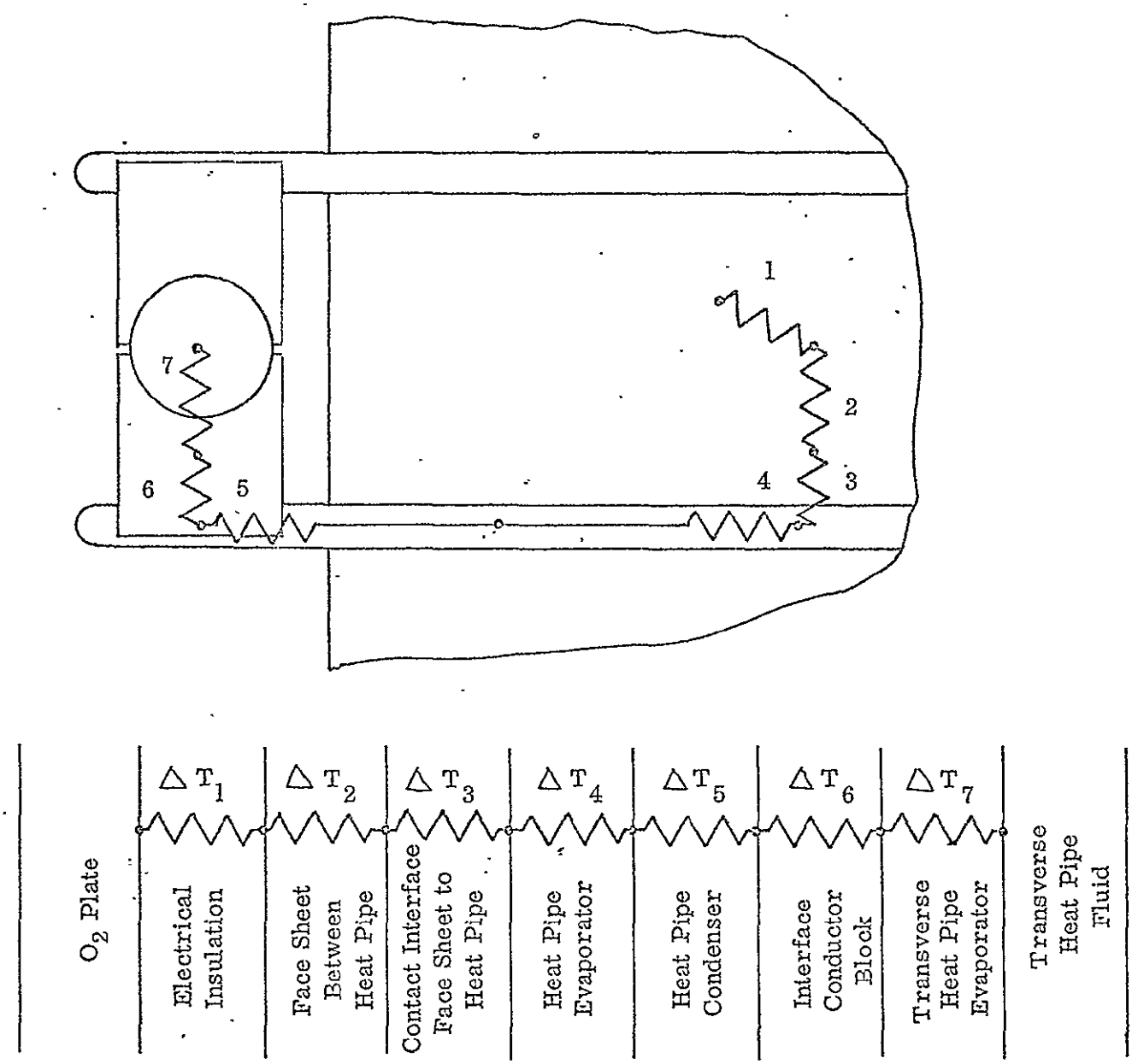

Figure 3.2-31. Temperature Gradient Schematic

Heat Generation Rate per Cell (Btu/Hr.Sq.Ft.)	ΔT_1	ΔT_2	ΔT_3	ΔT_4	ΔT_5	ΔT_6	ΔT_7	ΔT Total
250	.44	.65	.30	.73	.83	1.10	1.06	5.11
500	.88	1.30	.60	1.46	1.66	2.20	2.12	10.22
750	1.32	1.95	.90	2.19	2.49	3.30	3.18	15.33

Table 3.2-16. Various Thermal Gradients in Grid Plate Design, °F

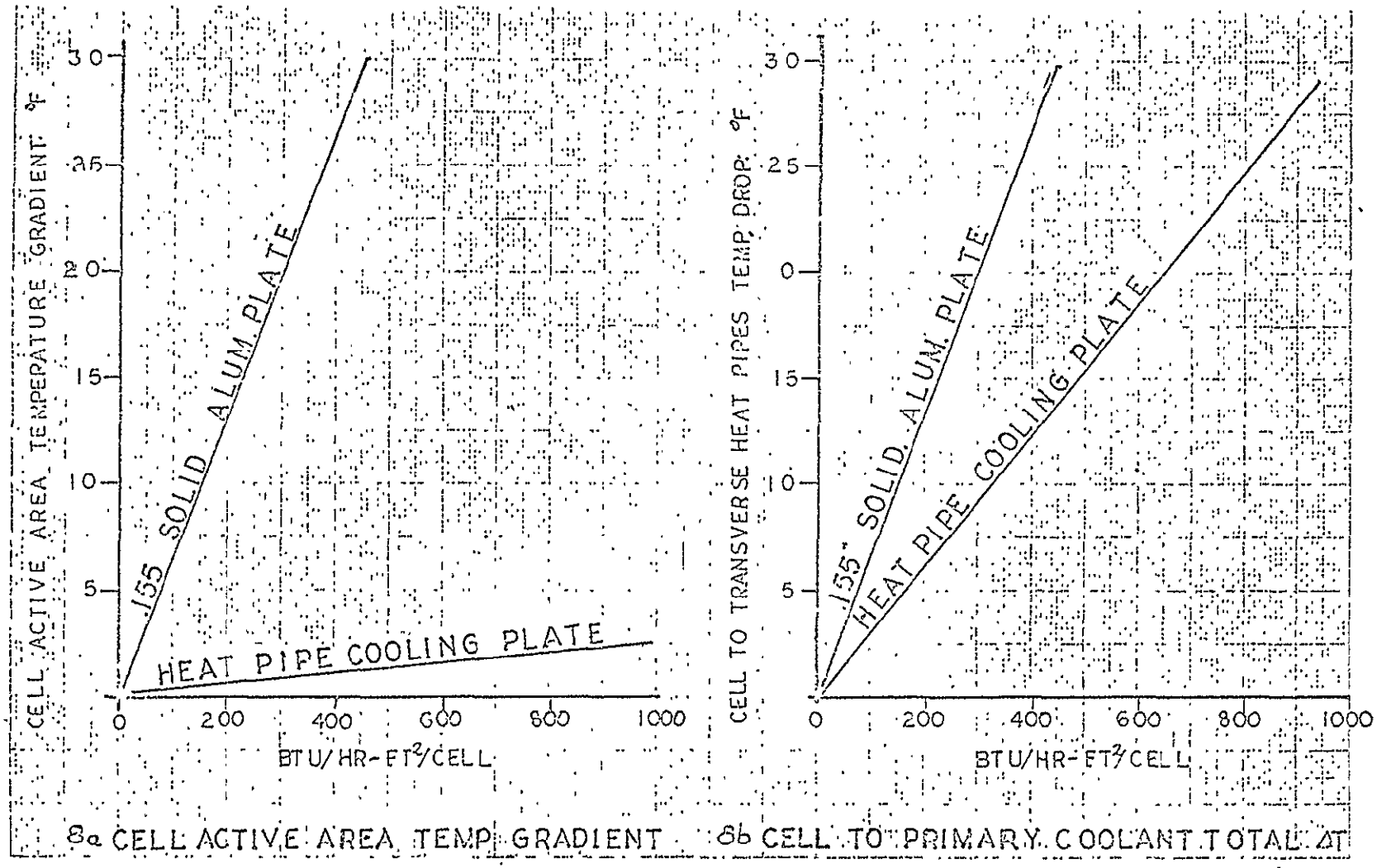

Figure 3.2-32. Comparative Performance Heat Pipe Internal Cooling Plate

(2) Change condenser geometry from flat to cylindrical. (Weight reduction).

(3) Use plastic wherever practicable. (Weight reduction).

(4) Increase coolant flow rate while maintaining the same pumping power requirements.

The analysis was based on the design criteria below:

- Condensate Flow Rate : $M = 2.5$ lb/hr.
- Condensate Pressure (Saturation) : $P_{sat.} = 3.4$ psia
- Asbestos Matrix Thickness : $\Delta X = .020$ in.
- Asbestos Matrix Pressure Drop : $\Delta P_m = .3$ psi
- Coolant : Ethylene Glycol-Water (60%-40%)

Asbestos matrix area was computed using the permeability relationship:

$$W_m = \frac{5.75 \times 10^{-12} A_m \Delta P_m}{(\Delta X)^4 \upsilon} \qquad (1)$$

where: ΔX = Matrix Thickness (inches)

W_m = Flow Rate (cc/min.)

A_m = Matrix Surface Area (in^2)

ΔP_m = Pressure Drop Across Matrix (PSI)

υ = Viscosity (ft^2/sec)

Tubular coolant channels were assumed with a projected area equal to 50% of the asbestos matrix surface area. That is, the tubular coolant loop size was governed by the relationship:

$$DL = .5 A_m \qquad (2)$$

where: D = Diameter of Coolant Loop Tube (feet)

L = Total Length of Coolant Loop Tube (feet)

A_m = Asbestos Matrix Surface Area (sq. ft.)

Coolant pressure drop as a function of coolant loop tube diameter was determined, using the above relationship and the equation:

$$\Delta P = f \frac{L}{D} \frac{\rho V^2}{2g} \tag{3}$$

where: ΔP = pressure drop (lb/ft^2)

$f = \frac{0.316}{R_e^{1/4}}$

R_e = Reynolds Number

P = Coolant density (lbs/ft^3)

V = mean coolant velocity (fps)

g = gravitational constant (32.2 ft/sec^2)

Loop ΔT's were calculated using the film coefficients below:

$$h_e = .023 \frac{K_e}{D} (R_e)^{0.8} (P_r)^{0.4} \tag{4}$$

where: h_e = coolant film coefficient

K_e = coolant thermal conductivity (Btu/hr-ft-°F)

P_r = Prandtl number

$$h_c = \frac{K_c}{S} \tag{5}$$

where: h_c = condensate film coefficient

K_c = condensate thermal conductivity (Btu/hr-ft-°F)

S = condensate film thickness (feet)

Condenser pumping power is determined from:

$$HP = \frac{\dot{m} \Delta P}{J} \tag{6}$$

where: HP = Pumping Power Required (Watts)

$\dot{m}$ = Mass Flow Rate of Coolant (#/hr)

ΔP = Condenser Pressure Drop (PSF)

J = 2655 ft-lb/watt-hr

Results for the case of a sample flow loop and coolant mass flow rate of 100 lbs/hr are summarized in Table 3.2-17, Case #1.

Since most of the condenser ΔT's occur between the coolant inlet and outlet, an increase in coolant flow rate was considered. Flow rates of 200 lb/hr and 300 lb/hr were evaluated. To retain the same pumping power requirement and coolant film coefficient, parallel flow paths within the condenser were introduced. The number of flow paths selected corresponds to the increase in flow rate over the 100 lb/hr single loop case. The results are summarized in Table 3.2-17, Case #2 and Case #3. The table also includes performance of the existing condenser for comparison. Figure 3.2-17 shows total condenser temperature drop (condensate saturation temperature minus coolant inlet temperature) as a function of mass flow rate. A conceptual design illustrating Case #3 is shown in Figure 3.2-23 including size and materials. A weight summary is shown in Table 3.2-18.

As a result of this evaluation, a sizeable improvement in condenser heat conductance was determined to be possible by the relocation of the coolant channels to the vapor side of the asbestos matrix. Additional gains in thermal performance can be achieved with higher coolant flow rates while maintaining a constant condenser pumping power requirement. This can be achieved by varying the number of parallel flow paths as a function of mass flow rate, which in turn allows a reduction of inlet versus outlet temperature drop. Finally a substantial weight reduction can be achieved.

A condenser design employing heat pipe cooling was also considered. Such a condenser could be coupled with a heat-pipe stack cold plate to provide for passive and self-controlled (no moving parts) fuel cell thermal control. Predicted performance is as follows:

Asbestos Matrix Thickness = .020 in.

Asbestos Matrix ΔP = .3 PSI

Ethyl. Glycol-Water Coolant (60% - 40%)

	Case #1	Case #2	Case #3
Condensate Flow Rate	2.5 lbs/hr	2.5 lbs/hr	2.5 lbs/hr
Asbestos Matrix Surface Area	87 in^2	87 in^2	87 in^2
Coolant Flow Rate	100 lbs/hr	200 lbs/hr	300 lbs/hr
Coolant Temp. Rise ($T_{in} - T_{out}$)	32°F	16°F	11°F
Condenser Temp. Drop ($T_{sat.} - T_{bulk}$)	8°F	8°F	8°F
Number of Coolant Flow Loops	1	2	3
Condenser UA	310 $\frac{BTU}{Hr - {}^oF}$	310 $\frac{BTU}{Hr - {}^oF}$	310 $\frac{BTU}{Hr - {}^oF}$
Coolant Loop Tube Diameter	3/16 in.	3/16 in.	3/16 in.
Total Tube Length	22 ft.	22 ft.	22 ft.
Estimated Weight (Approx.)	4 lbs.	4 lbs.	4 lbs.

EXISTING SYSTEM	
Flow Rate	100 lbs/hr
Asbestos Matrix Area (.030" Thick)	435 in^2
Coolant Temp. Rise ($T_{in} - T_{out}$)	32°F
Condenser Temp. Rise ($T_{sat.} - T_{bulk}$)	46°F
Condenser UA	55 $\frac{BTU}{Hr - {}^oF}$
Weight	15 lbs

Table 3.2-17. Predicted Condenser Performance

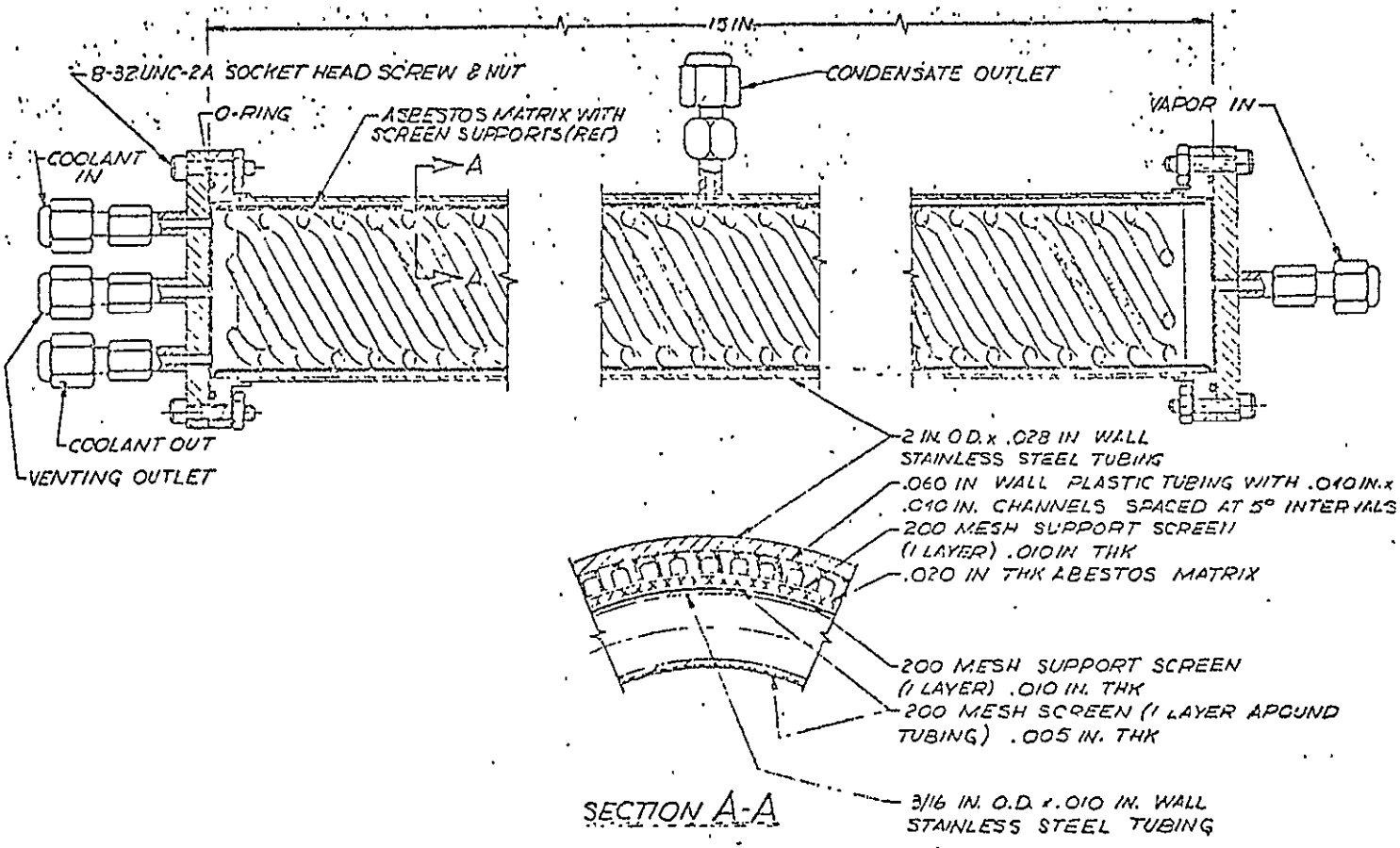

Figure 3.2-33. Cylindrical MCS Condenser Concept (Forced Flow Coolant)

Component	Weight
Condenser Jacket: Stainless Steel	.57 lbs
Flanges (2): Stainless Steel	.29
Covers (2): Stainless Steel	1.05
Condensate Collector: Plastic	.31
Asbestos Matrix	.21
Asbestos Matrix Retainer: Stainless Steel Screen	.20
Coolant Tube: Stainless Steel	.48
Coolant: Ethyl Glycol-Water (60% - 40%)	.26
Coolant Headers: Stainless Steel	.28
Misc. Hardware: Bolts, Fittings, Gaskets	.35
TOTAL	4.00 lbs

Table 3.2-18. Condenser Weight Summary - Case #3

•	Total Temperature Rise (Including Cold Plate to Spacecraft Interface)	10°F
•	Estimated Weight (Including Cold Plate)	4.5 lbs

Proportional Moisture Removal Valve

Techniques to provide a sensing link between a remotely located proportional MRV and the fuel cell were considered. The existing A-C MRV design requires that the valve be imbedded within the stack so that its sensing fluid is at the same temperature as the stack. Concepts evolved for a remotely located MRV include:

1) Redesign of the existing MRV to include a sensing fluid reservoir (bulb) and a capillary tube linkage (Figure 3.2-34). Only the reservoir need be imbedded in the stack.

2) Mounting of the MRV to a heat pipe which is thermally linked to the stack.

Each approach appears to be technically feasible. Final selection requires further evaluation of relative reliability, ease of integration, operational stability and accuracy, and maintenance impact.

Demonstration Prototype

As a result of the heat pipe application studies conducted in the first phase of this program, a number of thermal design improvements were identified. A major area requiring improvement is the thermal link between the fuel cell stack and the spacecraft coolant loop. With heat pipes mounted to the edge of the stack major improvement in thermal performance and weight can be achieved over the existing system. Therefore, a representative section of the fuel cell stack with edge cooling heat pipes was selected as the demonstration prototype.

In order to retain the technology of the existing 2-kW stack, a design was developed which

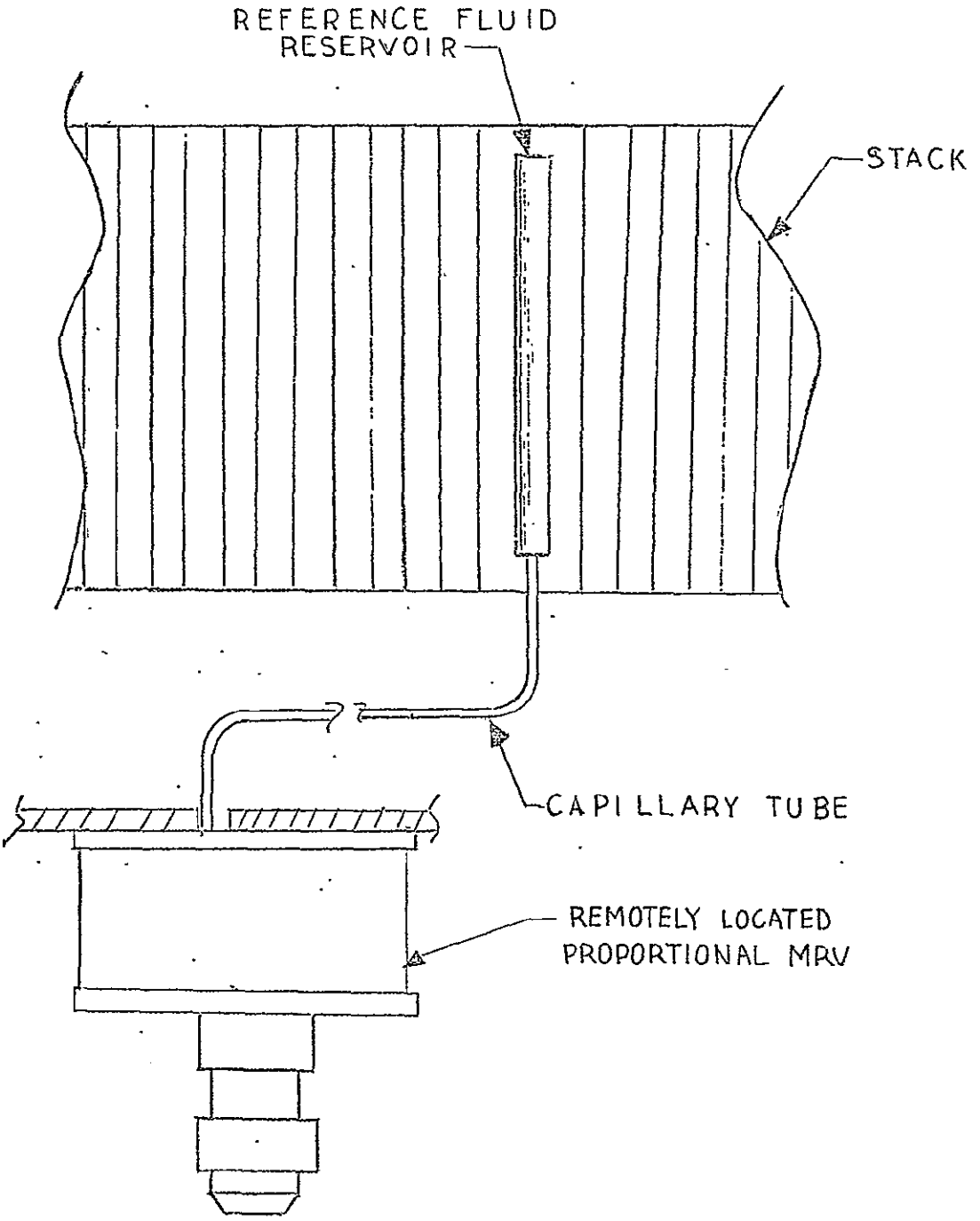

Figure 3.2-34. Remote Location Proportional MRV Concept

requires no changes in the internal construction of the stack. This design can be attached to the stack by removing (machining) the existing convective fins and clamping the edge cooling heat pipes to the stack. Thermal design of this concept was based on thermal loads of the present 2 kW system.

The demonstration prototype design which was fabricated to simulate this concept is shown in Figure 3.2-35. Its size represents the full height and length of the stack. while the width is approximately 1/6 of the actual stack width. Since approximately twelve heat pipes (six on each side) would be used on a actual stack, the 1/6 section was selected as a representative thermal model. The fuel cell plates were simulated with a series of .090" aluminum plates held together with two 1/2" diameter stainless steel threaded rods. To simulate the cell and transport matrix, 1/16" phenolic spacers were used between the aluminum plates. Finally, silicon rubber heaters were attached to two sides of the plate stack assembly to simulate the heat generated by the fuel cell.

Interfacing of the heat pipes with the simulated fuel cell stack was achieved by clamping of the heat pipes to two opposite sides. These sides were machined to provide a flat surface to minimize temperature drop across the interface. The tubular heat pipes are mounted on aluminum saddles which provide the necessary transition between the flat edge of the simulated stack and the round heat pipe tubes. In order to provide a valid simulation of the heat pipe to stack interface, electrical insulation consisting of .004" Teflon tape was placed between the heat pipe saddle and the edge of the plates. Finally, an aluminum filled silicone grease thermal compound was used to fill any gaps due to uneven surfaces and coupling force. To simulate the spacecraft cold plate, the heat pipes were bent 90° and clamped between two aluminum blocks. Aluminum tubes (1/4" diameter) were brazed to these blocks for water cooling. A photograph of the demonstration prototype appears in Figure

The heat pipe design was based on the evaluation conducted in the study phase of this program. The construction consists of a 1/2" O.D. stainless steel tube with a wick fabricated from a fine pore size structure. The working fluid is water. Water was selected as the working fluid because of its high figure of merit and because of its ability to wick substantial heights on a "One-G" environment. To provide the necessary

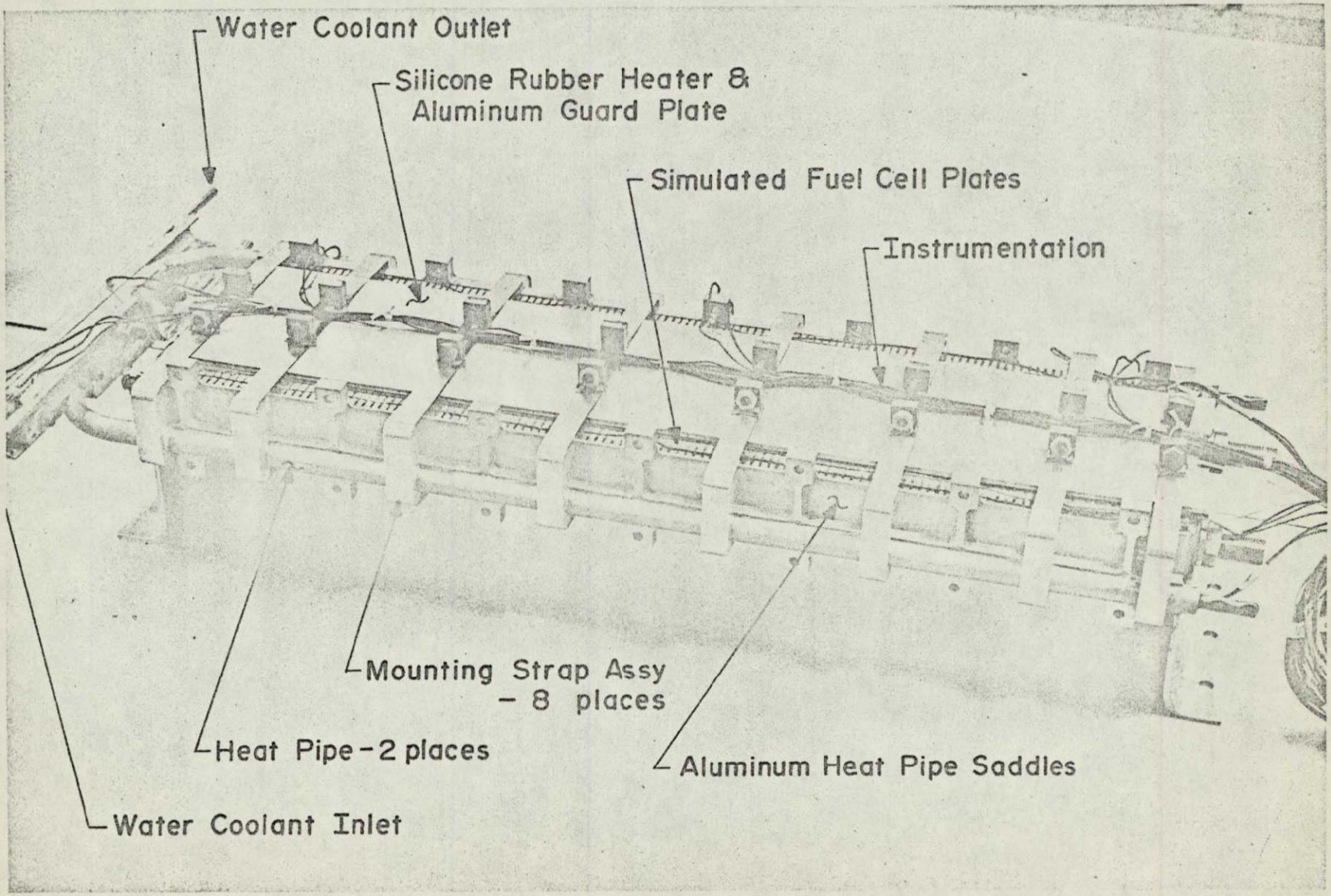

Figure 3.2-35. Fuel Cell Stack Edge Cooling Heat Pipe - Demonstration Prototype

compatibility with water, stainless steel was selected as the tube and wick material.

Initially, the stainless steel heat pipes were attached to the aluminum saddles and cold plate aluminum blocks with Eccobond-Al thermal epoxy. This approach proved to be inadequate when separation of the bonded interface occurred as a result of differential thermal expansion and stresses due to the clamping of the aluminum saddles to the edge of the stack. This bonded interface was modified to include aluminum filled silicone grease compound at the heat pipe to saddle and the heat pipe to cold plate interfaces. Although this compound offers a lower thermal conductivity, it allows relative growth of the aluminum and stainless steel during expansion and contraction. To accommodate this modification, the heat pipe to stack clamping arrangement was changed from tie rods connecting the aluminum saddles to straps which span the stainless steel heat pipes as well as the saddles.

The predicted temperature drops for the demonstration prototype are summarized in Table 3.2-19. These were calculated on the basis of a 150 watt thermal load which is equivalent to the thermal load of the 2 kW fuel cell system at 500 Atw/hr-ft^2. Performance prediction for both the bonded assembly (Eccobond-Aluminum) and the pressure contact interface assembly using aluminum grease are both shown in Table 3.2-19. As can be seen, slightly better performance was predicted for the bonded approach. However, since integrity of the bond could not be maintained, performance data could only be obtained for the case of aluminum grease interfaces. Results are summarized in Table 3.2-19. The correlation between measured data and predictions is excellent.

	Predicted Bonded Assy.	Predicted Aluminum Grease Interface	Measured Aluminum Grease Interface
Stack to Saddle Interface ΔT	7°F	7°F	6.6°F
Heat Pipe and Saddle ΔT	3°F	5°F	5.75°F
Heat Pipe and Cold Block ΔT	10°F	13°F	14.5°F
Total ΔT	20°F	25°F	26.85°F
Stack Temperature Uniformity	7°F	7°F	7.75°F

Table 3.2-19. Predicted versus Measured Prototype Performance

3.2.4 Subtask 2.4 - Advanced Fuel Cell Component Studies

Introduction

The objectives of this effort were:

- To prepare a plan for developing subsystems and components suitable for use in an advanced fuel cell
- To investigate improvements of the following hardware:
  - An electro-mechanical moisture removal valve
  - An integrated reactant control subsystem
  - An advanced stack compression device
  - Stack seals
  - Product water pump
  - Alternate glycol coolant pump
  - Deionizer techniques

3.2.4.1 Electromechanical Proportional Moisture Removal Valve

A review of the operation and performance of the Allis-Chalmers oxygen/hydrogen fuel cell indicates that a moisture removal valve that can control the water cavity pressure continuously over a wide range of operating temperatures will improve both life and performance characteristics. Two approaches have been identified; a mechanical temperature compensated back pressure regulator and an electronically controlled flow control valve. Because of the potential increased flexibility of control, the electro-mechanical valve was studied for future application. This type of valve allows for multi-location temperature sensing and preprograming of the KOH concentration as a function of mission time.

Procurement specification number 49157083 and source control drawing number 49602895 were prepared and sent to eight (8) suppliers (on bid package AEPD-556).

Of the eight, only Carleton Controls Corporation elected to bid on this valve. The valve proposed by Carleton Controls Corporation is a poppet valve driven by a gear motor through a rack and pionion drive. Position feedback is sensed by a linear variable differential transformer linked to the valve stem. The proposal review resulted in no major questions. The approach appears sound and is feasible for this application.

3.2.4.2 Integrated Reactant Control Subsystem (RCS)

Because the inlet reactant control functions are common to all stacks, the possibility of integrating the hardware offers weight, simplification and maintainability advantages. In addition, since the components of the RCS operate on a common media, integration of hardware offers simplification.

Three basic approaches to an integrated reactant control subsystem were established and are shown in Figures 3.2-36 through 3.2-38. The first approach uses essentially a separate RCS for each Stack. The second approach uses one regulator for a two stack combination.

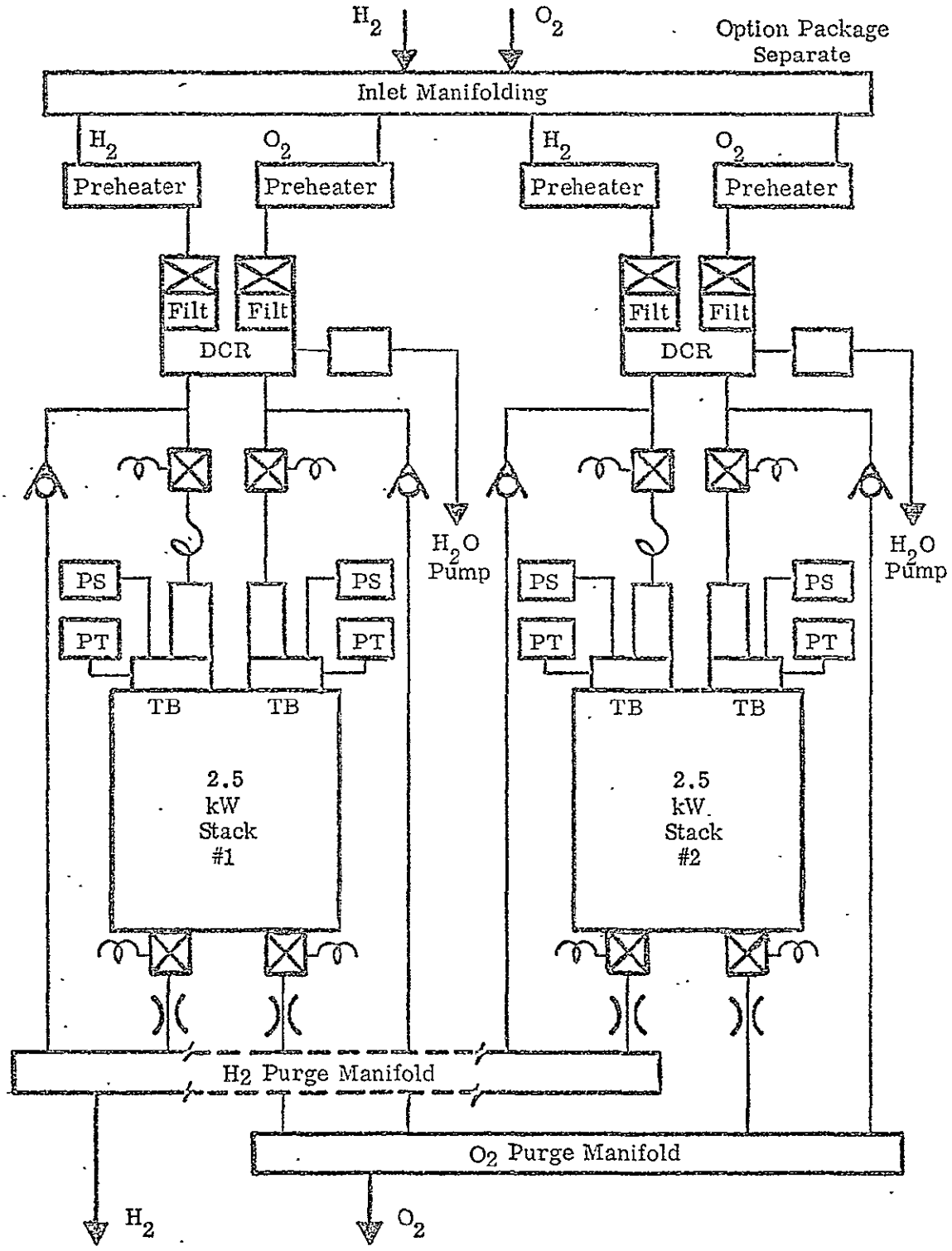

Figure 3.2-36. Integrated Reactant Control Subsystem, Approach 1 (One Regulator for Each Stack)

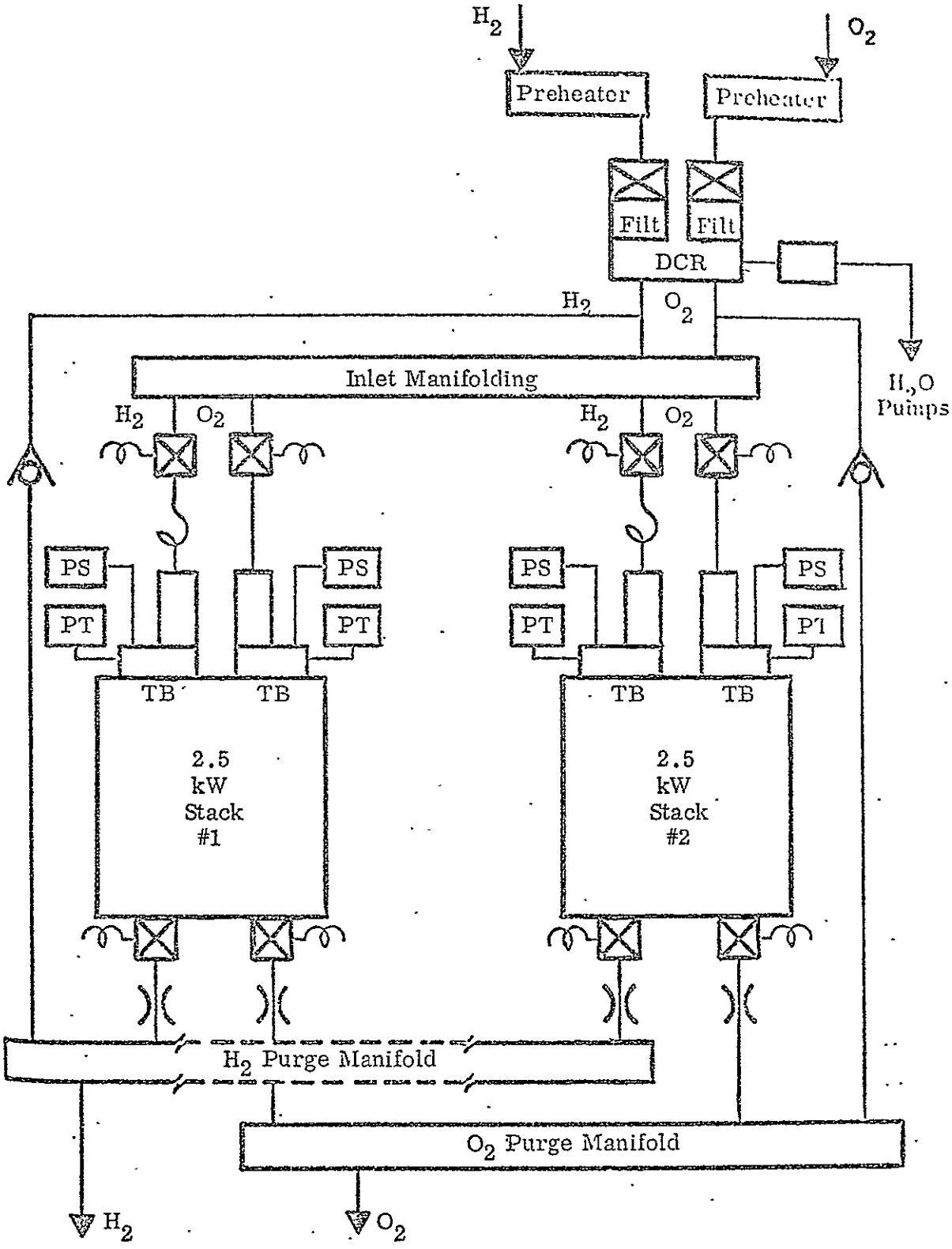

Figure 3.2-37. Integrated Reactant Control Subsystem, Approach 2 (Two Redundant Regulators for a Two-Stack Combination)

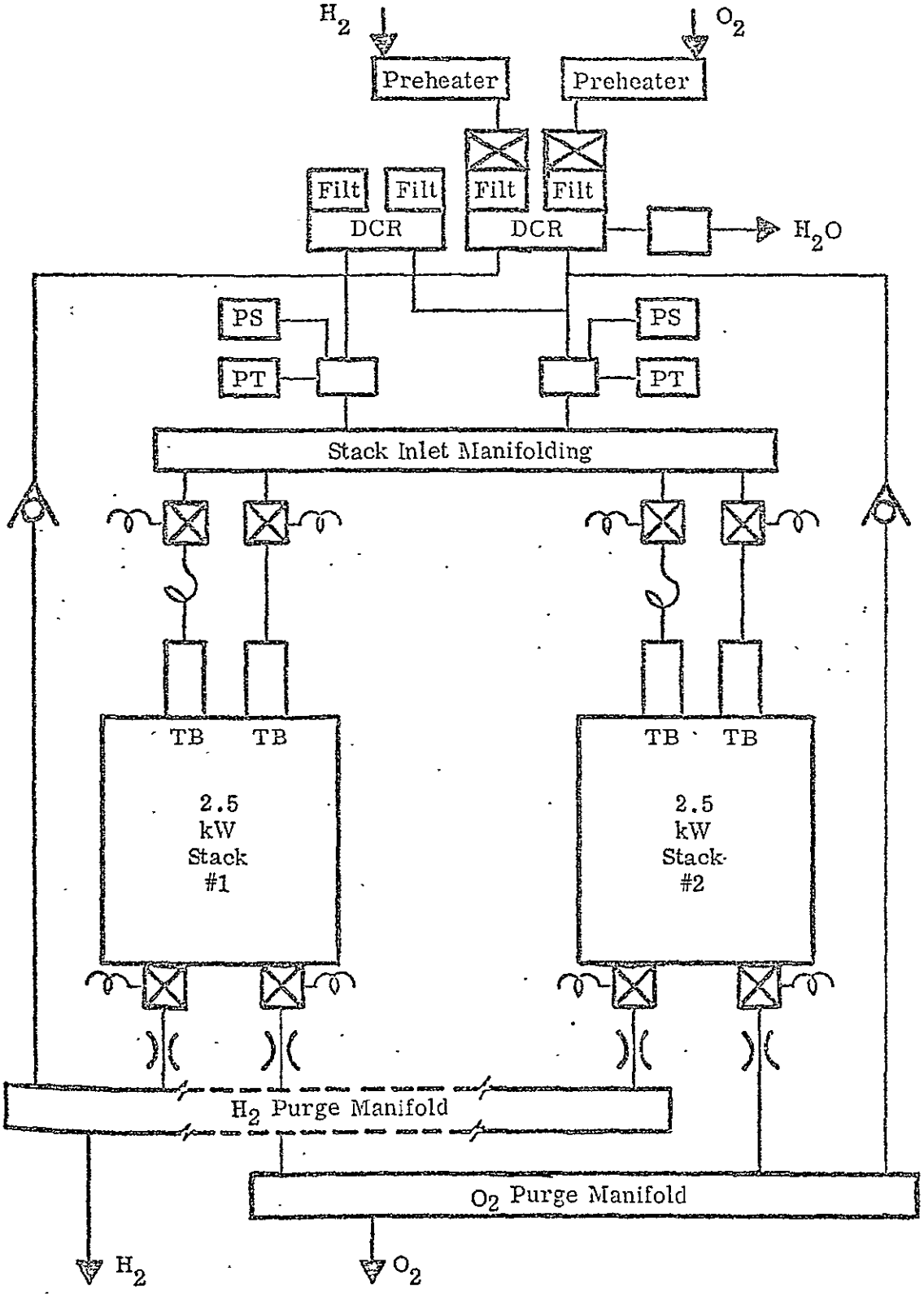

Figure 3.2-38. Integrated Reactant Control Subsystem, Approach 3 (One Regulator for a Two-Stack Combination)

The third approach uses two redundant regulators for a two stack combination.

Each approach provides the following functions:

- Preheats inlet gases
- Filters inlet gases
- Regulates pressure of inlet gases
- Provides Regulated gas to the water pump
- Provides for overpressure relief
- Provides separate stack isolation
- Provides inlet pressure sensing
- Provides individual stack purging

Since the 5 kW building block approach has no failure criteria or reliability requirement other than "fail safe", redundancy is not an advantage. Further, it is not advantageous to retain half power capability. With this in mind, a review of the three RCS approaches reveals that the lightest and simplest approach uses one regulator for a two stack combination (Figure 3.2-39).

Further examination of the RCS reveals that three basic design approaches can be taken for the valves and transducers: 1) obtain separate components and plumb together; 2) integrate "close" components together as a package; 3) optimize separate components into common mounting and manifolding. Separate components plumbed together results in inefficient packaging, significant weight penalties and increased leakage but does offer easy maintenance. Fully integrated components results in efficient packaging but also has high maintenance costs. The optimization of individual components into a common structure with integral manifolding combines the advantages of the other approaches without their disadvantages. On this basis, the concept for the Integrated RCS would be the preheater, filter, regulator and relief valve packages as a separate unit with the inlet and purge valves and transducers integrated into stack bottom end plated (See Figure 3.2-37).

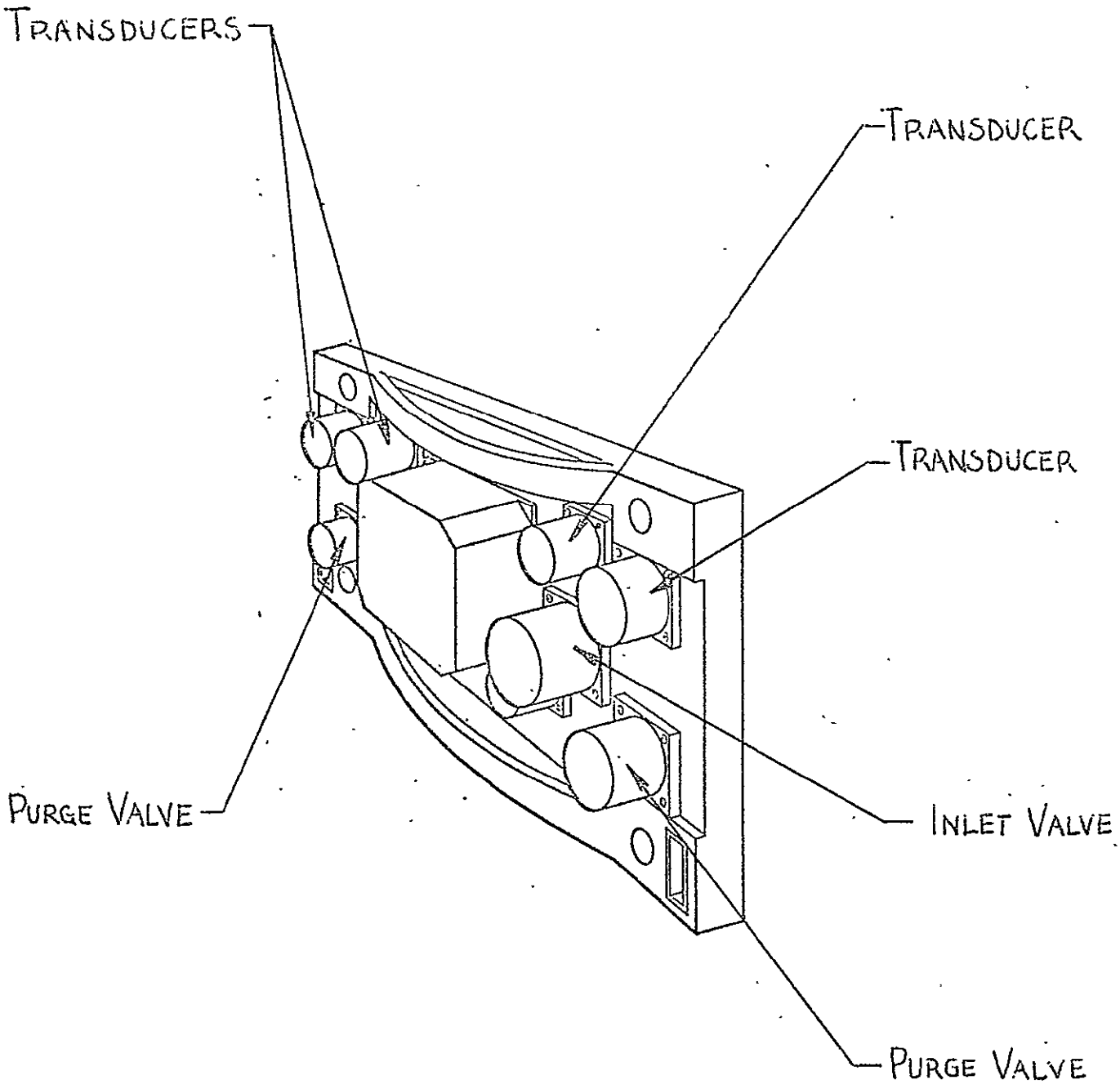

Figure 3.2-39. Bottom End Plate Assembly

3.2.4.3 Stack Compression Study

The objectives of this study was to identify improvements in the area of stack compression.

The details of this investigation are presented in the "stack compression/relaxation test interim report" (80045-TR-0006). The interim test report states that the fuel cell module end-plate force may be prudently halved from 20,000 to 10,000 pounds. The interim report also states that the stack remains a rigid body under vibration until the end-plate force declines below 2900 pounds compression load. The interim report thus bracketed the permissible end-plate force to be used on the MSC stack.

The next item to be established was the anticipated total stack relaxation, through 10,000 hours of operational life. The predicted stack relaxation was fixed at 0.134". This is the aggregate of fuel cell plate and insulation spacer creep and of thermal expansion difference between the components and the stack studs. The majority of the creep occurs during the stack acceptance test, i.e., during the first heating cycle. Data for two stacks, showing the stack relaxation after stack acceptance tests, is found in Table 3.2-20. The MSC stack utilizes the 10,000 lb end-plate force while the MSFC stack end-plate force was maintained at 20,000 lb.

The centerline stack compression devices (Belleville washer assemblies used on the MSC stack) were redesigned, using the new end-plate force and stack relaxation criteria as described above. The redesign was attained by regrouping existing Belleville assembly components into an array of two Belleville spring washers in parallel and twelve in series. This grouping nominally deflects 0.140" with force variations from 375 to 1250 lb per assembly. The total weight of all eight assemblies is 3.835 lb.

The investigation into alternate devices to maintain the stack end-plate force, between 3,000 and 10,000 lb, covered the following designs:

- Helical Compression Springs (round and square wire)
- Cantilever Type Flat Springs
- Hub with Radial Spring Arms

Date	Stack I.D.	Force (TOT) End-Plate lbs.	Stack Length-Inches Corner			
			A	B	C	D
4/22/70	MSFC	20,000	21.130	21.125	21.130	21.121
7/ 7/70	MSFC	20,000	21.034	21.040	21.039	21.036
	MSFC	Length Change	0.096	0.085	0.091	0.085
5/26/70	MSC	10,000	21.089	21.085	21.094	21.095
6/12/70	MSC	10,000	21.013	21.014	21.022	21.022
	MSC	Length Change	0.076	0.071	0.072	0.073

Table 3.2-20. MSC and MSFC Relaxation Rates

- Torque Nut Design
- Spring Plate
- Torsion Springs as Stud Nut Tighteners
- Elastomeric Devices

The devices were compared to the existing compression device with respect to weight and reliability. Another constraint which had to be considered was the space requirements of existing fuel cell module design.

Of all the devices which were evaluated, only the elastomeric pad, consisting of a piece of silicone rubber 7" x 4.5" x 1" compressed 50% between the stack end-plate and insulation spacer, fulfilled the force/deflection and weight requirements. The silicone pad weighed about 2 lb. The creep magnitude for the silicone was low as described by vendor literature (11% at 212°F) but further information including in-house testing would be required.

3.2.4.4 Seal Evaluation

Introduction

The principal objective of these tests were to evaluate the Apollo seal material, with respect to the present 2 kW stack seal design for 10,000 hours of service life.

Summary

The Apollo material excels, over other known TFE compounds, in its creep resistance. The Apollo material resembles other TFE compounds with respect to seal force requirements. The seal force requirements for the Apollo seal material, and for TFE in general, prohibits its use as a direct replacement for the present EPT seals. An estimated end-plate force of 15,000 lb would be required to compress a 0.099" TFE gasket to 0.075" ($\sim$25% compression). Force magnitudes in this range would necessitate a complete module redesign.

The Apollo seal material analysis should be continued, even though the material does not have a direct application as a seal in the 2 kW module. The materials' excellent creep resistance coupled with TFE's general inertness and wide temperature range, makes the material very versatile with possible applications as valve seats, high pressure seals, etc.

Alternate seal materials and configurations were identified for their potential use in the fuel cell.

- Apollo Seal Material Evaluation

  The objective of the tests were to assess the Apollo fuel cell seal material for 10,000 hour life in our current 2 kW seal configuration and environment. The test was concerned with the establishment of the force magnitude required to initiate and maintain an integral gas seal, and in predicting the creep behavior of the material at this force level and nominal fuel cell stack operating temperature.

  The Apollo seal material evaluated was Polyflon Corporation's stabilized polytetrafluoroethylene (PTFE) processed per Pratt and Whitney aircraft specification E 3810 (March 15, 1964). Six samples were received (1-1/2" x 1" x .1").

- Seal Force Test Results

  The seal force test results are displayed by Figure number 3.2-40. A gas seal was not attained with any of the four test samples. Leak rates, of 0.5 to 1.0 cc/min, were established at the completion of the compression hold during which samples were subjected to a constant stress (1365 psi), for assorted periods of time (20 minutes to 2 hours).

  Figure number 3.2-40 compares the stress/strain characteristics of the four test samples to that of a typical TFE sample and to our present seal material EPT (DuPont Fairprene 50-004 Nordel). The four test samples

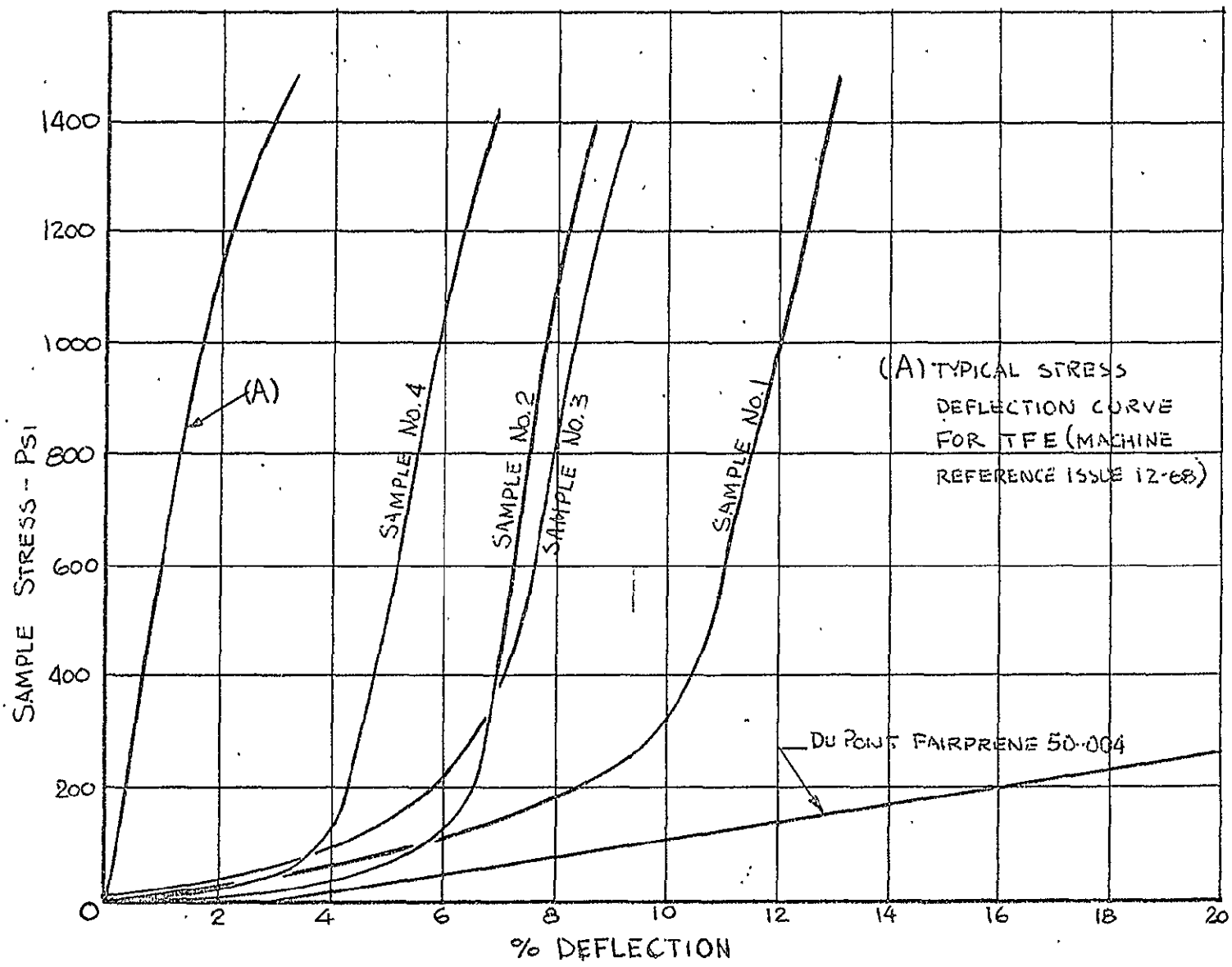

Figure 3.2-40. Apollo Seal Material, Seal Force Test

and the TFE sample had essentially the same slopes from 300 to 1365 psi. Attempts to correlate the curves below this stress level would be impracticable due to system limitations. Sample thickness irregularities of up to 0.008" were measured prior to testing. Assuming that the curves are linear from 0 to 1365 psi stress, the average strain is about 3%, which is typical for TFE at this stress level and temperature.

- Creep Test Results

Due to the limited supply of test material, only one creep test run was performed. The data generated by this run is displayed graphically by Figure number 3.2-41.

A test non-conformance was discovered during the strip chart recording audits. The pressure chart recordings indicated that the pressure to the pneumatic actuator fluctuated between the 13th and 20th hour of the test, the period of unattended operation. The pressure fluctuations caused the sample stress to oscillate from 2000 to 1860 psi. This non-conformance presumably produced the higher creep modules shown in Figure number 3.2-41 during the later stages of the test.

Creep test data of TFE, plotted on logarithmic coordinates, will show a linear relationship between creep modulus and time. Utilizing this principal, the data was extrapolated to 10,000 hours using the best fit line, i.e., only the data points recorded prior to the pressure fluctuations were used. Results arrived at indicate that the creep does not exceed 20% for the Apollo material.

- Alternate Seal Materials and/or Seal Configurations.

The objective of this section is to illustrate the fuel cell plate modifications required to allow for alternate seal designs, and to list several commercial seal materials and configurations, which have a 10,000 hour potential life in our existing fuel cell module environment.

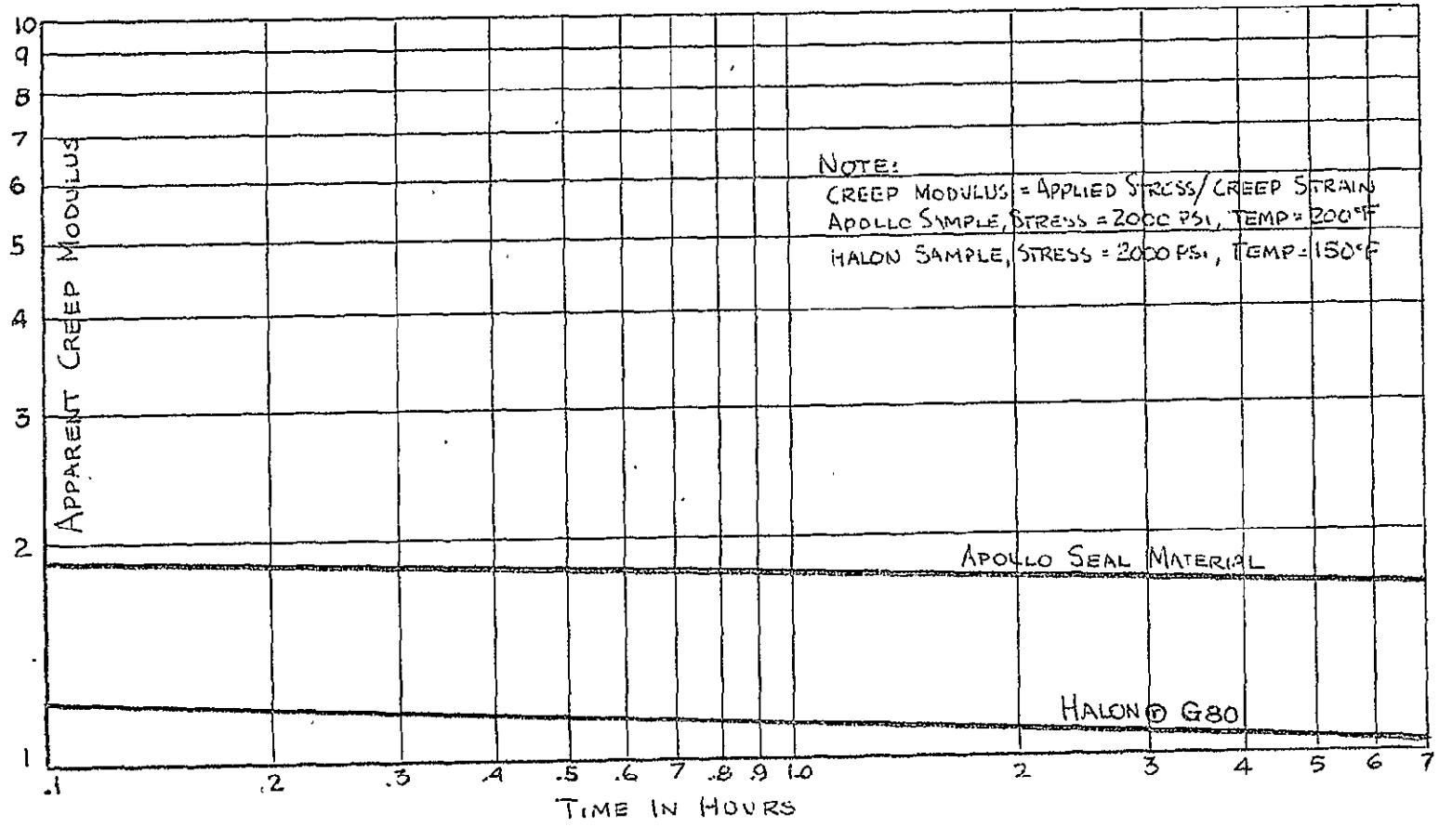

Figure 3.2-41. Log-Log Curves - Creep Modulus versus Time for Seal Materials

The current plate design is shown in Figure 3.2-42. Two alternative designs are shown by Figure 3.2-43 and Figure 3.2-44. The alternative designs permit o-rings. quad-rings, expander seals, etc., to be utilized by increasing the corner radius. The seal frame and cell matrices are the only components requiring modification. These designs utilize separate o-rings for sealing the ports and for peripheral sealing.

The following commercial seal designs, have the potential for 10,000 hour service life in our existing fuel cell environment. They include:

- Aeroquip, "Omniseal"(r)

  The Omniseal consists of a flat stainless-steel helical spring inside a C-section ring of Teflon. Aeroquip Corporation/Aircraft Division, Western Plant, P.O. Box 270, Burbank, California.

- A. W. Chesterton Company, "Vanway - O-Ring"

  The Vanway seal consists of a silicone rubber core ring with a complete encapsulation of Teflon. A. W. Chesterton Company, Ashland Street, Everett, Massachusetts.

- Tec Seal Corporation, "Tec-Ring Seals"

  The Tec-Seal is a continuous Teflon ring with an annular cavity to accept a resilient member. A variety of elastomeric and metallic expander materials are available. Tec Seal Corporation, Division of Tanner Engineering Company, P.O. Box 4646, 22624 Avalon Boulevard, Wilmington, California.

3.2.4.5 Improved Product Water Pump

A trade-off study was conducted to evaluate the relative merit between the existing (2 kW) water delivery subsystem and an alternate, torque motor driven water-delivery subsystem. It was concluded on the basis of this study that the alternate approach is markedly inferior to the present unit. The effective weight, including electrical power

COMPONENT	TYPE OF TEST									
	Operational Performance	Life	Vibration	Temperature	Vacuum	Shock	Humidity	EMI	Proof and Burst	Dielectric Strength
(ICS) Start/Stop Controller	X	X	X	X	X	X	X	X	-	X
Current Sensor	X	-	-	-	-	-	-	-	-	-
Purge Sequencer	X	-	-	-	-	-	-	X	-	-
(RCS) Pressure Regulator										
Adjustable	X	X	X	X	X	X	-	-	X	-
Nonadjustable	X	X	-	-	-	-	-	-	X	-
Relief Valves	X	X	X	X	X	X	X	-	X	X
(SS) Stack	X	X	X	X	X	X	X	X	X	X
Power Conditioner	X	X	X	X	X	X	X	X	-	X
(TCS) Coolant Control Valve	X	X	X	X	-	X	-	-	X	-
Cold Plates										
Liquid	X	-	X	X	X	-	-	-	X	-
Heat Pipe	X	-	X	X	X	X	X	-	-	X
(BRS) Purge Valves	X	X	-	-	X	-	-	-	X	-
Purge Restrictors	X	-	-	-	-	-	-	-	-	-
Moisture Removal Valve										
Thermo-mechanical	X	-	-	-	-	-	-	-	-	-
Electro-mechanical	X	X	X	X	X	X	-	X	X	-
(WDS) Condenser	X	-	-	X	X	-	-	-	-	-
Vent Regulator	X	-	-	-	-	-	-	-	-	-
Deionizer	X	X	-	-	-	-	-	-	-	-
Water Pump	X	X	-	-	-	-	-	-	-	-

Table 3.2-28. Component Test Program

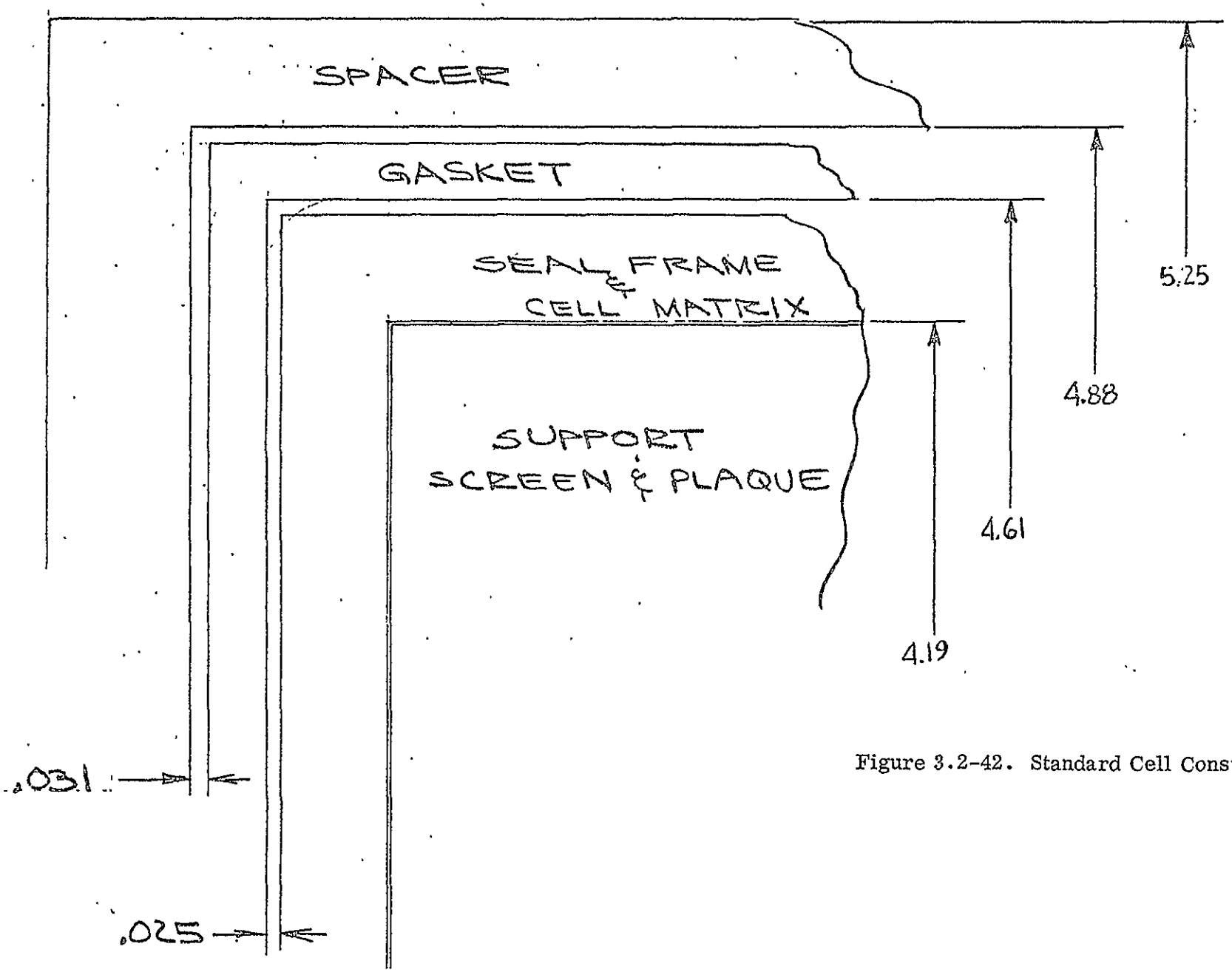

Figure 3.2-42. Standard Cell Construction

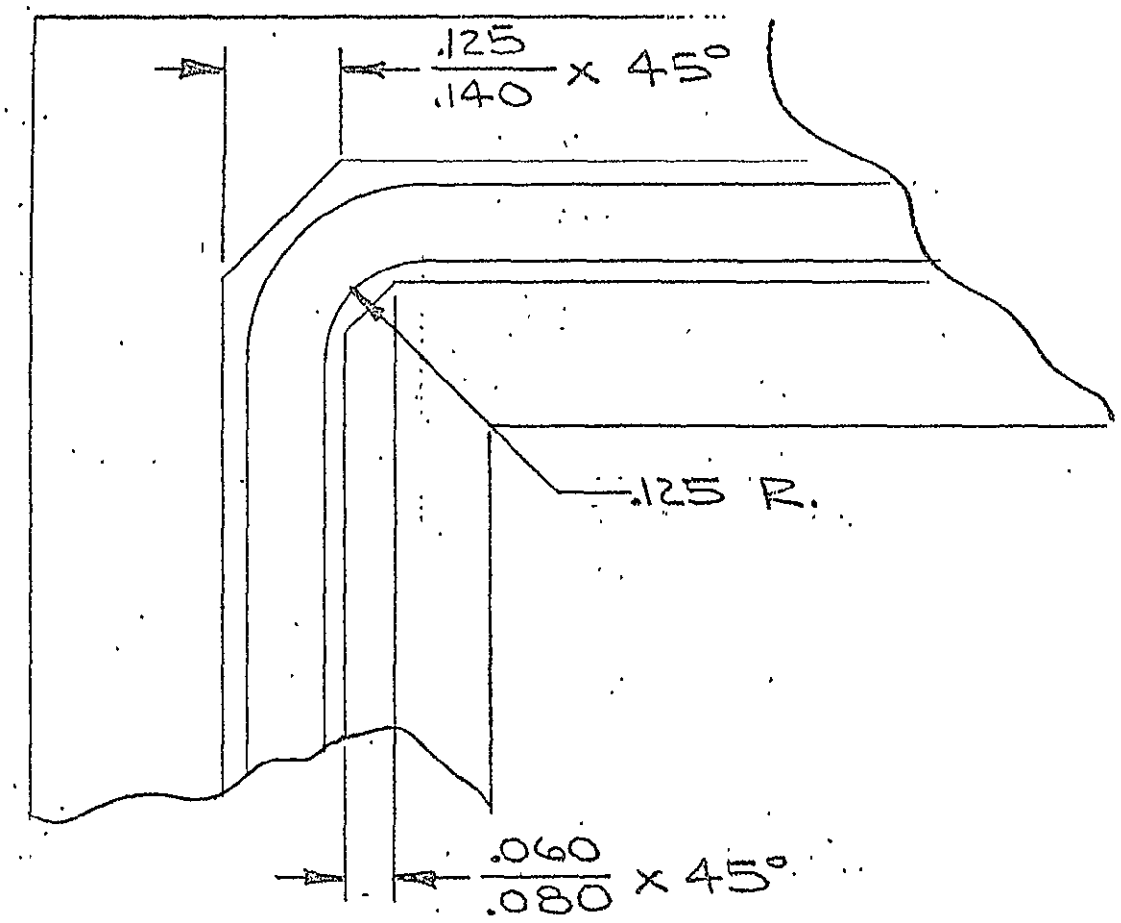

Figure 3.2-43. Modified Cell Configuration "A" Version

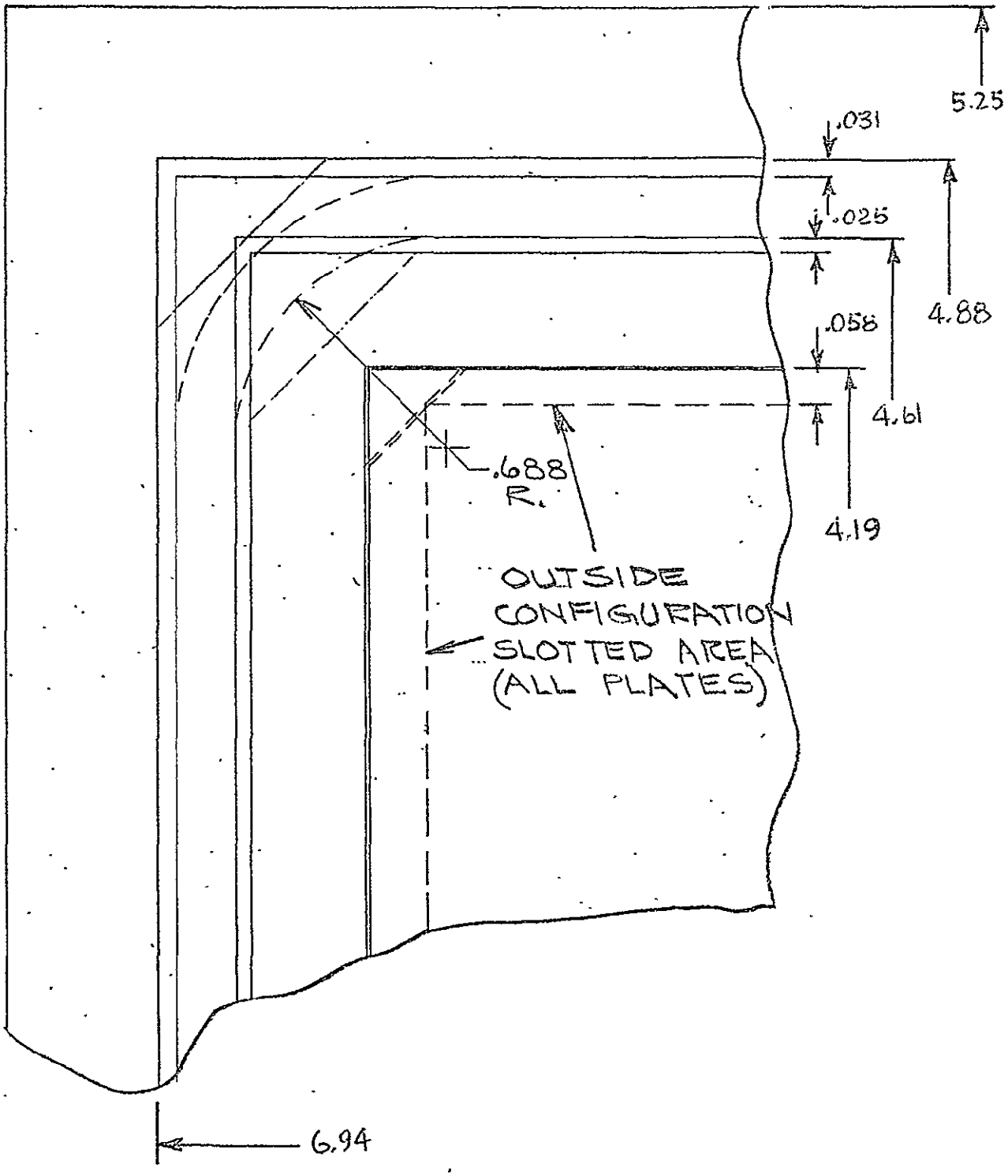

Figure 3.2-44. Alternate Cell Configuration "B" Version

requirements, of the alternate system is prohibitive. Fundamentally, the existing subsystem consists of a gas operated diaphragm water pump, and the auxiliary components for controlling the pneumatics.

Moisture flowing from the fuel cell via a condenser and deionizer, is collected in the water pump cavity. The pump cavity is sized to hold the amount of water (approximately 10 in^3) produced by the fuel cell in converting 16 ampere hours of output energy. Each 16 ampere hour, the pump control valve and gas stop valve are commanded to actuate admitting oxygen at the nominal pressure of 70 psig into the pump, thus forcing the collected water out. Water back flow is prevented by check valves at the pump inlet and outlet.

Oxygen used for driving the water pump is bled from the high pressure system supply line upstream of the dual channel pressure regulator. Prior to entering the pump, the oxygen pressure is reduced and controlled by a regulator.

At the end of the pump cycle the flow of oxygen to the pump is terminated by closing the gas stop valve, and the pump control valve is actuated to effect venting of the oxygen in the pump to space. The rate of oxygen venting is controlled by a pressure regulator in the vent line. The small differential pressure between the water side of the pump and the oxygen side, which is referenced to space vacuum, maintain the pump diaphragm in position to permit readmission of water to the pump in preparation for another pumping cycle.

The existing system has considerable merit. The hardware has been developed to a high degree. The component designs in the subsystem have undergone an average test time of 10,000 hours. No significant difficulties or problem areas were encountered during subsystem development. The subsystem does, however, have one significant disadvantage - complexity. The relatively large number of components required to manage the oxygen inhibit the versatility of the subsystem. A change in operating requirements, such as increased flow capability, could force redevelopment of several components.

The present subsystem could be simplified slightly by replacing the gas vacuum regulator

with an orfice. A more significant simplification could be effected if the required water tank head (subsystem back pressure) could be reduced to 35 psia or less. This would permit driving the water pump with oxygen bled from the low pressure side of the dual channel pressure regulator. Hence, the gas stop valve and regulator could be replaced by a low pressure rated solenoid valve. A weight savings of 1.26 lb would be realized as a result of these two modifications. The additional flow throughput burden placed upon the dual channel regulator, as a result of bleeding-off regulated pressure oxygen, would not force a redesign of the unit. The present capacity of the dual channel regulator is sufficient to handle the additional load.

With system simplicity as an objective, several alternate methods for pumping water to the vehicle storage tank were considered. Among the candidate approaches were a continuously operating, motor driven gear pump; a continuously operating, motor driven piston pump; and a intermittantly operating, motor driven diaphragm pump.

The motor driven gear pump approach was deemed impractical due to the problems involved in providing a sufficient NPSH to the pump. Any technique, such as a pilot diaphragm pump, for maintaining a sufficiently high pressure at the gear pump inlet to prevent caviation, would be more complex than the existing subsystem. Further, the efficiency of the unit would be very low.

Likewise, the motor driven piston pump approach was rejected due to potential pump lubrication problems, water contamination problems, and low unit efficiency.

Use of a unit with a diaphragm or bellows pump driven by a dc motor via a cam assembly appeared to have merit. Hence, this approach was evaluated and a comparison with the existing system was made.

Before a meaningful comparison between the two type units can be made, the alternate system must be optimumly sized. A large number of parameters influence the pump driver size. These parameters are:

- Maximum water production rate
- Pump cycle rate

- Tank head (system back pressure)
- Reliable cycle life of diaphragm or bellows
- Motor torque rating as a function of weight
- Motor torque as a function of input power

Based on supplier data, a reliable cycle life or 100,000 cycles is reasonable for bellows used in the application. At an average module current of 50 amps over 5000 operating hours on average cycle rate of 1 cycle per 2.5 ampere hours is permissible. This corresponds to an average time cycle rate of 20 cycles per hour.

The maximum water production rate for the advanced 2-1/2 kW module is 2.3 lb/hr, or 64 in^3/hr. In order to handle this quantity of water without exceeding the design cycle life of the bellows, the pump must have a minimum capacity of 3.2 in^3/cycle.

The head against which the pump must operate was assumed to be 75 psia. This value is identical to the requirements of the present pump.

The minimum motor torque required to operate the pump is given by the product of pump head, bellows effective area, and cam rise. It is desirable, of course, to minimize the weight and power requirements of the unit. Both weight and required input power increase with rated torque. This dictates that the effective area of the bellows must be minimized. However, to achieve a bellows life of 100,000 cycles with an internal to external pressure differential of 75 psid, the ratio of effective diameter to stroke of the bellows (rise of the cam) should be at least five.

With the diameter to stroke ratio of five and 3.2 in^3 capacity as constraints, a 2.75 inch effective diameter by 0.50 inch stroke bellows was selected for study purposes.

In order to be competitive with the present subsystem, the alternate subsystem must have the following characteristics:

- Greater reliability
- Less or equal total weight (including parasitic power penalty)

A comparison of the MTBF of the existing (centerline) subsystem and the alternate subsystem was made. Based on an operating life of 2000 hours the MTBF, at the present centerline subassembly, is 94,300 hours; whereas, the predicted MTBF of the alternate unit is 196,000 hours. The marked superiority of reliability of the alternate unit is largely the result of simplicity.

The minimum torque required to drive the pump is 306 lb/in. This torque value corresponds to a combined torque motor and controls weight of 23 lb. The input power required is 575 watts.

An "effective" weight comparison of the two subsystems is presented in Table 3.2-21. Included in this comparison are the weight penalties associated with oxygen usage in the centerline system and parasitic power usage in the alternate system. The predicted "effective" weight of the alternate unit is 39.7 lb as compared to 14.3 lb for the centerline system.

Although the predicted reliability of the alternate approach is considerably higher than that of the present system, the weight and power penalties are prohibitive. On the basis of this study, the motor driven, diaphragm pump water delivery approach is deemed impractical.

3.2.4.6 Water Glycol Pump

The water glycol coolant pump is presently a single source procurement item. An attempt was made to develop an alternate supplier.

Procurement specification number 49157059 and source control drawing number 49350059-001 were reviewed and it was established that they were general enough to be used to develop an alternate source. A procurement package was assembled (see bid package AEPD 526) and sent to the following five suppliers:

- Eastern Industries
- Pesco Products Division of Borg-Warner Corporation
- Romec Division of Lear-Siegler Incorporated

EXISTING SUBSYSTEM

COMPONENT	WEIGHT
Gas Pressure Regulator and Stop Valve	0.88
Pump Control Valve	0.37
Gas Vacuum Regulator	0.26
Pump Relief Valve	0.06
Water Pump Assembly	3.80
Check Valves (3)	0.21
Tubing and Fittings	1.75
Oxygen Usage Penalty (for 6250 kwh)	7.45
Total "Effective" Weight	14.78

ALTERNATE SUBSYSTEM

Torque Motor and Controls	23.00
Water Pump Assembly	3.80
Check Valves (2)	0.21
Tubing and Fittings	0.67
*Electrical Power Penalty, lb oxygen (for 6250 kwh)	12.00
Total "Effective" Weight	39.68 lb

*0.955 lb oxygen = 1.0 kwh

Table 3.2-21. Subsystem Weight Comparison

- Carleton Controls Corporation
- Kearfott Division of Singer-General Precision Incorporated

All five suppliers elected not to bid on this item. The apparent lack of enthusiasm stems from the fact that the suppliers could not justify the expenditure of time and effort to design, develop, tool and quality a new pump that offered limited production potential and which would be a high cost, non-competitive item.

3.2.4.7 Deionizer

Methods of eliminating the deionizer by containment of the electrolyte have been investigated; these methods are reported in Subtask 1.4 under the diffusion membrane work.

3.2.4.8 Component Development Plan

Introduction

This plan was prepared as part of Task 2.0, Subtask 2.4 of contract NAS 9-10443.

As a result of assessing the status of the present 2 kW hardware, defining an advanced fuel cell system and analyzing its future applications, specific development needs have been identified. This plan identifies the components and subsystems that require development efforts, describes the hardware approach in terms of existing hardware and presents a test matrix.

Discussion of Subsystems

- Instrumentation and Control Subsystem (ICS)

  The ICS performs the functions of data management, vehicle data interfacing, and control of the FCPS purge valves. The following is a preliminary list of ICS components:

  - H_2 pressure sensor

- O_2 pressure sensor
- Stack temperature sensor
- Water cavity pressure sensor
- Stack current sensor
- Electrical leads
- Valve position indicators
- Signal conditioners
- Valve and sensor excitation
- Purge sequencer
- Start/stop controller

Table 3.2-22 compares these components to those used on previous systems, identifies the relative hardware concepts and states the development status.

- Reactant Control Subsystem (RCS)

The RCS performs all functions necessary for supplying reactants to the stack subsystem and water delivery pump on demand.

The following is a preliminary list of RCS components:

- Thermal interface
- Filter
- Pressure regulator
- Relief valve
- Manifolding

Table 3.2-23 compares these components to those used on previous systems. identifies the relative hardware concepts and states the development status.

Item	Prior Use	Approach	Development Status
Basic control & instrumentation function	All systems to some degree	Provide information to computer interface Receive commands from interface	Requires tailoring for specific application Requires interface testing
Pressure Sensors	All systems	Same as previously employed	Fully developed
Temperature Sensors	All systems	Same as previously employed	Fully developed
Current Sensors	All systems	Resize	Fully developed
Electrical Leads	All systems	Same as previously employed	Fully developed
Valve position indicators	MOL systems	Micro switch	Fully developed
Signal conditioners	All 2 kW systems	Same as previously employed	Fully developed
Purge sequencer	Similar to all systems	Purge stacks individually	Fully developed
Start/Stop controller	New item	Automatic start/stop with command from interface	Requires full development
Packaging	Similar to all other systems	Modularize Integrate sensors with applicable other modules	N/A

Table 3.2-22. Instrumentation and Control Subsystem (ICS)

Item	Prior Use	Approach	Development Status
Basic Reactant control function	All systems	Control and condition inputs only	Fully developed
		Resize	Requires testing to verify resizing
Preheaters	All NASA 2kW Systems	Cold Plate	See TCS
Filters	All systems	Resize for life and maintainability	Fully developed
Pressure regulator	All systems	Minor Resize	Fully developed
		Make adjustable	New modification
Relief valves	2kW systems	Size to 67 psi	Requires full development testing
Packaging	200 watt & 5kW	Modularize	N/A

Table 3.2-23. Reactant Control Subsystem (RCS)

- Stack Subsystem (SS)

  The Stack Subsystem converts reactant energy to electrical power and provides by-product removal interfaces.

  The following is a preliminary list of SS components:

  - Stack
  - Electrical connectors
  - Thermal interface
  - Purge gas outlet
  - Water vapor outlet
  - Power conditioner

  Table 3.2-24 compares these components to those used on previous systems. identifies the relative hardware concepts and states the development status.

- Thermal Control Subsystem (TCS)

  The TCS performs the function of waste heat removal from the FCDS.

  The following is a preliminary list of TCS components:

  - Condenser heat sink
  - Electronics heat sink
  - Proportional coolant control valve
  - Stack heat sink
  - Reactant preheater

  Table 3.2-25 compares these components to those used on previous systems. identifies the relative hardware concepts and states the development status.

Item	Prior Use	Approach	Development Status
Basic Stack function	All System (NASA systems	Static moisture removal	Fully developed Required tailoring for specific needs
Stack	All systems	Use 34 cells	Fully developed EMA
KOH matrix	(was 30 mil JM1945)	Use improved matrix	Fully developed RAM
Reactant pressure	(was 37 psia)	Use 30 to 55 psia reactants	Fully developed past experience
Electrodes	(was AB-40 and HYSAC)	Use A-C XIV anodes	Fully developed substitution
Degradation per cell section	(EDS#1 was 27.5μv at 110 amps)	15μv at 110 amps	Reduce KOH contamination Reduce KOH loss Reduce lateral cell gradients
Cold plate	200 watt system (was gas cool)	Establish thermal contact with plates	See TCS
Power conditioner	Other power source applications	Pulse-width-modulate 9 cell sections	Feasibility established Requires demonstration testing with a stack
Packaging	Similar to all prior systems	Modularize Weight reduce	N/A

Table 3.2-24. Stack Subsystem (SS)

Item	Prior Use	Approach	Development Status
Basic Thermal Control Function	All systems	Indirect liquid cooled (cold plates) or Heat pipes	Developed and used on other A-C systems Requires testing for adaptation New item requiring full development for this application
Coolant control valve (liquid)	All 2kW systems used on-off valves	Proportional flow control valve	Feasibility established Requires full development testing
Cold plates	200 watt unit used plate technique	Circulate coolant in plates which are thermally shorted to the heat source or Integrate evaporator end of heat pipe into plate	Feasibility extablished Requires development testing
Packaging	No prior similarity	Integrate manifolding into structure Separate cold plates from other modules	N/A

Table 3.2-25. Thermal Control Subsystem (TCS)

- By-Product Removal Subsystem (BRS)

  The function of the BRS is to control removal of by-product media from the fuel cell stacks. Control of KOH concentration is an integrated part of this function.

  The following is a preliminary list of BRS components:

  - Purge valves
  - Purge restrictors
  - Purge manifolds
  - Proportional moisture removal valve

  Table 3.2-26 compares these components to those used in previous systems, identifies the relative hardware concepts and states the development status.

- Water Delivery Subsystem (WDS)

  The WDS receives steam from the By-Product Removal Subsystem and performs the condensation and conditioning functions necessary to deliver potable liquid water to the vehicle.

  The following is a preliminary list of WDS components:

  - Thermal interface
  - Condenser
  - Vent regulator
  - Deionizer
  - Water pump

  Table 3.2-27 compares these components to those used in previous systems, identifies the relative hardware concepts and states the development status.

Item	Prior Use	Approach	Development Status
Basic by-product removal function	All systems but not as a separate functional subsystem	Modularize Unitize	Fully developed
Purge valves	All systems	Redesign solenoid and seat	Requires life tests
Purge restrictor	All systems	Resize; same as prior NASA units	Requires only performance check of resize
Moisture removal valve	200 watt	Thermo-mechanical, temperature compensated back pressure regulator OR Electro-mechanical flow control valve	Fully developed Requires resize verification New item not previously developed
Packaging	Similar to all prior systems	Integrate into bottom end plate of stacks	N/A

Table 3.2-26. By-Product Removal Subsystem (BRS)

Item	Prior Use	Approach	Development Status
Basic water delivery function	All systems	Modularize	Fully developed
		Delete components to combine functions	Requires resize and repackage verification
		Resize for increased capacity	
Thermal interface	All systems	Recirculate liquid coolant	Requires resize and optimization; fully developed
		OR	
		Heat pipes	Requires development; feasibility established
Condenser	2kW & 5 kW	Same as prior NASA units with thermal options (see Subtask 2.3 trade-off)	Fully developed; requires resize verification
		Resize and weight reduce	
Vent regulator	All systems with condenser	Resize	Fully developed
			Requires resize verification
Deionizer	All systems with condenser	Make maintainable	Fully Developed
		Resize (see Subtask 1.4 for study results)	
Water pump	All systems with condenser	Same as prior NASA units	Fully developed
		Resize	Requires life testing
Packaging	5kW design similarity	Modularize to handle entire 2-stack system	N/A

Table 3.2-27. Water Delivery Subsystem (WDS)

Development Test Matrix

As shown in the subsystem discussions, sixteen components require development and associated testing.

Ten (10) basic development test types were used to define the extent of testing required to develop a component. Depending upon the component type (electrical, hydraulic, etc.) operational performance tests include exercising the component over its full performance limits under extremes of operating conditions at nominal environments. Life tests exercise the component through equivalent time or cycle requirements under nominal operating conditions. Vibration tests are performed on the component at levels which the component is expected to see taking into account the way in which the component is packaged and mounted in its final application. Temperature tests exercise the component through its operation during environmental temperature extremes. Vacuum tests exercise the component through its operation during vacuum environmental conditions. Shock tests are performed to enable evaluation of component operation after exposure to shock. Humidity tests are performed to evaluate corrosion resistance and susceptability to moisture. EMI tests are performed on electrical components to ensure that they are not susceptable to outside interference and do not produce unacceptable interference. Proof and burst tests are conducted to insure adequate design safety. Dielectric strength tests are performed to insure proper materials and design practice in electrical applications.

Each component was reviewed and an estimate of required testing was made. This is shown in Table 3.2-28.

COMPONENT	TYPE OF TEST									
	Operational Performance	Life	Vibration	Temperature	Vacuum	Shock	Humidity	EMI	Proof and Burst	Dielectric Strength
(ICS) Start/Stop Controller	X	X	X	X	X	X	X	X	-	X
Current Sensor	X	-	-	-	-	-	-	-	-	-
Purge Sequencer	X	-	-	-	-	-	-	X	-	-
(RCS) Pressure Regulator										
Adjustable	X	X	X	X	X	X	-	-	X	-
Nonadjustable	X	X	-	-	-	-	-	-	X	-
Relief Valves	X	X	X	X	X	X	X	-	X	X
(SS) Stack	X	X	X	X	X	X	X	X	X	X
Power Conditioner	X	X	X	X	X	X	X	X	-	X
(TCS) Coolant Control Valve	X	X	X	X	-	X	-	-	X	-
Cold Plates										
Liquid	X	-	X	X	X	-	-	-	X	-
Heat Pipe	X	-	X	X	X	X	X	-	-	X
(BRS) Purge Valves	X	X	-	-	X	-	-	-	X	-
Purge Restrictors	X	-	-	-	-	-	-	-	-	-
Moisture Removal Valve										
Thermo-mechanical	X	-	-	-	-	-	-	-	-	-
Electro-mechanical	X	X	X	X	X	X	-	X	X	-
(WDS) Condenser	X	-	-	X	X	-	-	-	-	-
Vent Regulator	X	-	-	-	-	-	-	-	-	-
Deionizer	X	X	-	-	-	-	-	-	-	-
Water Pump	X	X	-	-	-	-	-	-	-	-

Table 3.2-28. Component Test Program